Investigation on the interface structure and thermal conductivity of hot-forged Cu/ (Ti /W-coated)-diamond composites

Jingnan Ma

Supervised by:

Dr Fei Yang

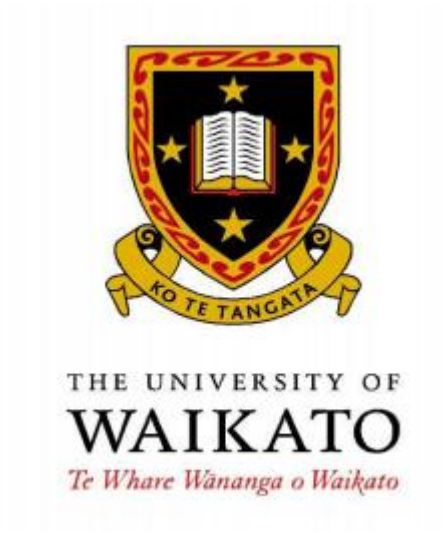

A thesis submitted in fulfilment of the requirement for the degree of Master of Engineering

The University of Waikato, 2020

Abstract

Effectively dissipating heat is required for the high-power electronic equipment to ensure the equipment has a safe working environment. Cu/diamond composite is considered as a new generation of heat sink materials because of its potential of achieving high thermal conductivity and tailorable coefficient of thermal expansion. The poor chemical affinity between the copper and the diamond is the main barrier for obtaining Cu/diamond composites that have high thermal conductivity. The interface layer between the copper and the diamond plays an important role in facilitating heat transfer in the Cu/diamond composites. However, it lacks deep understanding on the influence of interface characteristics on the Cu/diamond composite's thermal conductivity.

We aim to tailor the thermal conductivity of Cu/diamond composites by modifying the interphase layer's phase composition and microstructure, and there are three primary research parts in this thesis. The first part is the study of the Cu/Ti-diamond composite prepared by induction heating and hot forging from pre-annealed Ti-coated diamond particles. Part two is the study of the Cu/W-diamond composite prepared with the identical process that used in the part one from the pre-annealed W-coated diamond particles. The third part presents Cu/Ti-diamond composites that are fabricated by the combination of vacuum sintering and hot forging from Ti-coated diamond particles. The fabricated composites' microstructure and the interface morphology of diamond particles that are extracted from the fabricated composites are examined by scanning electronic microscopy (SEM) and atomic force microscopy (AFM), respectively, and the phase composition of the fabricated composites is analyzed by X-ray diffraction (XRD).

Results show that both TiC and W_2C particles are easier to nucleate on the diamond-{111} facet than on diamond-{100} facet during pre-annealing, and the reaction temperature for forming TiC is 800℃ and W_2C is 1050 ℃, respectively, and the higher the annealing temperature is, the more carbides nucleation and growing locations present on the diamond surface. It finds that the un-reacted diamond coating (titanium or tungsten) further reacts with the diamond to form metal carbides during the process of hot forging at 800 ℃. Ti-800-Cu/Dia composite has the highest thermal conductivity among the hot-forged Cu/Ti-diamond composites, with a value of 350W/ (mK), attributed to the formation of a continuous interface, almost no interfacial layer spallation, and a rough interface formed on the diamond particle surface. Due to a large amount of WC interface is formed after hot forging, W-1050-Cu/Dia composite shows the highest thermal conductivity (223 W/ (mK)) among the hot-forged Cu/W-diamond composites. After vacuum sintering, the Ti coating is fully reacted with the diamond to form TiC, however, the preformed TiC

particles are easy to spall from the diamond surface during hot forging. This leads to weak interfacial bonding strength between the diamond and the copper. The thermal conductivity of the Cu/Ti-Dia-VS is only 46W/ (mK) because of its low relative density. After hot forging, the thermal conductivity of Cu/Ti-Dia-VSHF composite is improved to 241W/ (mK), due to the significant increase of the hot-forged composite's relative density. It is possible to design the interface characteristics of Cu/diamond composites by changing the pre-annealing temperature of the coated-diamond particles prior processing.

List of Publication

J. N. Ma, L. Bolzoni, F. Yang, Interface manipulation and its effects on the resultant thermal conductivity of hot-forged Cu/Ti-coated diamond composites, Diamond and Related Materials (Submitting)

Acknowledgment

This research work was completed under the supervision of Dr. Fei Yang. His supervision and work are rigorous and meticulous. He helped me to improve my research and academic writing, increased my confidence, and inspired my research ideas. Thank you very much for your help in topic selection, experimental design, and revising my master thesis. The skills I have learned from Dr. Fei Yang will have a profound impact on my future study and work, they are my precious and lucky harvest.

This year was hard, everyone is suffering the impacts of COVID-19. I need to thank the members of the research group, Shanquan Jia and Lei Lei, who helped me with the operation of experimental equipment and also shared their research experience, especially at the start of my project. I have finished my master study successfully due to their help.

Thanks also goes to Yingchao Guo and Yutao Zhai under the supervision of Dr. Fei Yang, for helping with their thoughtful discussion. My appreciation to Jiangang Wang from HEBUST, China, for helping with carrying out the AFM testing.

Sincere thanks to my parents, for their silent dedication and full support. Although we are separated from each other in different countries, they did not neglect their concern for my life and study. Their financial support ensured my master study could be finished without any hindrances, and also their understanding encourages me to follow the difficult life of studying abroad.

Thanks, my friends, Yulu Sun and Yaqi Chang, for accompanying me in the master life, we learn from each other and encourage each other, which makes life more exciting, so we have the most sincere friendship.

My thanks to the many others who I could not specify directly.

Table of Contents

Abstract II
List of Publication IV
Acknowledgment V
Table of Contents VI
List of Figure VIII
List of Table X
List of Symbols XI
List of Abbreviations XII
1 Introduction 2
2 Literature Review 4
2.1 Overview of heat sink materials 4
2.2 The development of heat sink materials 5
2.3 Metal/diamond composites 7
2.3.1 Introduction of diamond 7
2.3.2 Fabricating process of metal/diamond composites 9
2.4 Metal/diamond composites 12
2.5 Research barrier in Cu/diamond composites 14
2.5.1 The interface of Cu/diamond composites 14
2.5.2 Interface modification of copper/diamond composite 17
2.5.3 Consideration of the Interface characteristics 20
2.6 Research significance and objectives 26
3 Experimental 28
3.1 Material preparation 28
3.2 Experimental procedures 28
3.3 Property testing 31
3.3.1 Materials characterization and analysis 31
3.3.2 Properties measurement and test 32
4 Interface characteristics and thermal conductivity of Cu/55vol%Diamond (Ti-coated) composites 34
4.1 Pre-annealing of Ti-coated diamond 34
4.1.1 Diamond phase transformation after annealing 35
4.1.2 Diamond surface characterization after annealing 37
4.2 Copper /55vol%Diamond (Ti-coated) composites 39

4.2.1 Relative density 40
4.2.2 Phase constitutions 41
4.2.3 Microstructure 42
4.2.4 Thermal conductivity 49
4.2.5 Theoretical thermal conductivity 50
4.2.6 Discussion 51
4.2.7 Summary 56

5 Interface characteristics and thermal conductivity of Cu/55vol%Diamond (W-coated) composites 58

5.1 Pre-annealing of W-coated diamond 58

5.1.1 Diamond phase transformation after annealing 59
5.1.2 Diamond surface characterization after annealing 61

5.2 Copper /55vol%Diamond (W-coated) composites 63

5.2.1 Relative density 63
5.2.2 Phase constitutions 64
5.2.3 Microstructure 66
5.2.4 Thermal conductivity 70
5.2.5 Theoretical thermal conductivity 71
5.2.6 Discussion 73
5.2.7 Summary 78

6 Effect of fabrication process on the interface characteristics and thermal conductivity of Cu/Ti-diamond composites 79

6.1 Cu/Ti-diamond composites 79

6.1.1 Relative density 79
6.1.2 Phase constitutions 80
6.1.3 Microstructure 81
6.1.4 Thermal conductivity 84

6.2 Discussion 85

6.2.1 Effect of vacuum sintering on Cu/Ti-diamond composites 85
6.2.2 Effect of hot forging on Cu/Ti-diamond composites 86

6.3 Summary 86

7 Conclusion 88
Reference 89

List of Figure

Figure 2-1 (a) Crystal structure of the diamond; (b) a diamond morphology [24] 7
Figure 2-2 Schematics of powder metallurgy [28] 10
Figure 2-3 Schematic diagram of SPS [24] 10
Figure 2-4 Schematics of vacuum hot pressing [30] 11
Figure 2-5 Schematics of Vacuum hot forging [33] 12
Figure 2-6 Diagrams of lattice and phonons [42] 17
Figure 2-7 Relations between volume fraction of diamond and thermal conductivity of composites [50] 19
Figure 2-8 Schematic diagram of heat transport along a metallic film assuming parallel grain boundaries and that the heat flux is perpendicular to the grain boundaries [51] 22
Figure 2-9 Ideal interface structure in Cu-Zr/ diamond composites [49] 24
Figure 3-1 Pre-annealing of coated-diamond (800℃) 29
Figure 3-2 Hydraulic press for hot forging 30
Figure 3-3 Vacuum sintering furnace 31
Figure 4-1 Diamond morphology: (a-b) non-coated diamond; (c-d) Ti-coated diamond 35
Figure 4-2 XRD patterns of the Ti-coated diamond after (a) magnetic sputtering; (b) heat treatment at different temperatures 36
Figure 4-3 EDS point analysis results of 1050℃-annealed Ti-coated diamond particles 37
Figure 4-4 Morphology of Ti-coated diamond after pre-annealing at (a)800℃; (b) 900℃; (c) 1050℃; (a1), (b1), (c1) are corresponding diamond-{100} facets and (a2), (b2), (c2) are the corresponding diamond-{111} facets 39
Figure 4-5 The measured relative density of Ti-800-Cu/Dia, Ti-900-Cu/Dia, and Ti-1050-Cu/Dia composites 40
Figure 4-6 XRD patterns of (a) Ti-800-Cu/Dia, (b) Ti-900-Cu/Dia, and (c) Ti-1050-Cu/Dia composites 41
Figure 4-7 SEM microstructure of (a-b)Ti-800-Cu/Dia; (c-d)Ti-900-Cu/Dia; (e-f) Ti-1050-Cu/Dia composites 43
Figure 4-8 EDS point analysis of (a) Ti-800-Cu/Dia; (b) Ti-900-Cu/Dia composites 44
Figure 4-9 Extracted diamond particles from (a)Ti-800-Cu/Dia; (b)Ti-900-Cu/Dia; (c) Ti-1050-Cu/Dia composites, (a1), (b1), (c1) are corresponding diamond-{100} facets and (a2), (b2), (c2) are corresponding diamond-{111} facets 46
Figure 4-10 3-D AFM microstructure of the TiC layer on diamond particles extracted from (a-b) Ti-800-Cu/Dia and (c-d) Ti-900-Cu/Dia, and (e-f) Ti-1050-Cu/Dia composites 48
Figure 4-11 3-D AFM microstructure of the TiC interfacial layer on diamond particles extracted from Cu/Ti composite [65] 49
Figure 4-12 Thermal diffusivity and thermal conductivity of the Ti-800-Cu/Dia, Ti-900-Cu/Dia, and Ti-1050-Cu/Dia composites 50
Figure 4-13 The nucleation and growth mechanisms of TiC carbides on diamond-{111} and -{100} facets [70] 53
Figure 4-14 Structure of the diamond-{100} and -{111} facets [59] 54
Figure 4-15 Further reaction mechanism between the diamond and titanium during hot forging 55
Figure 5-1 SEM microstructure of as-received W-coated diamond particles 59
Figure 5-2 XRD patterns of the W-coated diamond after (a) magnetic sputtering; (b) pre-annealing at different temperatures 60
Figure 5-3 EDS point analysis of 1050℃-annealed W-coated diamond particles 61

Figure 5-4 SEM microstructure of: (a) W900; (b) W1050. (a1) (b1) are corresponding diamond-{100} facets and (a2) (b2) are corresponding diamond-{111} facets 62
Figure 5-5 The detailed SEM microstructures of W1050 diamond particles: (a) diamond-{100} facet; and (b) diamond-{111} facet 63
Figure 5-6 The measured relative density of W-0-Cu/Dia, W-900-Cu/Dia, and W-1050-Cu/Dia composites 64
Figure 5-7 X-ray diffraction of (a) W-0-Cu/Dia; (b) W-900-Cu/Dia, and (c) W-1050-Cu/Dia composites 65
Figure 5-8 Microstructure of (a-c) W-0-Cu/Dia, (d-f) W-900-Cu/Dia, and (g-i) W-1050-Cu/Dia composites 67
Figure 5-9 Extracted diamond particles from: (a)W-0-Cu/Dia; (b) W-900-Cu/Dia; (c)W-1050-Cu/Dia composites, (a1), (b1), (c1) are corresponding the diamond-{100} facets and (a2), (b2), (c2) are the corresponding the diamond-{111} facets 70
Figure 5-10 Thermal diffusivity and thermal conductivity of W-0-Cu/Dia, W-900-Cu/Dia, and W-1050-Cu/Dia composites 71
Figure 5-11 Interface structure in Cu/W-diamond composites 73
Figure 5-12 The fabrication process of Cu/W-diamond composites 76
Figure 5-13 Further reaction in W-1050-Cu/Dia composite during hot forging 76
Figure 6-1 XRD patterns of Cu/Ti-Dia composites prepared by (a) vacuum sintering (Cu/Ti-Dia-VS); (b) the combination of the vacuum sintering and hot forging (Cu/Ti-Dia-VSHF); (c) hot forging (Cu/Ti-Dia-HF [65]) 80
Figure 6-2 SEM microstructure of (a-c) Cu/Ti-Dia-VS; (d-f) Cu/Ti-Dia-VSHF; (g-i)Cu/Ti-Dia-HF [65] composites 82
Figure 6-3 Microstructure of diamond particles extracted from (a) Cu/Ti-Dia-VS; (b) Cu/Ti-Dia-VSHF composites 84
Figure 6-4 Thermal diffusivity and thermal conductivity of composites Cu/Ti-Dia-VS and Cu/Ti-Dia-VSHF composites 85

List of Table

Table 2-1 Properties of some metal and composite materials [21-23] 7
Table 2-2 Fundamental properties of diamond [26] 8
Table 3-1 Pre-annealing parameters for the encapsulated specimens 29
Table 3-2 The fabricating parameters for composite specimens 30
Table 4-1 Details of copper/ 55vol%diamond (Ti-coated) composites 40
Table 4-2 Phase constitutions of copper/55vol%diamond (Ti-coated) composites before and after hot forging at 800℃ 42
Table 4-3 Coverage rate of the diamond by coating before and after hot forging 45
Table 4-4 Materials properties for theoretic thermal conductivity calculation of Cu/Ti-diamond composites [3, 66] 51
Table 5-1 Coverage rate by tungsten coating after pre-annealing 62
Table 5-2 Details of copper/55vol%diamond (W-coated) diamond composites 63
Table 5-3 Phase constitutions of Cu/55vol%diamond (W-coated) composites before and after hot forging at 800℃ 66
Table 5-4 Coverage rate of the diamond by coating before and after hot forging 70
Table 5-5 Material properties for theoretic thermal conductivity calculation of Cu/W-diamond composites [66], [71] 73
Table 6-1 The measured the relative density of the Cu/Ti-Dia-VS and Cu/Ti-Dia-VSHF composites 79
Table 6-2 Coverage rate of the diamond by TiC interface 83

List of Symbols

c_p	Heat capacity per unit volume
Ti-1050-Cu/Dia	Cu/Ti-diamond composite (Ti-diamond particles are pre-annealed at 1050℃)
Ti-800-Cu/Dia	Cu/Ti-diamond composite (Ti-diamond particles are pre-annealed at 800℃)
Ti-900-Cu/Dia	Cu/Ti-diamond composite (Ti-diamond particles are pre-annealed at 900℃)
W-0-Cu/Dia	Cu/W-diamond composite (W-diamond particles are without pre-annealed)
W-1050-Cu/Dia	Cu/W-diamond composite (W-diamond particles are pre-annealed at 1050℃)
W-900-Cu/Dia	Cu/W-diamond composite (W-diamond particles are pre-annealed at 900℃)
d	Thickness of interface
G	Thermal conductance
k	Thermal conductivity
N	Phonon velocity
q	Fraction of phonons incident within a critical angle
R	Radius of diamond
Ti1050	1050℃-annealed Ti-diamond particles
Ti800	800℃-annealed Ti-diamond particles
Ti900	900℃-annealed Ti-diamond particles
Vd	Volume fraction of diamond filler
Cu/Ti-Dia-HF	Cu/Ti-diamond composite prepared by hot forging
Cu/Ti-Dia-VS	Cu/Ti-diamond composite prepared by vacuum sintering
Cu/Ti-Dia-VSHF	Cu/Ti-diamond composite prepared by vacuum sintering and hot forging
W1050	1050℃-annealed W-diamond particles
W900	900℃-annealed W-diamond particles
Z	Acoustic mismatch
α	Transmission coefficient of phonons

List of Abbreviations

AFM	Atomic Force Microscopy
CTE	Coefficient of Thermal Expansion
EDS	Electron Dispersive Spectroscopy
MFP	Mean Free Path
SEM	Scanning Electron Microscopy
TC	Thermal conductivity
XRD	X-ray Diffraction

1 Introduction

In this information age, smaller size and better performance are the main requirements for the development of electronic applications. However, the miniaturization and versatility of electronic devices lead to a rapid increase in power density and heat generation of electronic devices, which will degrade work efficiency or even decrease the lifetime of electronic devices. This has become a potential challenge in the fields of communication, information, energy harvesting, and lighting technology [1]. In order to ensure a stable working environment for high-power electronic devices, effective heat dissipation is a key issue that needs to be resolved. Usually, a suitable heat sink material can help increase the heat dissipation of electronic devices. The development of highly integrated and high-power electronic devices requires advanced heat sink materials with superior thermal conductivity, suitable coefficient of thermal expansion, and reliable mechanical performance [2]. The early heat sink materials are mainly made of pure metal, ceramic, or plastic materials, however, their low thermal conductivity cannot meet the thermal dissipation requirements for high-power electronic devices. Thus, more and more attention has been paid to the research of developing a material that is able to rapidly dissipate the heat generated during electronic device operation.

Diamond (1800-2200 W/ (mK)) has the highest thermal conductivity in nature, and a relatively low coefficient of thermal expansion (CTE) of about 1.5×10^{-6}-4.8×10^{-6}/K. Copper is common for the heat sink material due to its advantages of high thermal conductivity, relatively low cost, and wide working temperature range, but its CTE is high, with a value of 17.5×10^{-6}/K [3]. Therefore, diamond reinforced copper composites have the potential of achieving high thermal conductivity and tailored CTE, meeting the requirements for next-generation heat sink materials for high-power electronic devices. However, the chemical affinity between the copper and the diamond is poor, and this easily leads to form a Cu/diamond composite that has high interfacial thermal resistance between the copper and the diamond, resulting in the composite has low thermal conductivity. Extensive research have proved that the formation of a carbide layer between the copper and the diamond in the fabricated Cu/diamond composites can improve the composite interface's integrity and adhesion by mechanical or chemical bonding, and it is beneficial for heat transport between the copper and the diamond, thus, improving the thermal conductivity of the composite [4]. Commonly, a medium interface can be introduced between the copper and the diamond to improve the interface quality of composites by using the methods of matrix alloying or pre-coating diamond. Metal elements like Cr, Zr, W, Ti, Mo, and W are always used for those purposes in the studies [5-8], which have made significant progress in improving the thermo-physical properties of

copper/diamond composites. Currently, it still lacks a deep study on how the interface characteristic influence the thermal conductivity of Cu/diamond composites. Knowing the affecting mechanism of the interface in copper/diamond composite is necessary for fabricating the heat sink materials for high-power electronic devices.

In this study, Cu-55vol% diamond composites are prepared by hot forging of the mixture of pure copper powder and annealed Ti-diamond/W-diamond particles. We will primarily investigate how the copper/diamond composites' interface microstructures are evolved before and after hot forging and how the respective interface microstructures affect the composite's thermal conductivity.

2 Literature Review

2.1 Overview of heat sink materials

Information technology is flourishing, which has a significant influence on our lifestyle, industrial manufacturing, and production. As an important part of the development of information technology, the renewal of assembly electronic technology and technology is forced to be improved. Gordon Moore ever predicted that the integration of circuits would rise fourfold, and the feature size would decrease two times for every three years, this is called Moore's law. From 1960 to 1990, the integrated circuits have experienced a series of developments in small-scale, medium-scale, large-scale, ultra-large-scale, and large-scale [9]. The number of the transistor was 10-100 per wafer rapidly increased to 10 million within the thirty years, this proves the correction of Moore's law [10]. In addition, with the continuous development of electronic technology, electronic devices are getting more and more complicated and assembled in recent years, so that the integration of electronic chips is much higher and the feature size is greatly reduced, these lead to unit power generated in the semiconductors urgently increase and a significant amount of heat is generated during its operation. Current heat sink material cannot rapidly dispel the heat generated away from the integrated chips and becomes the barrier that restricts the further revolution of the electronic technology, therefore, finding a new heat sink material has become a key problem researcher faced in material science. The requirements for ideal heat sink materials should include these properties:

(1) High thermal conductivity. The heat accumulated in the equipment makes its working temperature rise rapidly. According to reports, as the operating temperature rises by 18 degrees, the probability of equipment failure will increase by 2-3 times [2]. Thus, to enable the efficiency and stable working environment of the electronic devices, a heat sink material that has high thermal conductivity is required to rapidly dissipate the heat generated away from the devices;
(2) A suitable coefficient of thermal expansion (CTE). Electronic equipment is always working at fluctuating temperatures. The matching CTE between the heat sink material and the integrated chip can help reduce the possibility of debonding and thermal stress between the heat sink and the chip during operation.
(3) High densification and good gas tightness. Lots of applications require electronic devices run in an environment of vacuum or dirty-free, in addition, humidity and corrosion also affect the normal working of devices. This requires the electronic packing materials have high densification, avoiding gas is trapped in devices;

(4) Good mechanical properties. The heat sink material may be impacted or bumped during the manufacturing or assembly process. Therefore, the heat sink material must have good mechanical properties, such as good stiffness or strength.
(5) Low density or low weight. In order to adapt to microelectronic devices, especially in the aerospace field. Reducing the density as much as possible while maintaining good mechanical and thermal properties.

2.2 The development of heat sink materials

There is a long development time for heat sink materials, according to the type of materials, electronic packing materials can be divided into ceramic, plastic, metal or alloy, and composites [11].

Traditional ceramic-like Al_2O_3, AlN,[12] are in good isolation properties and have a similar CTE with electronic devices, but they have low thermal conductivity, their fabrication and processing are complicated, and the cost is very high, these bring difficulties for mass production for the ceramic heat sink materials. Epoxy materials [12] are much popular in plastic. Plastic heat sink materials are in good ductility, which can protect the devices from the external load. And also the production of plastic is saving money and time. However, the poor gas tightness of the plastic material will lead to equipment failure. In addition, the plastic heat sink material has a relatively low thermal conductivity which cannot satisfy the requirement of the current and future electronic devices. Comparing with ceramic and plastic, metals are in high conductivity and strength, and good process ability, researchers spend much time researching metal packing materials. Copper and aluminum are common in this field, heat transfer with the motion of free electrons leads to metals having high thermal conductivity. But pure metals have a very high CTE value that is not compatible with that of semiconductors. As the working temperature changes, the gas tightness of the devices will be affected due to the generation of the thermal stress, leading to the failure of the packing system. To modify the properties of the metal, researchers try to make metal packing materials with suitable CTE by alloying. Invar ($Fe_{58}Ni_{42}$) [13] and Kovar ($Fe_{54}Ni_{28}Co_{18}$) [14] is the first generation of metal alloy packing materials. The Invar and Kovar alloy are prepared by adding a large quantity of Co and Ni into the iron phase, this leads to the fabrication cost is quite high, and the thermal conductivity of them is only 11-17W/ (mK). Therefore, pure metals and metal alloys cannot meet the requirements of heat dissipation materials for high-power electronic devices. And researching on composite materials have become the trend in the field of the new heat sink material.

Composite materials are multi-phase materials prepared by two or more materials from metals, ceramics, polymers, etc. via appropriate processing techniques. In composite materials, the components complement each other in performance and produce a synergistic effect, making the composite material's comprehensive performance better than the original composition material to meet various requirements. Metal matrix composites with high thermal conductivity and tailorable coefficient of thermal expansion are widely used as a new generation of electronic packing materials, this is because [15]: (1) Metal matrix composites are designable. The composites' properties can be tuned by controlling the types of matrix and also the volume fraction and distribution of the reinforcement; (2) metal matrix has excellent formability. The near-final molding of the metal matrix composite material can be obtained by a suitable manufacturing method. This is conducive to improving and expanding the working efficiency and scope of use of the heat sink materials; (3) relatively high thermal conductivity and tailorable CTE. This is of vital importance to enhance the performance and life cycle of electronic devices.

In the metal matrix composites, the type of matrix and reinforcement have a significant influence on the final properties of the composites. The properties of some materials are listed in Table 2-1. Al and Cu are the most common metals that are considered as the matrix because of their relatively high thermal conductivity, and the reinforcements are usually ceramic or other metals. In order to adjust the composites' thermal expansion, W, Mo, and Si are used as reinforcements, while they are not good for the high thermal conductivity of composites. SiC_p is considered an ideal reinforcement for fabricating heat sink material, which has been used in aerospace, such as Hornet fighter, typhoon fighter, etc [16]. However, the thermos-physical properties of SiCp have been developed to the limit [16, 17], but it cannot be applied to high-power electronic devices. Therefore, researchers have discovered new reinforcing materials. The latest advances in reinforcement of metal matrix composites are graphite [17], diamond, graphene[18], and carbon nanotubes[19, 20]. Chen and Huang [10] fabricate Al/Graphite composites by hot pressing, and its thermal conductivity along the distribution of graphite direction can reach to 783W/ (mK) but is quite low along the perpendicular direction. Anisotropic thermal conductivity of the graphite limits the metal-graphite composites that have high thermal conductivity in all directions and causes the poor heat dissipation capability of electronic devices. And it is the same problem for carbon nanotubes and graphene. Diamond is the substance that has the highest thermal conductivity in nature. Moreover, other properties of diamonds also attracted the attention of researchers, such as suitable CTE, low density, and isotropic thermo-physical properties. Thus, diamond particles reinforced metal matrix composites are the next generation heat sink materials.

Table 2-1 Properties of some metal and composite materials [21-23]

Material	**Thermal conductivity (W/(mK))**	**Coefficient of thermal expansion ($\times 10^{-6}$)**	**Density (g/cm^3)**
Al	234	23.6	2.7
Cu	400	17.8	8.9
Invar (Fe58Ni42)	11	1.3	8.1
Kovar (Fe54Ni28Co18)	17	5.9	8.3
Cu/68vol%SiC_p	270	10.5	5
Cu10W90	209	6.5	17
Cu10Mo90	108	7	10
Al30Si70	120	6.2	2.4

2.3 Metal/diamond composites

2.3.1 Introduction of diamond

Diamond is composed of carbon atoms, which is an allotrope of graphite. The characteristic of the diamond structure is the regular octahedral crystal, the carbon atom is located at the top corner, and center of the tetrahedron and has a high degree of symmetry. The common crystal shapes of the diamond are octahedron, diamond dodecahedron, cube, tetrahedron, and hex-octahedron. Diamond is the hardest substance and can withstand high temperature, is widely used in the fabricating of artwork and cutting tools. Besides, the diamond is a metastable phase of carbon. The unique structure, as shown in Figure 2-1 [24], is specifically described as a three-dimensional network structure with an equiaxed crystal system.

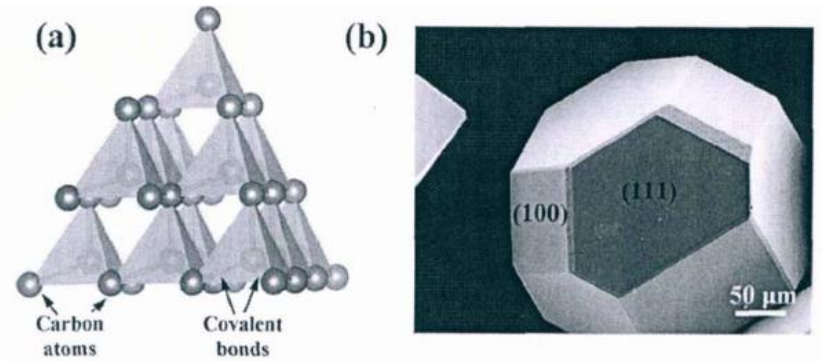

Figure 2-1 (a) Crystal structure of the diamond; (b) a diamond morphology [24]

In the structure of the diamond, each carbon atom has four closest neighbors and twelve sub-nearest neighbor atoms, and there are eight carbon atoms in each cell. All the outermost atoms can form

bonds and there are no free electrons in the crystal, this is because each carbon atom will generate four covalent bonds, and the length of each bond is 0.15nm and the angle between each other is 109°28´, with four closest atoms by sp^3 hybridizing. This characteristic of the diamond structure makes itself have high hardness and stability. To keep diamond at a stable state and low free energy, the dangling bonds of carbon atoms in diamond structure tend to attract gas or connect with others. This leads to diamond hardly react with other metals or alloys in common situations.

Diamond particles used in my research are Hexagon-octahedron, it is composed of six hexagons facets and eight octahedron facets, called diamond-{100} and diamond-{111} facets respectively. The intersection angle between different facets is different. Moreover, the surface energy of diamond-{111}and diamond-{100} facets are 5×10^{-5} J/cm^2 and 8×10^{-5}J/ cm^2 , respectively [25]. Because of the low surface energy of the diamond-{111} facet, the atoms on the diamond-{111} facet are not as active as that on the diamond-{100} facet. Diamond has lots of excellent physical and thermal properties, such as high hardness and elastic modulus, having the highest resistance to plastic deformation compared to any other materials, high thermal conductivity (the highest in nature), low thermal expansion coefficient, and the fundamental properties of diamond are listed in Table 2-2. Therefore, diamond is a good material for heat sink materials. With the development of fabrication technology, the price of artificial diamond is getting cheaper and affordable, which makes its wide application practical.

Table 2-2 Fundamental properties of diamond [26]

Density (g/cm^3)	3.52
Hardness (GPa)	50-100
Fracture toughness (MPa.m$^{1/2}$)	3.4
Young's modulus(GPa)	1000-1100
Poisson's ratio	0.07
Tensile strength (MPa)	1050-3000
Compression strength (GPa)	9
Thermal conductivity (W/mK)	600-2000
Thermal expansion coefficient (10^{-6}/K)	1.5-4.8

2.3.2 Fabricating process of metal/diamond composites

Fabricating processing has a significant influence on the microstructure and interface structure of composites. The fabricating process can be divided into solid-phase methods and liquid-phase methods. The solid-phase methods include powder metallurgy, vacuum hot pressing, and hot forging and spark plasma sintering, etc. The liquid methods are including high-temperature high-pressure method, pressure infiltration, and pressure-less infiltration.

The temperature prepared by the solid-phase method is generally lower than the melting point of the base metal. It is usually completed by applying pressure on the specimen. The solid-phase method is low cost, high efficiency, and suitable for large-scale production. For liquid-phase methods, the fabricating temperature is always higher than the melting point of the metal matrix, thus, the gaps between diamond particles will be infiltrated with the molten metal liquor, and the composite materials can be obtained after the metal solidification. The most widely used method is infiltration, however, its energy cost is much higher because of the need for higher manufacturing temperatures than that of the solid-phase methods. And also, it is quite difficult for filler to distribute uniformly in the composite, especially for composites that have a low volume fraction of reinforcement [27]. This study will fabricate copper/diamond composites by the solid-phase method. Therefore, only introduce some solid-phase methods below.

Powder metallurgy

Powder metallurgy is a traditional processing technique to prepare a metal matrix composite. The flowchart of preparing composite materials by powder metallurgy method is shown in (Figure 2-2). The main process is mixing metal powder and diamond particles in a certain proportion. The mixed powder will be loaded into a mold by compressor injection. After that, the metal matrix composite is fabricated by sintering under a protective atmosphere. The advantage of this approach is that it can control physical properties accurately by adjusting the volume fraction of metal matrix, reinforcement, and adhesive. Besides, it is suitable for mass production because the required temperature is relatively low which can decrease the probability of phase transformation from diamond to graphite, and also low equipment requirements. However, the relative density of the fabricated composites is quite low because of the existence of high porosity in the composites.

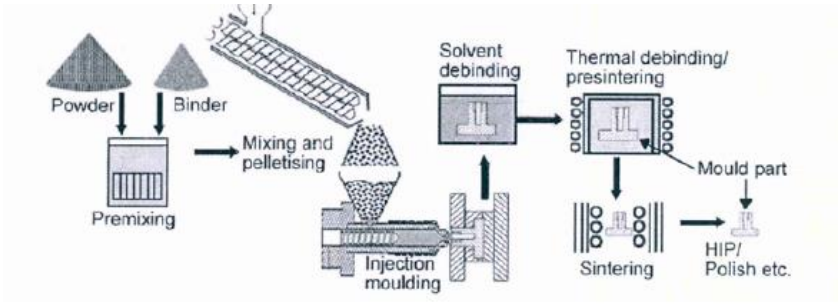

Figure 2-2 Schematics of powder metallurgy [28]

Spark plasma sintering

In spark plasma sintering (SPS), a high pulse current is applied onto powder particles under a vacuum atmosphere and a small uniaxial pressure to discharge pulsed plasma between the powder particles, which generate localized high temperatures to sinter the powder. The diagram of SPS is shown in Figure 2-3. A local high temperate state is generated at the contact points between particles, which leads to evaporation, cleaning, and melting on the surface of the powder particles. In the SPS process, a sintered neck can be formed between the powder contacts, and the powders are consolidated in a relatively short time. Moreover, it is easy to control the composition of composites. Abyzov [29] fabricates Cu/W-diamond composites by SPS, they study the effect of diamond coating on the properties of composites, the thermal conductivity is 720W/ (mK). However, Chu [27] finds that SPS cannot densify the composite due to bad connections between the matrix and the diamond when the diamond particles are in large size. This leads to the poor thermos-physical properties of the composite.

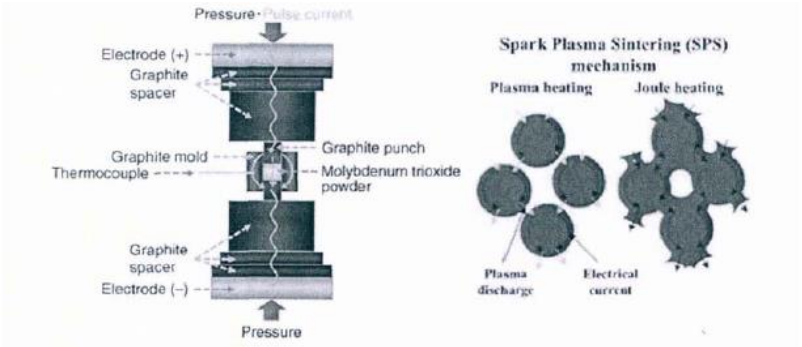

Figure 2-3 Schematic diagram of SPS [24]

Vacuum hot pressing

Hot pressing sintering is one of the powder metallurgy methods. The diagram of vacuum hot pressing shows in Figure 2-4. The main procedure is pressing the mixed powder in a graphite die to form composites with high densification under high temperatures and a vacuum atmosphere by

using the uniaxial pressure. This process would enable to press and sintering at the same time, which will shorten the sintering time. The high temperature can lead to the chemical reaction between the additional elements and the diamond particles which will improve the interfacial bonding strength at the interface of the composite, and the applied stress will reduce the porosity of the final product so that getting the composite material with high densification. Moreover, comparing with the SPS method, the relatively long holding time can ensure sufficient diffusion between the metal particles and the filler particles, which helps to optimize the chemical affinity at the interface in the composite material.

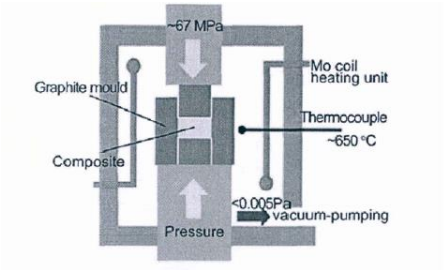

Figure 2-4 Schematics of vacuum hot pressing [30]

Powder hot forging

Hot forging is also one of the methods of powder metallurgy methods. The schematic of the hot forging is shown in Figure 2-5. The process of hot forging includes powder mixing, powder compaction, and compact forging. The powder mixture is pre-cold-pressed before forging to gain a composite compact with high relative density and strength. After that, the compact loaded in a steel can is heated to the desired forging temperature and then forged into a pancake in a protection atmosphere using an induction furnace. Hot forging is a metalworking process in which the metal is plastically deformed above their recrystallization temperature, which allows the material to retain its deformed shape as it cools. The grain structure of the metal is improved during the hot forging process, which leads to the forged composites will be tough and strong. Besides, forged materials always have good ductility, excellent surface quality, and flexibility [31]. As an alternative method, hot forging is very cost-effective and it has been proved that hot forging is a feasible method to produce copper/diamond composites with acceptable mechanical thermos-physical properties for heat sink materials [32]. Therefore, our experiment prefers to use this process to fabricate copper/diamond composites.

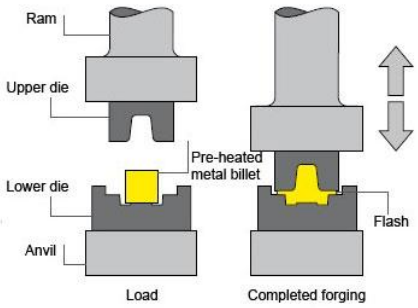

Figure 2-5 Schematics of Vacuum hot forging [33]

2.4 Metal/diamond composites

Diamond has excellent thermos-physical properties, such as high thermal conductivity, and relatively low thermal expansion coefficient, therefore, diamond particles can be used to reinforce other metals to fabricate the composite materials with high thermal conductivity. Au, Ag, Al, and Cu are the widely used metals in the current researches.

Ag/diamond composites

Ag has the highest thermal conductivity among these metals, which is 429W/ (mK), and it is quite stable in air. Tang [34] produces Ag/diamond composites by SPS, using Cr-coated diamond to increase the connection between matrix and diamond particles. The results show that Cr can improve the interface, and the thermal conductivity can be 695 W/ (mK) as the diamond volume fraction is 60%. Edtmairer [35] studies the effect of the chemical state of the diamond surface on the thermal conductivity of the Ag-Si/diamond composite. It reports that diamonds can be oxidized and form more C-O and sp^2 after pretreatment on diamonds. The thermal conductivity of the Ag-3wt%Si/diamond composite is 960W/ (mK) at 150K. His study finds that diamond surface treatment is a good method to improve the thermal conductivity of the composite. However, the cost of Ag is very high, it is not affordable and practical to use Ag/diamond composites.

Al/diamond composites

Aluminum has a relatively high thermal conductivity and much cheaper than Ag, which has attracted more attention. Long[36] fabricates Al/diamond composites by vacuum hot pressing sintering. The thermal conductivity of composites is 327W/ (mK), CTE is 9.3×10^{-6} K^{-1} as the volume fraction of diamond is 50%, and sintering pressure is 60MPa. Tan [37] also finds that there are optimum values of sintering temperature, pressure, and time. At that point, the thermal conductivity can reach the highest. The highest value was 567 W/ (mK), as diamond volume fraction is 55% at 650℃ and 67MPa for 90 min. Al/diamond composites have low density and high

thermal conductivity, however, Al_4C_3 will be generated at the interface, it is easy to decompose into Al $(OH)_3$ with water to reduce the composite's thermal conductivity, thus leading to the composite is not stable while working under normal air environment.

Cu/diamond composites

Copper is an alternative matrix, the thermal conductivity of Cu is a bit lower than that of Ag, but it is quite economy friendly. The barrier for Cu/diamond composites is the poor chemical affinity between the copper and the diamond. This limits the prepared Cu/diamond composites have high thermal conductivity. Therefore, interface modification is the most important issue researchers faced. The method of diamond surface alloying and Cu matrix alloying helps improve the chemical affinity between the copper and the diamond. Schubert [38] adds alloy elements into the copper matrix to study the effect of different elements on the thermal conductivity of composites. It shows that the alloying elements can effectively improve the interfacial bonding of the composite material, thereby enhancing the thermal conductivity of the composite material. The thermal conductivity of Cu-0.3wt%B/diamond (40vol %) composite material is up to 500W/ (mK). And the thermal conductivity reaches 639W/ (mK) for the Cu-0.8wt%Cr/diamond composites. Abyzov [29] prepares Cu/diamond composites with W-coated diamond particles by SPS, the thermal conductivity of composites is 720W/ (mK).

The thermal conductivity of Cu/diamond composites, prepared by SPS or other liquid methods, can reach a relatively high value. Hot forging can be an alternative cost-effective and feasible method for the fabrication of Cu/diamond composites. Besides pursuing good thermal properties of the composite, a deep study on how to control properties of the composite needs to be investigated in the future.

2.5 Research barrier in Cu/diamond composites

The high-quality interface between the copper and the diamond contributes to the excellent thermos-physical properties of copper/diamond composites, which can improve the chemical affinity between the matrix and the filler. Therefore, the study of the interface in copper/diamond composites is essential for the research of copper/diamond composites.

2.5.1 Interface of Cu/diamond composites

The interface of copper/diamond composites plays an important role in the thermal conductivity of the composites. The wetting angle between copper and diamond is 145° at 1150℃, which means non-invasive. The poor chemical affinity of copper on the diamond surface is determined by the valence electron arrangement of copper. From the valence bond theory, it can be seen that the valence electrons of carbon atoms enter the empty *d* orbitals of the transition metal to form metal carbides. The more empty *d* orbitals, the stronger bonding can be formed between the carbon atoms and the metal atoms and there will be no chemical reaction between carbon atoms and metals without empty *d* orbitals. The electron arrangement of Cu is $3d^{10}4s^{1}$, which indicates that the *d* orbitals are full of electrons, thus, the metal carbides cannot form at the interface of copper/diamond composites, resulting in chemical inertness between copper and diamond. Thus, weak bonding in Cu/diamond composites causes poor thermos-physical properties. In order to maximize the properties of both matrix and diamond, a transition layer is always introduced to enhance the connection of the diamond and the copper.

2.5.1.1 Theory of interface

The interface in the composite is a boundary area between the matrix and the reinforcement, where has different chemical compositions, elastic modulus, thermal expansion coefficient, and thermodynamic properties from the matrix and the reinforcement phase [39]. In metal-based composite materials, the interface area significantly affects the thermal conductivity of the composites. An ideal interface can make the metal matrix and the reinforcing phase tightly connected, realize the effective transfer of performance between the phases, and ensure the effective play of the excellent performance of the matrix and the reinforcing phase in the composite material. In addition, the interface can achieve continuous and effective load transfer in the composite. The interface area should also suppress the propagation of cracks in the composite material, reduce the stress concentration at the interface, and improve the overall strength, toughness, and other mechanical properties of the composite material. Finally, the interface has the effect of absorbing

and scattering electrons, photons, and other carriers, which will change the intensity of heat, light, sound, and vibration when passing through the interface. This feature can be used to adjust the composites' functions according to the application.

The interface of Cu/diamond composite is the main barrier for the research of heat dissipation materials because it significantly affects the thermal conductivity of the composite. Most of the current reports about copper/diamond composites did not explain how to control the thermal conductivity of composites by adjusting the interface. They simply obtain the relationship between the thickness of the interface and thermal conductivity of composites by varying coating thickness or calculating thermal conductance from the known thermal conductivity by different modes like Maxwell, or Hasselma-Johnson [4]. Time-domain thermo-reflectance (TDTR) is widely used in the nanostructure of Cu/diamond composites to know the relationship between interface and thermal conductance [40] in the researches. However, directly adjusting the microstructure or phase composition of the interface to control the thermal conductivity of copper/diamond composites has not yet been achieved, this limits the present research on the Cu/diamond composites for efficient heat sink materials. Therefore, it is crucial to understand the interface characteristics for further improving the Cu/Diamond composite's thermos-physical properties.

2.5.1.2 Phonon scattering

Phonon scattering can be explained as phenomena that can lead to a change in direction, momentum, or energy of the phonon [41]. In copper/diamond composites, phonons are the main carrier for heat transport that affects thermal boundary conductance at the interface because researchers normally ignoring the function of the electrons. Phonon is a quantum of lattice vibration.

Generally, the interface of Cu/diamond composite is a metal carbide layer, which is ceramic. The main source of heat transport of ceramic mainly depends on the lattice vibration. When lattices are subjected to external force, phonons will be released as the "carrier" for heat transport. To get a better understanding of the concept of the phonon, the relationship between the lattice and the phonon is usually represented by a spring-mass diagram [42] (as shown in Figure 2-6). The propagation of the heat and load in the composite material propagates is reached by the phonon transport. A material where the phonons serve as heat carrier can travel without any hindrance will lead to better heat transport, which means composites are with high thermal conductivity [43]. Actually, phonons are always scattered when encountered with the interface or grain boundaries. Phonon scattering is the main source for limiting the thermal conductivity of composites, as it

results in the generation of thermal resistance at the interface of the composite. In copper/diamond composites, more energy is required for phonons to pass through the carbide interface to break the perfect lattice bond due to the lattice mismatch and the existence of the tiny grain boundaries that produced by the breaking of perfect lattice bonds during the deposition of carbide film between the copper and the diamond. This will lead to phonons scattering, which can reduce the heat dissipation efficiency and lead to the low thermal conductivity of the cooper/diamond composite. Thus, reducing the phonon scattering is the key to improve the thermal conductivity of the composite system.

Due to the complicated relationship between interface and thermal conductivity, thermal boundary conductance is always used to measure interface behaviors, which is more visualized than thermal conductivity. Thermal boundary conductance can describe the quantities of phonons transfer across the boundary, where will cause a temperature gradient in two solid materials. Thus, the value of thermal boundary conductance is intimately related to the morphology and thickness of the interface carbide layer, it is investigated that the high thermal boundary conductance is associated with a thin and continuous interface carbide layer [4]. Understanding the thermal boundary conductance can help to design the interface of Cu/diamond composites so that control the thermal conductivity of the bulk material. Two macroscopic theories to model the thermal conductance, one is the acoustic mismatch model (AMM), and the other one is diffusion mismatch theory (DMM). AMM model assumes that there is no phonon scattering at the interface which is used to calculate the acoustic impedance difference at the boundary of two different materials. AMM does explain the interfacial thermal conductance well at the low temperature due to few phonons are considered in the thermal transfer process. Whereas the DMM model assumes that all the phonons at the interfaces are completely elastic scattered, which means there is no energy dispersion after scattering. It also estimates the transmission probabilities of the phonons at the interface employs differences in phonon density of state. Due to the assumption of complete scatterings, the thermal conductivity that calculated by DMM is always larger than the experimental values, which normally works better in high-temperature regimes [31]. DMM model is widely used in current works due to the thermal conductivity of the theoretical is closer to the experiment results than that from AMM.

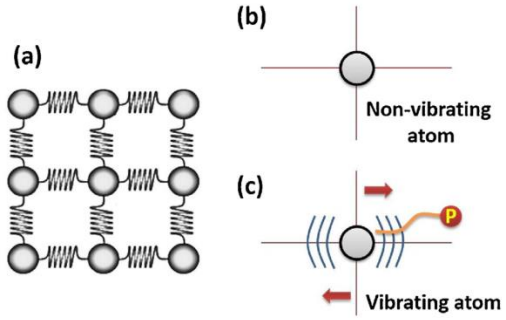

Figure 2-6 Diagrams of lattice and phonons [42]

2.5.2 Interface modification of copper/diamond composite

In the previous section, it has been known that the interfacial characteristic of diamond/metal composites has a very important influence on the stress distribution, load conduction, heat transmission, and mechanical properties in the composites. Therefore, optimizing the interface structure of composites is an important method to improve the performance of composites. In order to improve the interfacial bonding and overall performance of composite materials, the common approaches used are (1) optimizing advanced fabrication technology, (2) metal matrix alloying, and (3) diamond surface metallization.

2.5.2.1 Metal matrix alloying

Adding alloy elements to the metal matrix can change the chemical affinity, and also inhibit the interface reaction between the metal matrix and the diamond. The second metal phase in the metal matrix should be a carbide-forming element, thereby, the formed metal carbides can improve the interfacial bonding of the composite. This is a relatively economical, simple, and effective interface modification method. However, the alloying elements will decrease the thermal conductivity of the metal matrix, resulting in a decrease in the thermal conductivity of the composite material.

Schubert [44] produces Cu-0.8wt%Cr/diamond composites by pulse plasma sintering. The experiment shows that the thermal conductivity of the composite was 640W/ (mK) as the volume fraction of the diamond was 50%. Observation through the two-phase interface reveals that the alloying element Cr added to the Cu matrix reacted with the diamond at the interface to form a layer of Cr_3C_2 (about 100 nm thick). The high thermal conductivity is attributed to the addition of the Cr element, which effectively improves the chemical affinity between the matrix and the diamond, and the forming of the Cr_3C_2 promotes the interfacial bonding of composite materials. Chuang[45] studies the effect of Cu-Ti on the interfacial structure and thermal conductivity of Cu/diamond

composites. The results reveal that TiC is formed by a chemical reaction between titanium and diamond. The formation of the TiC improves the chemical affinity between copper and diamond. The highest thermal conductivity of Cu-2at%Ti/diamond composites is 608W/ (mK) in Chung's study. Chu [46] and Bai [47] prepare Cu-Zr/diamond and Cu-B/diamond composites, their experiment agree that the addition of a second metal phase in the copper matrix is beneficial for preparing Cu/diamond composites with high thermal conductivity. However, they find that the thermal conductivity of composites increases first and then decreases with the increase of the Zr/B elements. The thermal conductivity of Cu-1.2wt%Zr/diamond and Cu-0.3wt%B/diamond composites are 615W/ (mK) and 868W/ (mK) respectively. This indicates that the thermal conductivity of the copper/diamond composites can be improved by metal matrix alloying, but the quantity of the addition elements should be in an appropriate amount. When the content of alloy elements is too small, the amount of carbides formed has little effect on the composites. When the content of the added alloy is too much, excessive carbides will be formed, reducing the overall thermal conductivity of the composite material.

2.5.2.2 Diamond surface metallization

Diamond surface metallization is to coat the diamond surface with alloying elements to improve the chemical affinity between the substrate and the diamond. The formed metal carbide layer is more continuous and denser by diamond surface metallization comparing with the metal matrix alloying method. The introduction of a continuous interlayer can effectively prevent the non-uniform nucleation of the reaction products at the interface. By adjusting the thickness of the coating on the diamond surface, the deterioration of the alloy element on the performance of the composite material can be reduced. Many researchers suggest that diamond metallization with the alloying element contributes a significant improvement in the thermal conductivity of Cu/diamond composites.

In Kang et al' s experiments [48], the thermal conductivity of the composite fabricated from a mixture of WC-coated diamond particles and copper powder is high enough to 658 W/ (mK). Besides, they also use Mo_2C-coated, Ti-coated, and Cr-coated diamond to fabricate copper/ coated-diamond composites, respectively. The thermal conductivity of the Cu/Mo_2C-diamond, Cu/Ti-diamond, and Cu/Cr-diamond composites are is 608W/ (mK), 514 W/ (mK), and 562 W/ (mK), respectively. These results suggest that WC coating is the best one to optimize the interface, following by Mo_2C, Cr_7C_3, and TiC. Wang et al. [49] prepare Cu/Zr-diamond and Cu/Ti-diamond composites by gas pressure infiltration. The result shows that Cu/Zr-diamond composite can obtain

the highest thermal conductivity, 735W/ (mK), when the thickness of Zr on the diamond is 47nm. While the thickness of Ti on the diamond is 220nm, the highest thermal conductivity of Cu/Ti-diamond composites is 811W/ (mK), and they think the thermal conductivity of the Cu/Ti-diamond composites can also be increased by decreasing the thickness of Ti. These results conclude that Ti coating is easier than Zr in changing the properties of the composites.

Cheng et al [50] fabricate copper/diamond, using Ti-coated diamond and Cr-coated diamond composites under the same processing to explore the relationship between the diamond volume fraction and thermal conductivity. The thermal conductivity of the composites decreases with the increasing of diamond volume fraction, this is due to the existence of voids between diamond and copper, as shown in Figure 2-7. After coating diamond particles with Ti or Cr, the thermal conductivity of composites is improved significantly. This is attributed to the Ti-coating and Cr-coating improve the linkage between copper and diamond. In addition, it is clear to see that regardless of the diamond volume fraction, the thermal conductivity of the Cu/Cr-coated diamond composites is higher than that of Cu/Ti-coated diamond composites. This means the interface formed via reacting with Cr has more significant effects on decreasing the interface resistance between the copper and the diamond than that is formed by the reaction with Ti.

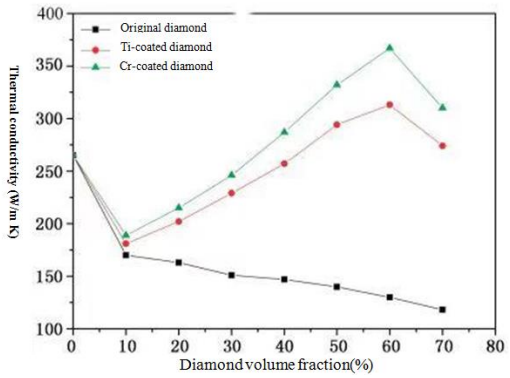

Figure 2-7 Relations between volume fraction of diamond and thermal conductivity of composites [50]

In all, the metallization of the diamond surface is able to help form a continuous, dense, and thickness-controllable interface between the copper and the diamond in the fabricated composites, thereby improving the thermal conductivity of the composite material. Moreover, varied metallization alloying elements have different degrees of influence on the thermos-physical properties of the composite material.

2.5.3 Consideration of the Interface characteristics

Generally, in copper/diamond composite materials, the thickness of the interface, the size of the metal carbide particles at the interface, and the interfacial bonding between the interface and the copper or diamond should be considered. Furthermore, due to the different properties on the diamond-{111} and diamond-{100} facets, the properties of the diamond facets also need to be taken into account. During the fabrication of copper/diamond composites, the carbides interphase layer is obtained by the chemical reaction between the transition metal and the diamond, which can effectively improve the interface bonding of composite materials. However, the carbides phase has relatively lower thermal conductivity than the copper matrix and the diamond. Therefore, in order to maximize the contribution of the interface to the thermal conductivity of the composites, studying and characterizing the interface structure of composite materials is necessary, which is helpful to understand the interface reaction mechanism, and then guide the adjustment of the preparation process.

2.5.3.1 Size effects

Size effects, including the interface thickness and the grain size of the metal carbides particles, which has a significant influence on the thermal conductivity of the Cu/diamond composites. The size effect is related to the mean free path (MFP) of the heat carrier, which means that the thickness of the interface and the particle size at the interface can be adjusted according to the MFP of the phonons in a specific material. The research reveals that the thermal conductivity is only a function of the effective phonon MFP in the thin films, this is suitable in the nanoscale of the Cu/diamond composite[51]. MFP is the distance that phonons traveled before scattering. The larger the MFP, the higher the thermal conductivity of the composites. When the size of the interface is equal or smaller to the MFP, parts of the phonons will across one side of the interface and transfer to the other side directly without diffusivity, namely ballistic transport, with no scattering of these phonons[52]. Ballistic transport results in a temperature gradient which attribute to the phonon heat transport. When the film thickness is bigger than MFP, phonon scattering will occur. The surface of the carbide layer is one of the locations that phonon scattering occurs, thus, controlling the layer thickness is quite essential. The interface thickness plays an essential role in the thermal conductivity of composites which can be designed depends on the MFP in the material.

A previous study [53] explores the relationship between the thickness of the interface and the thermal conductivity of Cu/diamond composite. In this experiment, the authors fabricate composite by gas pressure infiltration. Four diamond samples are prepared with a Ti coating of 65nm, 220nm, 340nm, and 850nm, respectively. The highest thermal conductivity of Cu/Ti-diamond composite

reached 811W/ (mK) when using the diamond with the Ti coating thickness of 220nm. As a result, the thermal conductivity of the Cu/diamond composites shows an evident dependence on the thickness of the interfacial carbide layer. It is reported [51] that if ignoring the effect of the grain boundary and the diffuse boundary condition of the interface, the thermal conductivity of the composite will improve with the increase of the interface thickness. Ideally, when the phonons have completely elastic scattering through a rough surface, the thermal conductivity of the composite will not be reduced. But because the carbide layer has a certain thickness, which will decrease the thermal conductivity of the composites due to interface has lower thermal conductivity than the copper and the diamond. Thus, thick interface will decrease the thermal conductivity of the composite due to the thick interface has resistance for heat transport.

It states that getting a thin and continuous interface carbide layer is ideal for the Cu/diamond composites. It is not beneficial for obtaining copper/diamond composites having high thermal conductivity if the composite has a continuous and either thick or a thin non-continuous interface [4]. It is also not good for composites that have an extremely thin interface. There is also a critical thickness value of the formed carbide layer to reach the highest thermal conductance of the composite. If the film is extremely thin, the phonon will be scattered more than once [51]. In a previous study, researchers study on the Cu/diamond composite, their results prove that an extremely thin or thick interface is not good for the thermal conductivity of the composites [54]. A report shows the thermal conductivity of the Cu/Cr-diamond composites decreases from 787W/ (mK) to 633W/ (mK) when changing the thickness of Cr from 210nm to 150nm. Andrey M. uses SDB1085 diamond and copper powder to prepare Cu/diamond composites. The results reveal that when the thickness of the interface is lower than 50nm, coated-diamond is not affinitive with copper anymore [55]. The wetting angle increases dramatically to 90°. This is because as the thickness of the interface decreases, the continuity of the interface becomes worse. Another study produces Cu/Cr-diamond composites (100μm of 70vol% diamond), the study reveals the optimum interface thickness is between 0.4-0.6μm [56]. If the interface thickness is below 0.4 μm, it is hard to form a strong linkage between the copper and the diamond. And as the thickness of the carbide layer is thicker than 0.6 μm, the interface will detrimental to heat transfer due to its low thermal conductivity. The result suggests that the Cu/Cr-diamond composite with a formation of 0.5μm-thick Cr_7C_3 has a thermal conductivity of 657W/ (mK).

The grain size of the interphase layer has a more significant effect than the thickness of the interface [51]. Thermal boundary conductance is affected via grain boundary scattering. When the carbide film deposited on the diamond, it would form tiny grains due to the mismatch of the lattice which

increases the interface thermal resistance causing lower thermal conductivity of composites. It has a similar function as surface, it takes much energy and time for phonons to pass grain boundary and grain boundaries also shorten MFP of phonons by R (grain boundary scattering coefficient). This is a negative effect on heat transport. Therefore, large grains facilitate heat transfer in the composite. From their experiment, regardless of the situation of the surface, the grain boundary scattering starts to dominate as R becomes larger than approximately 0.3. This proved that the fine-grained structure exhibits a substantial contribution to the size effect.

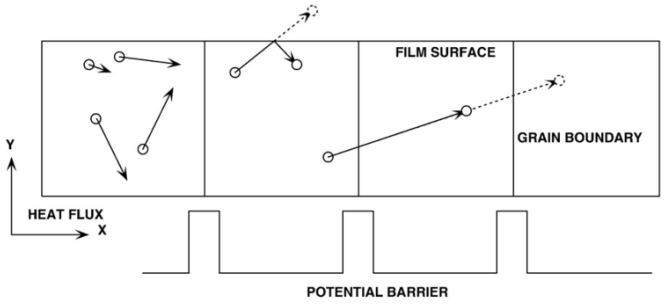

Figure 2-8 Schematic diagram of heat transport along a metallic film assuming parallel grain boundaries and that the heat flux is perpendicular to the grain boundaries [51]

The effective mean free path is determined by the thickness of the film and the size of grains, as shown in Figure 2-8 [51]. It also needs to notice that the grain size highly depends on fabricating processing parameters such as pressure, temperature, and holding time. Jianwei et al. [57] add element Ti(x=0.3, 0.5, 2.0wt%) into copper matrix by gas pressure infiltration. The results show that the size of the TiC carbide grows up as adding more Ti element. When x=0.3wt%, the fabricated composite has an optimized thermal conductivity of 752W/ (mK). And the size of the carbide is 200-300nm. It explains that the heterogeneous nucleation of carbides at the interface and the following preferential growth along with certain crystal orientation from diamond into the Cu matrix. Causing the reduction in thermal conductivity of copper. This is why thermal conductivity will decrease when x=2wt%. Interface thickness and grain size affect the thermal properties of composites in different stage regime. There should be a relationship between thickness and grain size. When they match each other well, thermal properties can be best. Finding this correlation is a hot topic in future studies.

2.5.3.2 Interfacial bonding

Thermal boundary conductance is enhanced in materials pairs with strong interfacial coupling, which influences the transmission probabilities [31]. As previously mentioned, matrix alloying or diamond coating can modify the low thermal conductivity of Cu/diamond composite caused by the

poor bonds between the copper and the diamond. This is because interfacial chemical bonding can be generated during the reaction between the diamond and the additional elements at the interface of the composite material. The generated interphase layer of Cu/diamond composite is usually a kind of ceramic, the main bonding in ceramic is covalent. Strong covalent bonds between different regions can maintain the stability of the system, which will reduce phonon scattering caused by lattice vibration. In general, the thermal resistance of a covalent bond through valence electron is about 10 times smaller than that of weak forces like the Van der Waals bond [42]. Therefore, researchers expect to establish a strong covalent bonding between the interface and the matrix or filler to provide an effective path for phonon transfer.

It is reported that large TiC carbide particles formed at the interface can improve the mechanical interfacial locking of the composites because TiC particles penetrated deeper into the copper matrix of Cu-Ti-diamond composites [57]. A similar conclusion is obtained from another report, Copper-tungsten-diamond composites are fabricated by vacuum sintering techniques. A tungsten layer is deposited on the diamond surface and following by a copper layer. The results show that the thermal conductivity of copper-tungsten-60vol%diamond composites is 661W/ (mK) [58]. The outstanding performance can be ascribed to the tungsten layer provides a good surface condition for copper deposition, which increases the bonding strength between the interphase layer and the copper matrix, and then leads to the high thermal conductivity of composites. In Clio Azina et al.'s [8] report, the effective thermal conductivities and heat transfers at the interphases of Cu(Cu-Zr)-D systems are investigated. In their study, the fracture pattern shows an intergranular fracture of the diamond, which confirms the strong bonds between the copper matrix and the diamond reinforcement. Comparing with Cu/diamond composites, the presence of ZrC interphases increases the thermal conductivities of the composite materials, which also confirms the strong bonding brought by the interphase layer. Zhang et al. [59] solve the interfacial debonding of copper/diamond composite by diamond metallization with Cr element. Their study verifies that increasing the interfacial bonding between the diamond and the copper is realized via the formation of different types of bonding at the interface in Cu/diamond composites. One is reaction bonding, caused by the chemical reaction between the diamond atoms and the additive Cr elements, which takes effect on the interfacial bonding between the diamond layer and Cr_3C_2 interphase layer. And the other is diffusion bonding which has an effect on interfacial bonding between the carbide layer and copper matrix.

In short, interfacial bonding can indeed improve the thermal conductivity of the composites, in particular, forming metal carbide layers at the composites' interface which are seen as a bridge to

provide more phonons heat transfer channels. However, some other reports think it is not wise to focus on increasing interfacial bonding. Andrey [60] prepares Cu-tungsten-diamond composites by PPS. In their study, using WC coating to replace the W coating to improve adhesion at the interface between the copper and diamond, it is surprising the thermal conductivity of the diamond-tungsten-copper composite decreases from 690 W/ (mK) to 550 W/ (mK). This suggests that the thermal conductivity is not always linearly rising with the increasing of the interfacial bonding. A small number of transition elements dissolving in the copper matrix and setting covalent bonding between the interphase layer and the diamond can strengthen the bond connection between the copper and the diamond. However, too much interfacial bonding between the interphase layer and the copper or the diamond, which means more metal carbides formed at the interface in the composite, will reduce the thermal conductivity of the composites, because the metal carbides have relatively low thermal conductivity and they can speed up the transformation from the diamond to the graphite phase [51]. In addition, the increasing interfacial bonding will gradually separate the copper matrix and the diamond, which results in bad thermal-physical properties of composites. Therefore, the best scenario is the formed carbide particles do not connect with each other but embed in the copper matrix. This will eliminate the acoustic mismatch between the copper and the diamond, and also have a minimum effect on the copper matrix. The expected interfacial bonding in CuZr/diamond composites is shown in Figure 2-9 [49].

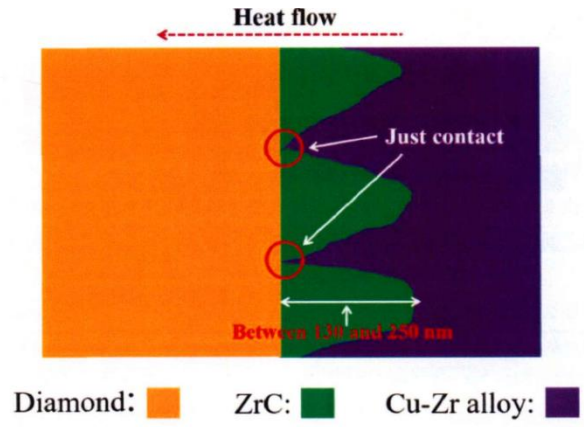

Figure 2-9 Ideal interface structure in Cu-Zr/ diamond composites [49]

2.5.3.3 Selection of interfacial bonding on diamond facets

The common diamond is in the form of hexagon-octahedral, which is comprised of {100} and-{111} facets. Because diamond-{100} facets have higher surface energy than that of the diamond-{111} facets, this results in forming a carbide with different morphology on the diamond facets.

Selection interfacial bonding is commonly used to explain the distinct morphology on diamond-{100} and -{111}facets. The selection interfacial bonding is firstly reported by P.W. Ruch et al. in diamond/Al composite as early as the year 2006 [61], the authors investigated the interfacial reaction of W-coated diamond particles after annealing. The results show that the selective interfacial bonding on the W-coated diamond surface is related to the atomic arrangement and chemical state of the diamond. From the microstructure analysis, the tungsten atoms prefer to react with the carbon atoms that on diamond-{100} facets and there are some micro-cracks between the copper matrix and diamond-{111} facets, which does not contribute to the thermal conductivity of composites. To modify this situation, authors use the ion beam bombardment pretreatment to suppress this reacting selection and diamond-{100} and -{111} facets, which is a way for diamond surface modification to change the reaction activity of the carbon atoms.

In another similar report, diamond/Al composites are fabricated by GPI methods [62]. Pre-annealing is used to eliminate the anisotropic reaction on diamond different facets during fabrication. The results show that the thermal conductivity of Al/diamond composites increases to 710 W/ (mK) from 540 W/ (mK) by increasing pre-annealing time on diamond particles. The pre-annealing result reveals that the transformation from sp^3 to sp^2 carbon transformation is preferential on diamond-{111} facets during pre-annealing and the authors think the amorphous carbon contributes to the interfacial reaction between the aluminum and the diamond. However, an opposite conclusion gained from Justyna Grzonka [63], who prepares diamond/Al composites by Pulse Plasma Sintering at 900°C. The results show that there is a strong graphitization on the diamond-{100} facets and the coverage rate by chromium carbide layer on diamond-{111} facets is higher than that on diamond-{100} facets. They explain that as the temperature is higher than 227°C, the chromium atom is more likely to react with diamond than graphite.

In summary, diamond-{111} and -{100} facets have different properties, more evidence proves that it is much easier to modify diamond-{100} facets than that of -{111} facets, but the opposite results are also gained from the previous experiments. This is because the selective interfacial bonding is related to the composites' producing parameters such as temperature, which has different effects on the chemical state of diamond-{111} and -{100} facets. The surface condition of the diamond is critical for carbide forming, and studies have found that pre-treatment on the diamond surface is an effective way to eliminate or decrease the effects of selection interfacial bonding of diamond facets during composite fabrication.

2.6 Research significance and objectives

From the extensive literature review, we know that the copper matrix has a very high thermal conductivity and a wide processing temperature range, and diamond has excellent thermos-physical properties. Therefore, copper/diamond composite materials is possible to have excellent thermos-physical properties (high thermal conductivity and tailorable coefficient of thermal expansion coefficient), and can be used as good heat sink materials for high-power electronic devices. However, the high thermal conductive Cu/diamond composite is dependent on the interface characteristics, which is affected by the fabrication process and types of carbide forming elements added. Currently, it significantly lacks a deep understanding on how the interface characteristics influence the thermal conductivity of Cu/diamond composites, and it is also necessary to well comprehend the affecting mechanisms of the interface formation in fabricating Cu/diamond composites to optimize the fabrication process for producing high thermal conductivity Cu/diamond composites.

Our research group developed and initiated a cost-effective process of fabricating copper/diamond composites and has successfully fabricated Cu-55vol%diamond composites with high thermal conductivity (up to 550W/ (mK)). This thermal conductivity value is higher than that of most reported copper/diamond composites fabricated with the similar range of diamond particle size. To advance the understanding on the copper/diamond composite's interface formation, and its affecting mechanisms and influence on the resultant composite's thermal conductivity, we will investigate how different types of interface are formed during hot forging and how the interface microstructure evolves and influences the composite's thermal conductivity. The specific research tasks are listed below:

(1) Modify the characteristics of the Ti-coated diamond by pre-annealing at various temperatures and analyze the effect of annealing temperature on the phase constitutions and microstructure of both diamond-{100} and -{111} facets, respectively;
(2) Prepare Cu/55vol%Ti-diamond composites from the mixture of annealed Ti-diamond particles and pure copper by hot forging at 800℃, and characterize the morphology and phase constitutions of the forged composites and the diamond particles that are extracted from the fabricated composites, to determine the interface evolution during the composites' fabrication;
(3) Using the same pre-annealing (1) and fabricating processes (2) to prepare Cu/55vol%W-diamond composites and evaluate the effect of different carbides forming metals on interface microstructures and thermal conductivity of the fabricated composites;

(4) Fabricate Cu/Ti-diamond composites from the as-received Ti-coated diamond particles by following different fabrication methods, and investigate the effect of fabricating methods on interface microstructures and thermal conductivity of the fabricated composites.

3 Experimental

3.1 Material preparation

1) Diamond particles:

   The high-quality synthetic diamond powder (MBD8), with an octagonal shape, is supplied by Henan Huanghe Whirlwind Co., China. It has two different facets on each diamond particle, denoted as diamond- {100} and -{111} facets. Generally, the thermal conductivity of diamond is up to 2000W/ (mK), due to the presence of nitrogen impurity of commercial diamonds reduce the diamond's thermal conductivity, and the estimation of diamond used in this research is about1500W/ (mK). Diamond particles are deposited with titanium and tungsten coating by magnetron sputtering, respectively. And the thickness of the titanium/tungsten coating on the diamond surface is about 50nm thick (measured by the gravimetric method by manufacturer). After the deposition, the particle size of the coated-diamond particles is about 70-80μm.

2) Copper

   Copper is used as the metal matrix for this experiment, supplied by Aldrich Company, NZ. The purity of the metal copper is more than 99.7% and its particle size is less than 45μm.

3.2 Experimental procedures

1) Pre-annealing of coated-diamond particles

Before mixing with the copper powder to make copper/diamond composites, the Ti/W-coated diamond particles were encapsulated in quartz tubes with a vacuum of 1×10^{-5} Pa first and then annealed at the desired temperature for holding 30 minutes, and the heating rate is 5℃/min. After that, the encapsulated diamond powders were furnace cooled down to room temperature. The detailed pre-annealing parameters for the coated-diamond diamond powders are listed in Table 3-1 and the process of pre-annealing of the encapsulated diamond powder is shown in Figure 3-1.

Table 3-1 Pre-annealing parameters for the encapsulated specimens

Sample	Heating rate (℃/min)	Temperature (℃)	Holding time (min)	Cooling
Ti-coated diamond	5	700/800/850/900/950/1050	30	furnace cooling
W-coated diamond	5	700/800/850/900/950/1050	30	furnace cooling

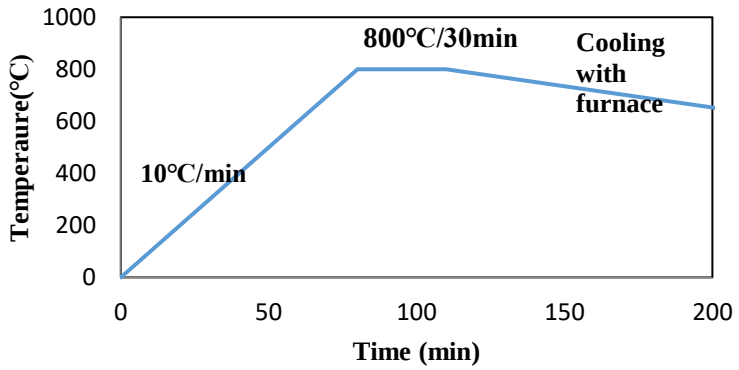

Figure 3-1 Pre-annealing of coated-diamond (800℃)

2) Fabrication of Cu/diamond composites

The copper/diamond composites with a nominal composition of copper/55vol%diamond was weighted first, and then the powder mixture of copper and the pre-annealed coated-diamond particles were blended in a V-type blender at 60rpm for 90mins. The powder mixture of the copper and the pre-annealed coated-diamond were mechanically pressed into a compact with a dimension of 12mm in height and 9mm in diameter or 37mm in height and 30mm in diameter. Then the compacts were filled in a specific steel can to hot-proceed into solid copper/55vo%diamond composites. Two processing routes were followed. In route one, the 9mm-diameter compact was located in a steel can to heat up to 800℃ and forged into a pancake in an argon atmosphere. After that, the forged pancake was slowly cooled down to room temperature. In route two, the 30mm-diameter compact was vacuum sintered at 800℃ for 2h. The heating process in a vacuum sintering furnace can divide into three stages, the composite was heated to 400℃ and then increased to 800℃, and the heating rate was 10℃/min. The pre-set program could start automatically after the furnace vacuum is low enough. After sintering, the sample was furnace cooling with the furnace to

room temperature. Then, the 30mm-diameter sintered composite was located in a steel can and hot forged at 800℃ following the process of route one. In Chapters 4 and 5, Cu/Ti-diamond composites and Cu/W-diamond composites were fabricated following route one. In Chapter 6, Cu/Ti-diamond composites were prepared following route two by different methods (vacuum sintering, and the combination of vacuum sintering and hot forging). The hot forging and vacuum sintering facilities are shown in Figure 3-2 and Figure 3-3, respectively. The details of the processing parameters are listed in Table 3-2.

Table 3-2 The fabricating parameters for Cu/Ti (W)-diamond composites

Samples	**coated-diamond annealing temperature (℃)**	**Heating rate (℃/min)**	**Holding time (min)**	**Cooling rate**	**Powder compact Vacuum sintering (℃/h)**	**Powder compact Hot Forging temperature (℃)**
Ti-800-Cu/Dia	800	5	30	furnace cooling	-	800
Ti-900-Cu/Dia	900	5	30	furnace cooling	-	800
Ti-1050-Cu/Dia	1050	5	30	furnace cooling	-	800
W-900-Cu/Dia	900	5	30	furnace cooling	-	800
W-1050-Cu/Dia	1050	5	30	furnace cooling	-	800
W-0-Cu/Dia	-	-	-	-	-	800
Cu/Ti-Dia-VS	-	-	-	-	800/2	800
Cu/Ti-Dia-VSHF	-	-	-	-	800/2	800

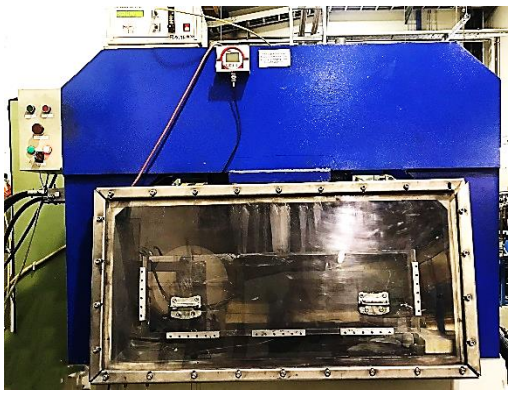

Figure 3-2 Hydraulic press for hot forging

Figure 3-3 Vacuum sintering furnace

3.3 Property testing

3.3.1 Materials characterization and analysis

1) Microstructure

Scanning electron microscope (SEM, HITACHI, S4700), equipped with EDS (Thermo Noran, accelerating voltage 20kV), was used to characterize the morphology of pre-annealed diamond particles and the fabricated copper/diamond composites and the diamond particles extracted from the fabricated composites. When observing diamond particles, it is necessary to spray gold on the diamond surface because the diamond is not conductive and the discharge phenomenon is serious.

The methods for preparing SEM samples to observe the composites microstructure and diamond morphology are, (1) the bulk Cu/diamond composites were ground with abrasive papers coded as 320 #, 1000 #, 2000 # and then polishing for 1h; and (2) the diamond particles were completely extracted from the composites with 30% nitric acid for 20min-60min for morphology observation. Besides, the coverage rate of diamond extracted from the fabricated copper/diamond composites by the interface is calculated by using Image-pro plus software using backscatter images with a magnification of 500. Three different areas across the whole specimen were selected to obtain the average value of the coverage rate.

2) X-Ray diffraction

X-ray diffraction (XRD, Philips X-pert x-ray diffraction system, CuKa radiation) was used to analyze the phase compositions of the diamond after pre-annealing and the fabricated composites.

3) Atomic force microscope

Atomic force microscope (AFM, Bruker Ltd) was used to characterize the surface morphology of the extracted diamond particles. AFM imaging was performed using a probe-tapping method with a scanning frequency of 0.9Hz.

3.3.2 Properties measurement and test

1) Density

The composites' density was tested following the Archimedes principle. The high-precision analytical balance was used to measure the sample mass before and after immersing the distilled water. Five measurements were carried out to obtain the average value. The density was calculated according to the following equation

$$\rho_c = \frac{m_0}{m_0 - m_1} \times \rho_w \qquad 3\text{-}1$$

where ρ_c is the density of the composites, m_0 is the dry mass of the specimens, m_1 is the mass of the specimen in distilled water, and ρ_w is the density of distilled water.

The relative density is equal to the experiment value divided by the theoretical values. The ideal density of copper/55vol%diamond composites should be 5.96 g/cm^3, the density of diamond is taken as 3.52 g/cm^3 and the copper's density is 8.92 g/cm^3.

2) Heat capacity

The specific heat capacity was calculated by the rule of mixture (ROM) which is based on the mass fraction of each component. The equation is shown below:

$$cp_c = \frac{m_m}{m_{mixture}} \times cp_m + \frac{m_f}{m_{mixture}} \times cp_f \qquad 3\text{-}2$$

where cp_c, cp_m, cp_f are the heat capacity of the composite, matrix, and filler respectively. m_m,m_f and $m_{mixture}$ are the mass of the matrix, filler, and composites, respectively.

3) Thermal diffusivity

The thermal diffusivity's measurement principle is to apply a one-dimensional laser pulse to one surface of a circular sample with a specific size, the temperature change of the other is measured with time, and then the thermal diffusivity is calculated according to the theoretical model of unsteady heat conduction.

The thermal diffusivity was measured by a laser flash technique using an LFA 467 instrument (Netzsch, Germany) at room temperature with an international standard dimension of Φ12.7 mm × 3 mm for the 30mm-diameter specimen and Φ10 mm × 2 mm for the 9mm-diameter sample. All samples were ground with abrasive papers coded as 320 #, 1000 #, and 2000 # and then cleaned ultrasonically in ethanol for 1min.

4) Thermal conductivity

The thermal conductivity was calculated by using the equation:

$$\lambda = \alpha \times \rho \times Cp \qquad 3\text{-}3$$

where λ (W/m/K) is the thermal conductivity of the composites, α (m^2/s) is the thermal diffusivity, ρ (kg/m^3) is the density of the composite and Cp (J/kg/K) is the specific heat capacity of the composites.

4 Interface characteristics and thermal conductivity of Cu/55vol%Diamond (Ti-coated) composites

(A journal article has been extracted from this chapter and is submitting to the Journal, Diamond and Related Materials)

In copper/diamond composites, the interface characteristics, including phase composition and microstructure, play an essential role in achieving high thermal conductivity for the composite. Optimal interface characteristics can facilitate effective heat transfer. However, the poor chemical affinity between the copper and the diamond results in the weak interfacial bonding formed in the fabricated copper/diamond composites, and this is easy to cause interface fracture or delamination. It is reported that the interface failure is the main reason causing the fabricated composites has a low thermal conductivity [57, 64].

Generally, introducing a suitable interface between the copper and the diamond in the copper/diamond composite is widely used to improve the composite's interface bonding, thus leading to obtaining high thermal conductivity. However, there is still a lack of knowledge about how the interface characteristics affect the thermal conductivity of copper/diamond composites. Thus, it is crucial to establish the relationship between the interface characteristics and the thermos-physical properties of copper/diamond composites for engineering the copper/diamond composites to meet practical requirements in the heat sink materials.

Cu/Ti-diamond composites have been successfully fabricated by hot forging at 800℃ and 1050℃ in our research group, and the thermal conductivity of the fabricated copper/diamond composite can reach up to 550W/ (mK) [65]. In this chapter, I am trying to tailor the interface characteristics of Cu/55vol%Ti-coated diamond composites through pre-annealing of Ti-coated diamond particles before the materials' fabrication process (hot forging), and investigate on how the phase constitutions and the interface microstructure of fabricated copper/Ti-diamond composites vary before and after hot forging, to access how those interface characteristics' variation affect the resultant thermal conductivity of copper/diamond composites.

4.1 Pre-annealing of Ti-coated diamond

Figure 4-1 shows the microstructure of non-coated diamond particles and Ti-coated diamond particles. The non-coated diamond particles have a flat surface and the diamond particles are in regular Cubo-octahedral shape (Figure 4-1a, b). Figure 4-1 c shows the main features of the Ti-

coated diamond particles. It is clear to see that the diamond particles are evenly coated with a uniform titanium layer. Titanium behaves much brighter on the backscatter images due to the atomic number of titanium is bigger than that of carbon. In the high magnification images (Figure 4-1 d), the white dots are visible and they are pure titanium particles, which are caused by technical limitations. And it also can see that the Ti-coated diamond surface is still flat except for the white dots. Since magnetic sputtering is operated under room or low temperature, there is no chemical reaction between titanium and carbon during this process.

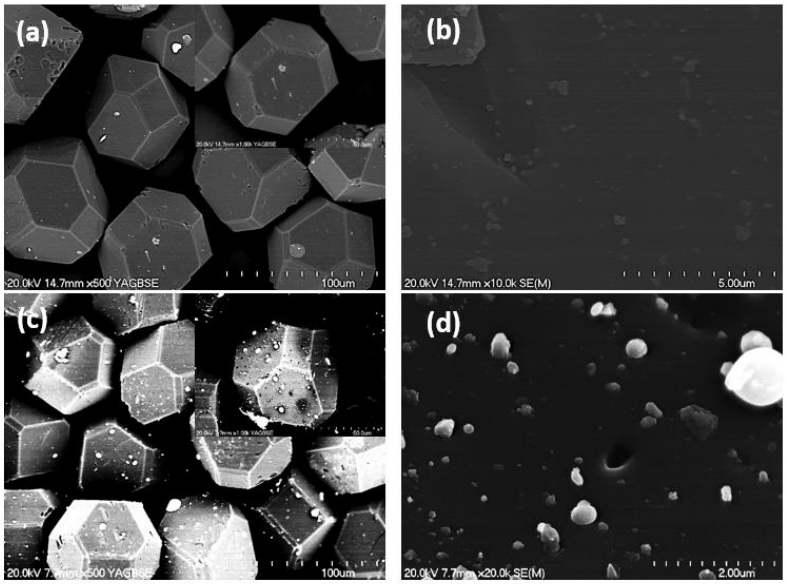

Figure 4-1 Diamond morphology: (a-b) non-coated diamond; (c-d) Ti-coated diamond

In order to tailor the diamond surface microstructures, Ti-coated diamond particles are annealed at different temperatures (see experimental procedure).

4.1.1 Diamond phase transformation after annealing

Figure 4-2 shows the XRD patterns of Ti-coated diamond particles before and after annealing. Only the titanium and diamond peaks can be detected for the as-received Ti-coated diamond particles, as shown in Figure 4-2a. It is clear to see that there are two phases in the 700℃-annealed diamond particles (Ti and diamond) and three phases (Ti, diamond, and TiC) of the diamond particles annealed above 800℃. In addition, with increasing the annealing temperature, the intensity of Ti is gradually weakened in the XRD patterns and the TiC peak intensity is increased. The peak of Ti nearly disappears when the annealing temperature is over 950℃. It suggests that when the pre-annealing temperature is below 800℃, the phase constitution of Ti-coated diamond particles is not significantly changed. When the pre-annealing temperature is over 800℃, the diffusion of carbon

and titanium atoms is significantly activated, leading to a chemical reaction happens between Ti coating and diamond in a relatively short time (the annealing temperature is held for 30min), as seen in equation 4-1, to form TiC. The reaction becomes more active with increasing the pre-annealing temperature.

$$Ti + C_{diamond} = TiC (\Delta G = -186600 + 13.2T \text{ J/mol}) \quad 4\text{-}1$$

The value of Gibbs energy is below zero, this means the annealing temperature can provide enough energy to activate this reaction. Furthermore, there is no graphite peak found in the XRD patterns, suggesting that the pre-annealing will not induce the graphitization of diamond to occur at the researched annealing temperatures with holding the temperature for 30min. In addition, it can conclude that the reaction temperature between the titanium atoms and the diamond is above 700℃. Pre-annealing at 1050℃ can cause the titanium coating on diamond particles to completely react with the diamond to form TiC, and this can be proved by EDS results as well.

In order to further confirm the phase constitutions of Ti-coated diamond particles after annealing, the EDS analysis is carried out the related results of Ti-coated diamond particles annealed at 1050 ℃are shown in Figure 4-3. At point 1, it contains 88.7wt% of titanium and 6.47wt% of carbon, suggesting that the particle at position 1 is likely uncoated titanium from the sputtering process. The composition of points 2 and 3 are composed of 65.45wt%C and 34.55wt%Ti, and 43.89wt%C and 56.11wt%Ti, receptivity. Combining with the results obtained from the XRD patterns, it can indicate that the original titanium coating layer on the 1050℃-annealed diamond surface is completely reacted with the diamond to form TiC.

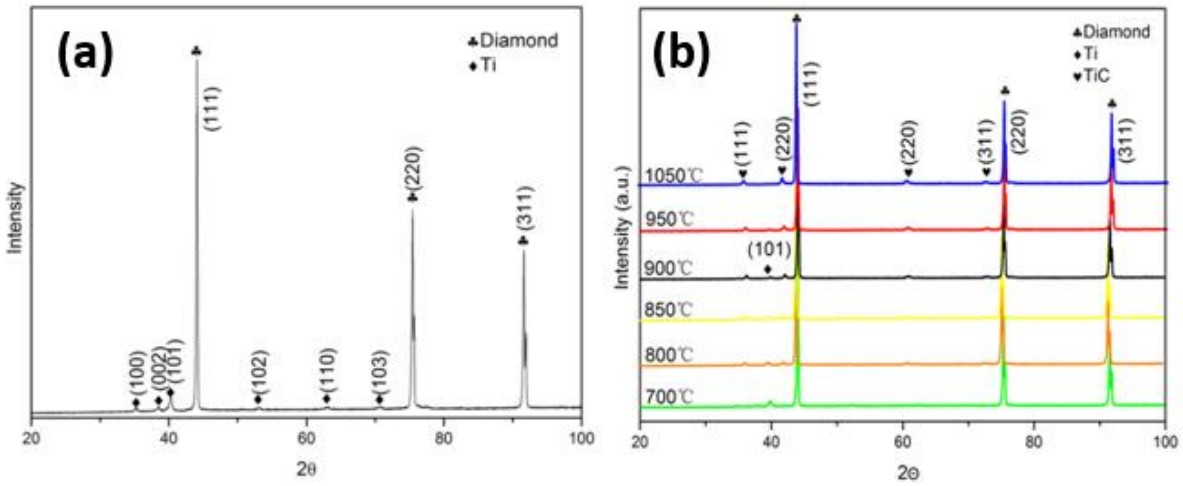

Figure 4-2 XRD patterns of the Ti-coated diamond after (a) magnetic sputtering; (b) heat treatment at different temperatures

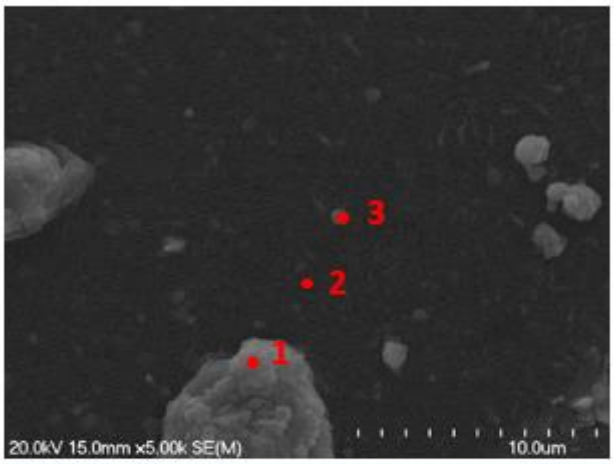

position	C-wt%	Ti-wt%
1	6.47	88.17
2	65.45	34.55
3	43.89	56.11

Figure 4-3 EDS point analysis results of 1050℃-annealed Ti-coated diamond particles

4.1.2 Diamond surface characterization after annealing

SEM microstructures of the Ti-coated diamond particles after annealing at 800℃, 900℃, and 1050℃ (referred to as Ti800, Ti900, and Ti1050) are shown in Figure 4-4.

After pre-annealing at 800℃, diamond particles are evenly enveloped with a coating layer observed from the backscatter image (Figure 4-4a). In the high magnification images, the morphology on both diamond-{100} and -{111} facets is distinct. The coating layer is relatively flat except for the existence of very few particle protrusions (as indicated by arrows in Figure 4-4a1) on the diamond-{100} facet, and the morphology is the same as the as-received Ti coated diamond particles (Figure 4-1d). For the diamond-{111} facet, more particle protrusions are visible and the diamond surface is relatively rough compared to the diamond-{100} facet (Figure 4-4a2). From the XRD results in Figure 4-2b, it suggests that TiC exists due to a small amount of titanium reacts with the diamond to form TiC particles when the annealing temperature is 800℃. It was reported in our previous work that the TiC formed by the reaction between the diamond and the titanium coating during hot forging at a temperature not lower than 800℃ [65]. We can speculate that the particle protrusions on both diamond-{100} and -{111} facets are the newly formed TiC. A large amount of TiC protrusions are observed on the diamond-{111} facet (Figure 4-4 a2) than that on the diamond-{100} facets (Figure 4-4 a3). Thus, it can conclude that TiC is easier to form on the diamond-{111} facet

than on the diamond-{100} facet under annealing at 800℃. The possible reason will be discussed in the later section.

Figure 4-4b shows the backscatter images of Ti900 diamond particles, it indicates that diamond particles are still completely coated with a uniform layer after pre-annealing at 900℃. In the high magnification, the morphology on diamond-{100} (Figure 4-4b1) and diamond-{111} facets (Figure 4-4b2) of Ti900 diamond particles are the same. The nucleation of TiC particles on both diamond-{100} and -{111} facets increase and this leads to a rough coating diamond surface compared to Ti800. After annealing at 900℃, the XRD result suggests that a large amount of titanium coating reacts with the diamond to form TiC (Figure 4-2b). This indicates that improving the pre-annealing temperature can active more TiC nucleation positions and stimulate the diffusion of the diamond and titanium atoms, and an annealing temperature of 900℃ is the critical annealing temperature which can make the nucleation of TiC particles occur on the diamond-{100} facet and diamond-{111} facets almost at the same time and similar nucleation rate.

Further increasing the annealing temperature to 1050℃, it can see that diamond particles are still fully covered by a coating layer in the low magnification images (Figure 4-4c). In the high magnification images, it is clear to see that diamond-{100} and -{111}facets have a similar terrace-structure (as shown in Figure 4-4 c1 and c2, respectively). However, the size of TiC particles on the diamond- {111} facet is bigger than that on the diamond-{100} facet, while the density of the TiC particles on the diamond-{100} facet is higher than that on the diamond-{111} facet. Ti coating is likely completely reacted with the diamond to form TiC for the 1050℃-annealed diamond particles, and this can be concluded from the XRD results (no titanium peaks are identified in Figure 4-2b). These indicate that the newly formed TiC particles start growing with increasing the annealing temperature to 1050℃ and it is easier for TiC particles to grow coarse on diamond-{111}facet than on diamond-{100} facet. The reason will be explained in a later section.

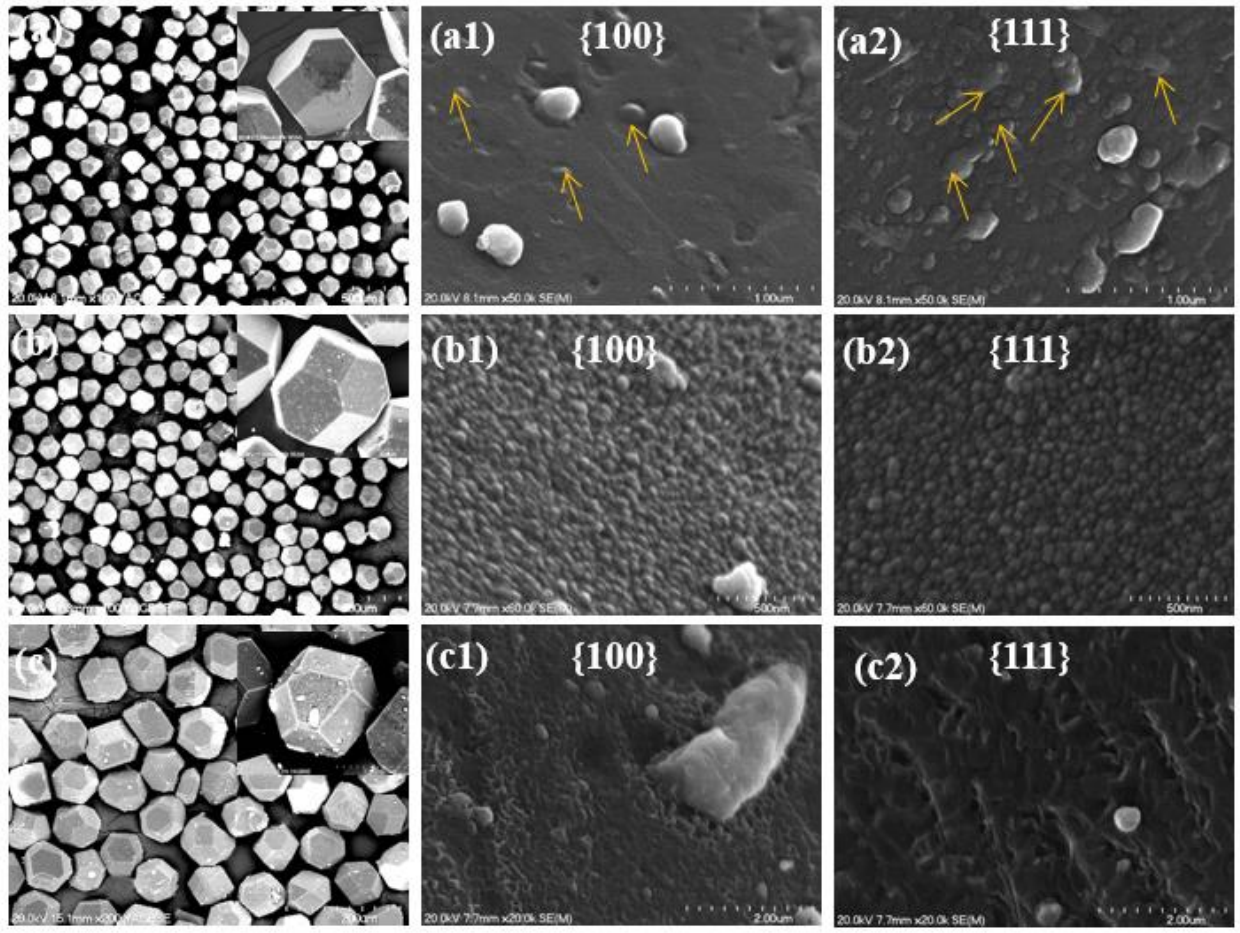

Figure 4-4 Morphology of Ti-coated diamond after pre-annealing at (a)800℃; (b) 900℃; (c) 1050℃; (a1), (b1), (c1) are corresponding diamond-{100} facets and (a2), (b2), (c2) are the corresponding diamond-{111} facets

4.2 Copper /55vol%Diamond (Ti-coated) composites

Based on the XRD and SEM results of annealed Ti-coated diamond particles, it can confirm that the phase constitutions of Ti-coated diamond are distinct after pre-annealing at 800°C (composed of Ti, diamond, and a very small amount of TiC), 900°C (consists of a small amount of Ti, diamond, and a relatively large amount of TiC), and 1050°C (primary diamond and TiC). Thus, we use the Ti-coated diamonds annealed at those three different temperatures as start materials to prepare copper/diamond composites by hot forging at 800°C, and the corresponding copper/diamond composites fabricated are denoted as Ti-800-Cu/Dia, Ti-900-Cu/Di, and Ti-1050-Cu/Dia, respectively. The detailed processing parameters are listed in Table 4-1.

Table 4-1 Details of copper/ 55vol%diamond (Ti-coated) composites

Samples	**Matrix**	**Diamond**		**Composites**
	Copper	Pre-annealing T (℃)	Holding Time (min)	Hot Forging T(℃)
Ti-800-Cu/Dia		800	30	800
Ti-900-Cu/Dia		900	30	800
Ti-1050-Cu/Dia		1050	30	800

4.2.1 Relative density

Figure 4-5 shows the measured relative density of fabricated copper/diamond composites. The relative density of the Ti-800-Cu/Dia is 94%. With increasing the Ti-coated diamond particles' annealing temperature, the fabricated composite's relative density is increased, with a value of 96.61% for Ti-900-Cu/Dia and 97.07% for Ti-1050-Cu/Dia. It is noticed that the increase in the relative density for the fabricated copper/diamond composites is not significant as increasing the diamond particles' pre-annealing temperature from 900℃ to 1050℃. This suggests that the large quantity of TiC particles formed during the pre-annealing process may contribute to improving the density of the fabricated composites.

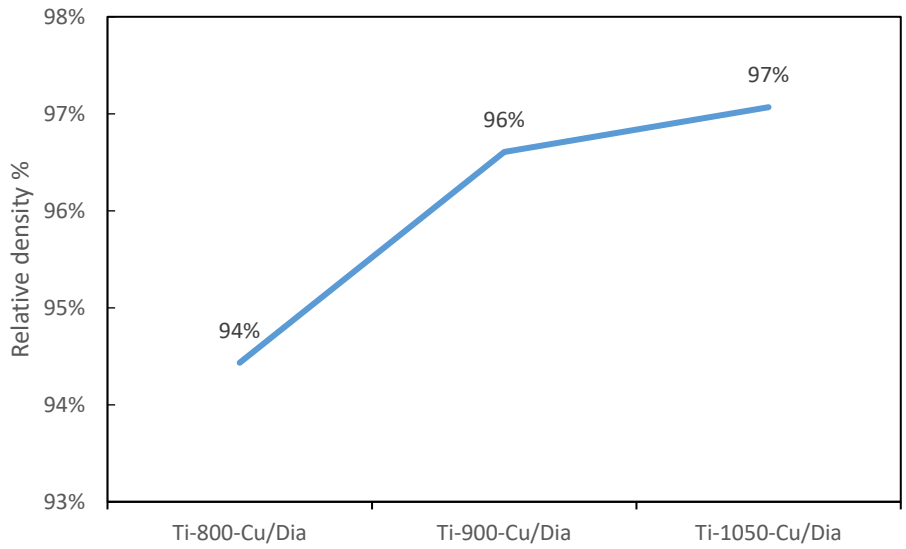

Figure 4-5 The measured relative density of Ti-800-Cu/Dia, Ti-900-Cu/Dia, and Ti-1050-Cu/Dia composites

4.2.2 Phase constitutions

Figure 4-6 illustrates the phase constitutions of the fabricated Cu/Ti-diamond composites (Ti-800-Cu/Dia, Ti-900-Cu/Dia, and Ti-1050-Cu/Dia). The reflection peaks at 43.3°, 50.4°, 74.1°, and 43.9°, 44.8° are corresponding to the peaks of (111)Cu, (200)Cu, (220)Cu, (111)diamond, and (111)diamond, respectively. Only one small peak of TiC at 35.9° is identified and the intensity of the TiC peak is similar in the three composites, and no Ti peaks are identified in the three fabricated composites. These suggest that the residual Ti on the Ti-coated diamond particles annealed at 800℃ and 900℃ is further reacted with the diamond to completely form TiC during 800℃-hot forging. Therefore, the TiC phase in these Ti-800-Cu/Dia, Ti-900-Cu/Dia, and Ti-1050-Cu/Dia composites are formed in two steps: one is formed in the pre-annealing process and the other is formed during hot forging at 800℃. The detailed phase compositions of Ti-800-Cu/Dia, Ti-900-Cu/Dia, and Ti-1050-Cu/Dia composites before and after hot forging are listed in Table 4-2.

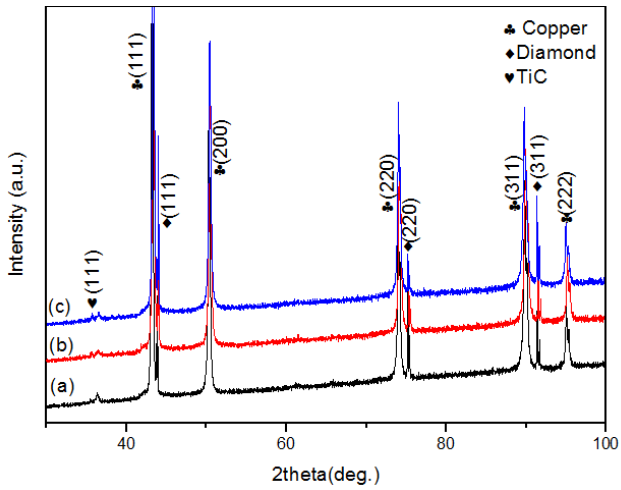

Figure 4-6 XRD patterns of (a) Ti-800-Cu/Dia, (b) Ti-900-Cu/Dia, and (c) Ti-1050-Cu/Dia composites

Table 4-2 Phase constitutions of copper/55vol%diamond (Ti-coated) composites before and after hot forging at 800℃

Specimens	Before hot forging	After hot forging
Ti-800-Cu/Dia	Copper, Diamond, a large amount of Ti, a small amount of TiC	Copper, Diamond, TiC
Ti-900-Cu/Dia	Copper, Diamond, a small amount of Ti, a relatively large amount of TiC	Copper, Diamond, TiC
Ti-1050-Cu/Dia	Copper, Diamond, TiC	Copper, Diamond, TiC

4.2.3 Microstructure

4.2.3.1 Microstructure of 800℃-forged composite materials

Figure 4-7 shows the SEM microstructures of Ti-800-Cu/Dia, Ti-900-Cu/Dia, and Ti-1050-Cu/Dia composites. It can see that the diamond particles are uniformly distributed in the copper matrix for all those three fabricated composites.

In Ti-800-Cu/Dia, the diamond particles are tightly attached on the copper matrix, and a thin interface layer (as indicated by the arrow in Figure 4-8c) can be observed between the copper and the diamond, which acts as a bridge to connect the diamond and the copper, and no obvious pores and voids appeared around the interface. The EDS analysis results at the positions that are close to the interface are shown in Figure 4-8(a). The composition at point 1 is composed of 26.03wt% C, 10.87wt% Ti, and 89.11wt% Cu, and point 2 is about 59.13wt% C, 14.71wt%Ti, and 21.71wt% Cu, however, the composition at point 3 and point 4 are nearly 100% Cu and 100% C, respectively. Therefore, point 1 and point 2 are located in the interface between the diamond and the copper matrix, and we can speculate that the interface is composed of the TiC phase combining with the XRD results (Figure 4-6).

In Ti-900-Cu/Dia and Ti-1050-Cu/Dia composites, several diamond particles are detached from the copper matrix that leaves a pit showing diamond particle shape on the copper matrix (indicated by the red arrow), as shown in Figure 4-7 d and g. The detachment of diamonds from the matrix is due to mechanical polishing as preparing SEM specimens. This suggests that weaker interface bonding formed in Ti-900-Cu/Dia and Ti-1050-Cu/Dia than Ti-800-Cu/Dia composites. For composite Ti-

900-Cu/Dia, it can see a thin interface exists between the copper matrix and diamond particles, and this thin layer is TiC, which is proved by the combination analysis from the results of XRD (Figure 4-6) and EDS. The chemical composition of point 3 is composed of 66.41wt%C, 6.48wt%Ti, and 25.01wt%Cu, and the composition for other points primarily consisted of C (point 1 and 2) or Cu (point 4), as shown in Figure 4-8b. Furthermore, gaps are visible in Ti-900-Cu/Dia composites (indicated by the blue arrow in Figure 4-7f), and this also deteriorates the interface bonding. For Ti-1050-Cu/Dia composite, more voids and clear gaps are observed compared to Ti-900-Cu/Dia, and no obvious interface layer is identified neither. This suggests that Ti-1050-Cu/Dia composites may have the worst interface bonding between the diamond and the copper among those three fabricated composites.

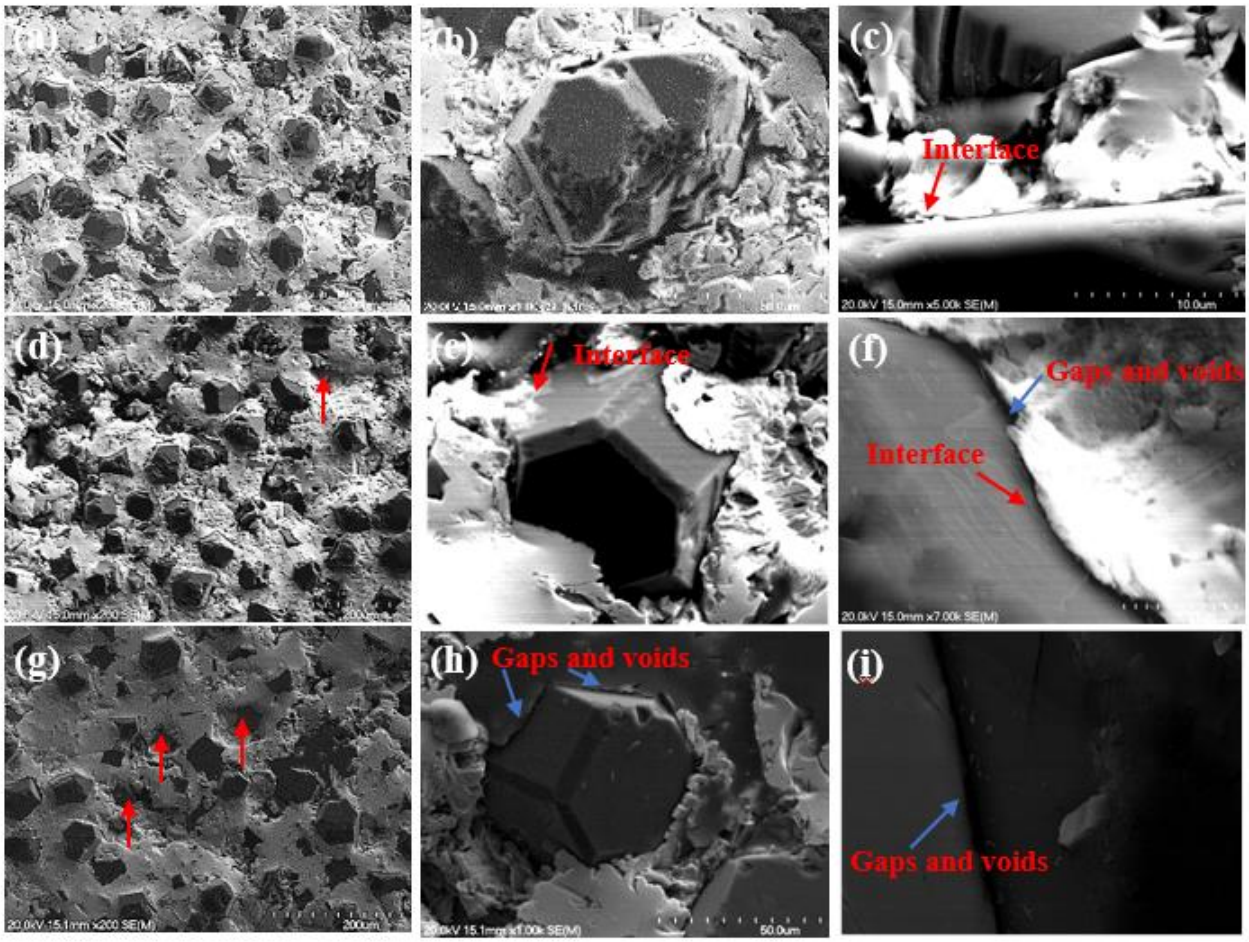

Figure 4-7 SEM microstructure of (a-b)Ti-800-Cu/Dia; (c-d)Ti-900-Cu/Dia; (e-f) Ti-1050-Cu/Dia composites

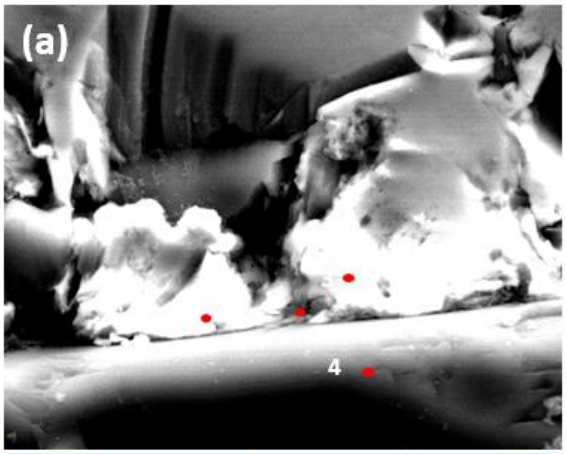

position	C- wt%	Ti- wt%	Cu- wt%
1	26.03	10.87	59.11
2	59.13	14.71	21.71
3	2.66	0.12	97.22
4	97.73		2.27

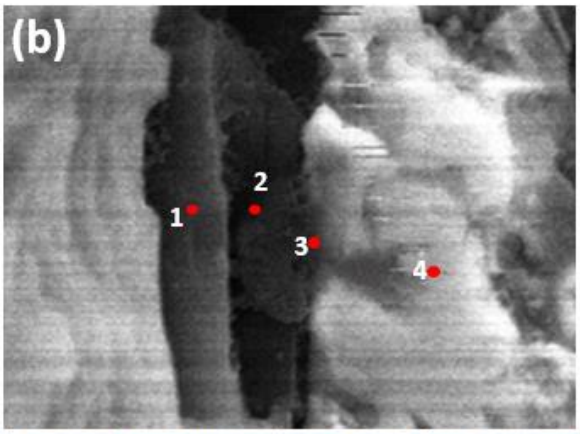

position	C-wt%	Ti-wt%	Cu-wt%
1	100.00		
2	97.72	2.28	
3	66.61	7.48	25.01
4	3.69	0.65	95.66

Figure 4-8 EDS point analysis of (a) Ti-800-Cu/Dia; (b) Ti-900-Cu/Dia composites

4.2.3.2 Morphology of the extracted diamond particles from the fabricated copper/diamond (Ti-coated) composites

To further investigate the interface microstructure of Ti-800-Cu/Dia, Ti-900-Cu/Dia, and Ti-1050-Cu/Dia, the diamond particles are extracted from the composites, respectively, to be analyzed by using SEM and the morphology of corresponding diamond particles are presented in Figure 4-9. It can see that most diamond particles extracted from those three composites are enveloped by the formed TiC interface layer (in a bright color in Figure 4-9a, b, and c), however, some formed interface layer is spalled from the diamond particles to expose bare diamond surface (in a dark color). The statistic coverage of diamond particles by formed TiC interface is about 79.5% for Ti-800-Cu/Dia, 65.3% for Ti-900-Cu/Dia, and 57.7% for Ti-1050-Cu/Dia, respectively, and the results are listed in Table 4-3.

From Figure 4-4, we know that, after pre-annealing (800℃, 900℃, and 1050℃), the Ti-coated diamond particles are completely enveloped by either original Ti-coating or the product of the reaction between titanium coating and diamond in the annealing process, and no spallation from the diamond particle surface is observed. This indicates that the spallation of the interface from diamond particles occurs during hot forging. The high coverage of diamond by the interface for the diamond particles extracted from the Ti-800-Cu/Dia composite agrees with the microstructure observation of bulk Ti-800-Cu/Dia: tight contact of diamond and copper matrix appears, no pores and gaps are exited, and clear interface layer is identified. Moreover, obvious pores or gaps are observed in Ti-900-Cu/Dia and Ti-1050-Cu/Dia composites.

Table 4-3 Coverage rate of the diamond by coating before and after hot forging

Coverage diamond area (%)	**Ti-800-Cu/Dia**	**Ti-900-Cu/Dia**	**Ti-1050-Cu/Dia**
Before hot forging	100	100	100
After hot forging (800℃)	79.5	65.3	57.7

The high magnification images in Figure 4-9 clearly show the detailed microstructure on the diamond-{100} facet (a1, b1, and c1) and diamond-{111} facet (b2, c2, and c2). Not like the 800-annealed-Ti-coated diamond particles surface (diamond surfaces very smooth and flat on the diamond-{100} facet and slightly rough (caused by the formation of particle protrusion) on the diamond-{111} facet), both diamond-{100} and -{111} facets are rough for the extracted diamond particles from Ti-800-Cu/Dia. This is likely caused by the further nucleation and growth of TiC particles through the reaction of Ti coating and diamond during hot forging. Furthermore, the diamond-{100} facet (Figure 4-9 a1) has a relatively rougher surface than that on the diamond-{111} facet (Figure 4-9 a2).

For the diamond particles extracted from Ti-900-Cu/Dia, the formed TiC layer tends to be flattened (Figure 4-9 b1 and b2). Compared to the diamond particles extracted from Ti-800-Cu/Dia, the TiC layers are denser and the grain boundaries are more visible on both diamond-{100} and -{111} facets. From previous results, we know that, after 900℃ annealing, a large amount of Ti coating reacts with the diamond to form fine TiC particles that are distributed on both diamond-{100} and -{111} facets, there still have a small amount of unreacted Ti coating left on the diamond particle surfaces. During hot forging, the performed fine TiC particles will grow and the unreacted Ti-coating will further react with the diamond to form TiC and the newly formed TiC particles grow as well. This leads to a dense TiC layer with clear TiC grains is formed in Ti-900-Cu/Dia.

For the diamond particles extracted from Ti-1050-Cu/Dia composites, the diamond surface becomes flatter and smoother and TiC grain boundaries are much clearer than that in Ti-900-Cu/Dia, but there are some voids to appear between grains (Figure 4-9 c1 and c2). Ti-coating on the diamond particles is completely transformed into TiC particles after 1050℃ pre-annealing for 30min (confirmed in Section 4.1), and thus the TiC particles continually grow during the hot forging process, and this leads to the TiC particles are much coarser and the grain size of the TiC is relatively bigger in Ti-1050-Cu/Dia than in Ti-900-Cu/Dia, resulting in forming a flat surface. Furthermore, pre-formed TiC particles may peel off from the diamond particle surface due to the

plastic deformation. The flat surface decreases the contact area between the interface and copper matrix, thus forming a weak interfacial bonding between the copper and the diamond. This is also the reason that causes diamond particles to detach from the copper matrix in the Ti-1050-Cu/Dia composites. In addition, the microstructures on both diamond-{100} and -{111} facets are similar for the Ti-1050-Cu/Dia, but the TiC grain boundary is more clearer and its grain size is much bigger on the diamond-{100} facet than on the diamond-{111}facet, suggesting that TiC grsin growth is faster on the diamond-{100} facet than on the diamond-{111} facet during hot forging.

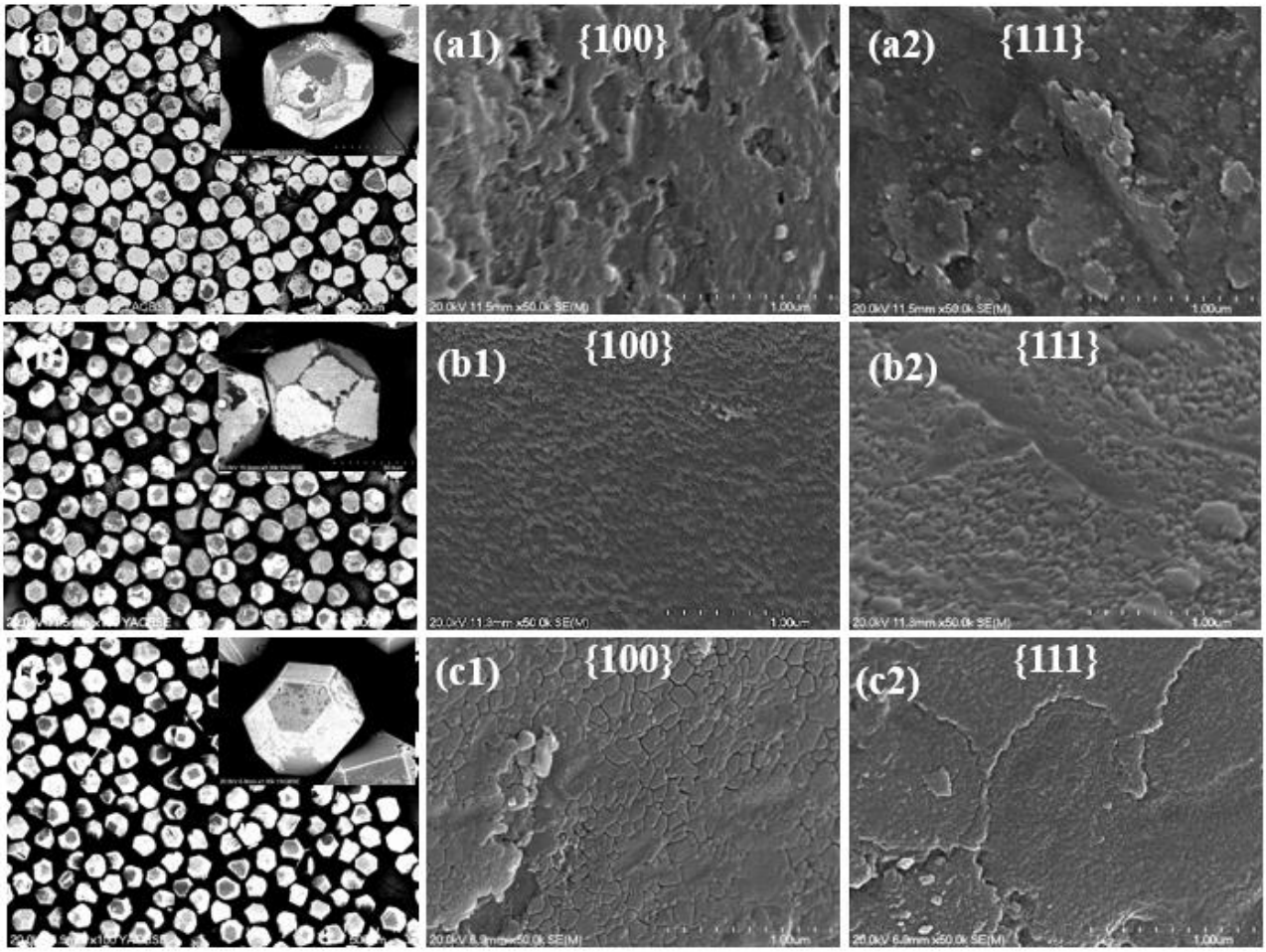

Figure 4-9 Extracted diamond particles from (a)Ti-800-Cu/Dia; (b)Ti-900-Cu/Dia; (c) Ti-1050-Cu/Dia composites, (a1), (b1), (c1) are corresponding diamond-{100} facets and (a2), (b2), (c2) are corresponding diamond-{111} facets

4.2.3.3 Atomic-force microscopy (AFM) microstructure

The interface bonding strength between the copper and the diamond is affected by the surface roughness of the formed TiC interface layer as well. Generally, it is using mean roughness, Ra, to represent the surface texture, which is the degree of deviation from an ideally smooth surface. The

Ra is the average value of the absolute deviation of the profile from the baseline. In this section, AFM is used to characterize the roughness of diamond particles extracted from the Ti-800-Cu/Dia, Ti-900-Cu/Dia, and Ti-1050-Cu/Dia composites.

The AFM morphology of formed TiC particles on the diamond particles extracted from Ti-800-Cu/Dia, Ti-900-Cu/Dia, and Ti-1050-Cu/Dia can be seen in Figure 4-10. It is clear to see that the size of the TiC particles are in nanoscale on both diamond-{100} and -{111} facets for Ti-800-Cu/Dia. However, the particle size of TiC on the diamond-{100} facet is slightly bigger than that on the diamond-{111} facet. In addition, the statistics show that the diamond-{100} facet (Ra=5.13nm) (Figure 4-10a) is rougher than the diamond-{111} facet (Ra=2.92nm) (Figure 4-10 b). This is consistent with the SEM observation (in Figure 4-9a1and a2). This is caused by varied TiC formation ability on the diamond-{100} and -{111}facets at 800℃.

Figure 4-10 c and d show the detailed surface morphology of TiC particles on the surface of diamond particles extracted from Ti-900-Cu/Dia. It can be seen that the morphology of TiC particles on the diamond-{100} and {111} facets are almost the same. In addition, there is a significant reduction in the roughness on the diamond surface extracted from Ti-900-Cu/Dia. The value of Ra is only 0.199nm for the diamond-{100} facet and 0.491nm for the diamond-{111} facet. It indicates the TiC particles become coarser and the interfacial layer tends to be flat and smooth with the increasing of the pre-annealing temperature. This agrees with the microstructure observation of diamond particles extracted from Ti-900-Cu/Dia (Figure 4-9b1 and b2). The diamond-{100} and -{111} facets of Ti-1050-Cu/Dia also obtain the close Ra value, as shown in Figure 4-10 e and f. The Ra value of diamond particles extracted from Ti-1050-Cu/Dia is very small, with a value of 1.14nm for the diamond-{100} facet and 1.54nm for diamond-{111} facet (a bit higher than Ti-800-Cu/Dia, the deviation of the results attributed to the spallation of the interface from the diamond particles, results in relatively large Ra). Considering (1) all the three composites, Ti-800-Cu/Dia, Ti-900-Cu/Dia, and Ti-1050-Cu/Dia are hot forging at 800℃ and (2) only a very small amount of TiC particles formed after Ti-coated diamond particles annealed at 800℃ on the diamond-{111} facet, a large amount of TiC particles are uniformly formed on both diamond-{100} facet and diamond-{111} facets after annealing the Ti-coated diamond particles above 900℃, we can speculate that the distinct anisotropic microstructure characteristics caused by TiC nucleation between the diamond-{100} and -{111} facets for the Cu/Ti-coated diamond composites could be eliminated by pre-annealing the Ti-coated diamond particles at 900℃ prior processing. This is because the high annealing temperature prompt the nucleation and growth of TiC particles on both diamond-{100} and -{111} facets during the annealing stage, and this create an equal nucleation

rate on both diamond facets during the forging process, leading to an almost isotropic interface microstructure is observed on both diamond facets.

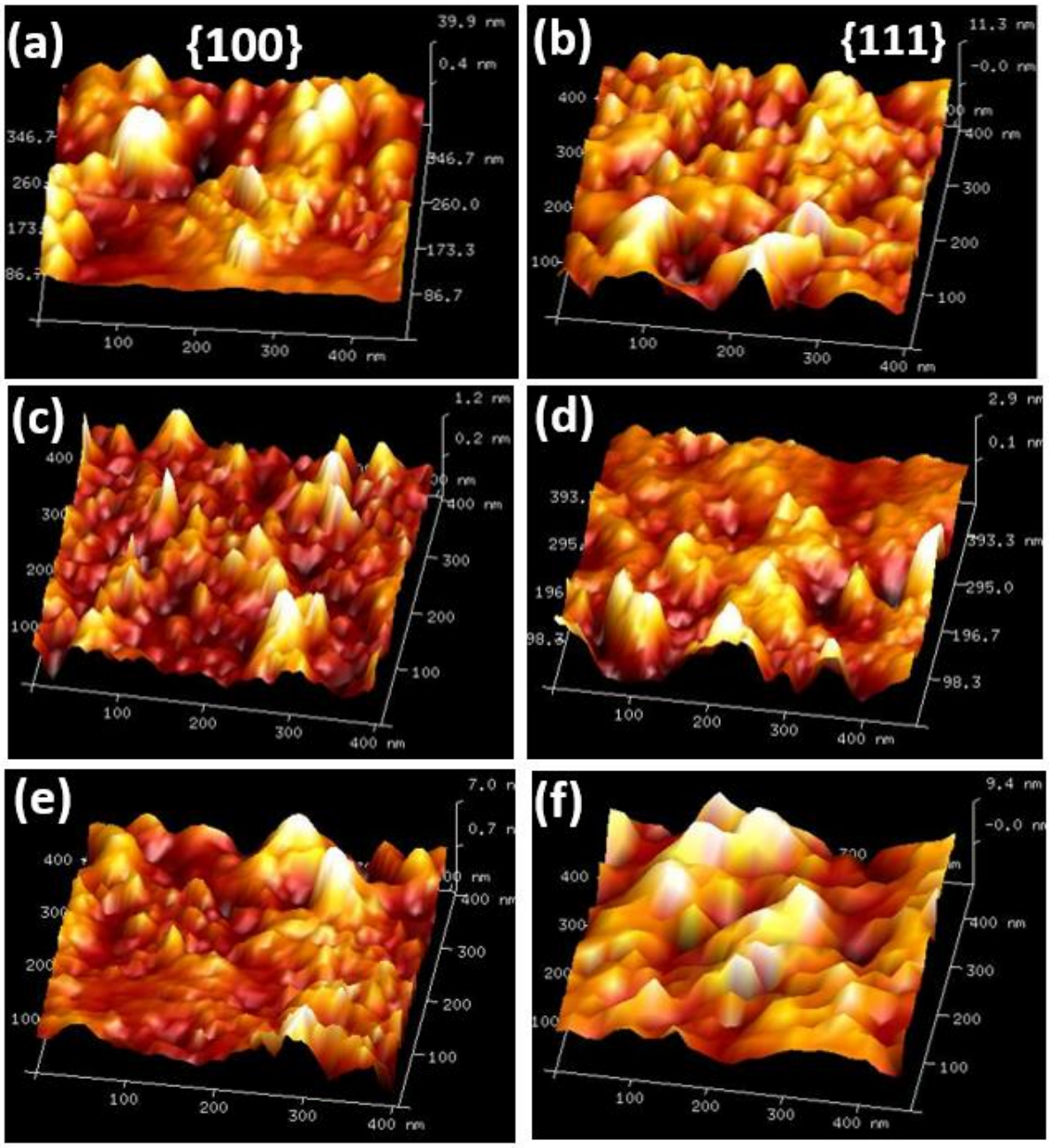

Figure 4-10 3-D AFM microstructure of the TiC layer on diamond particles extracted from (a-b) Ti-800-Cu/Dia and (c-d) Ti-900-Cu/Dia, and (e-f) Ti-1050-Cu/Dia composites

Comparing with the 3-D AFM microstructure of the diamond extracted from the Cu/ Ti-diamond composite directly fabricated by hot forging at 800℃ (Figure 4-11) [65], both diamond-{100} and -{111} facets for the Ti-800-Cu/Dia are less rough, and the TiC particles are coarser. This is mainly

attributed to the pre-annealing that helps to facilitate the TiC nucleation before forging, leading to relatively fast growth during forging.

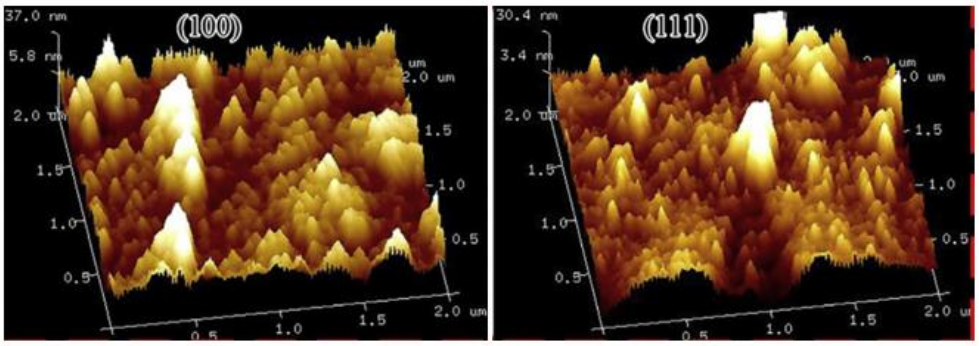

Figure 4-11 3-D AFM microstructure of the TiC interfacial layer on diamond particles extracted from Cu/Ti composite [65]

4.2.4 Thermal conductivity

The thermal diffusivity (α) and thermal conductivity (k) of the Ti-800-Cu/Dia, Ti-900-Cu/Dia, and Ti-1050-Cu/Dia composites are presented in Figure 4-12. The Ti-800-Cu/Dia composite has the highest thermal conductivity in the three composites, which is 350 W/ (mK), and it is about 1.5 times higher than that of the processed copper matrix, 224W/ (mK) [65]. The thermal conductivity for Ti-900-Cu/Dia and Ti-1050-Cu/Dia composite is very close, with a value of 250 W/ (mK) and 266 W/ (mK), respectively. Ti-800-Cu/Dia has a higher TC but lowers relative density than those of Ti-900-Cu/Dia and Ti-1050-Cu/Dia composites, and this indicates that the formed interface structure in Ti-800-Cu/Dia make more contribution than the density does.

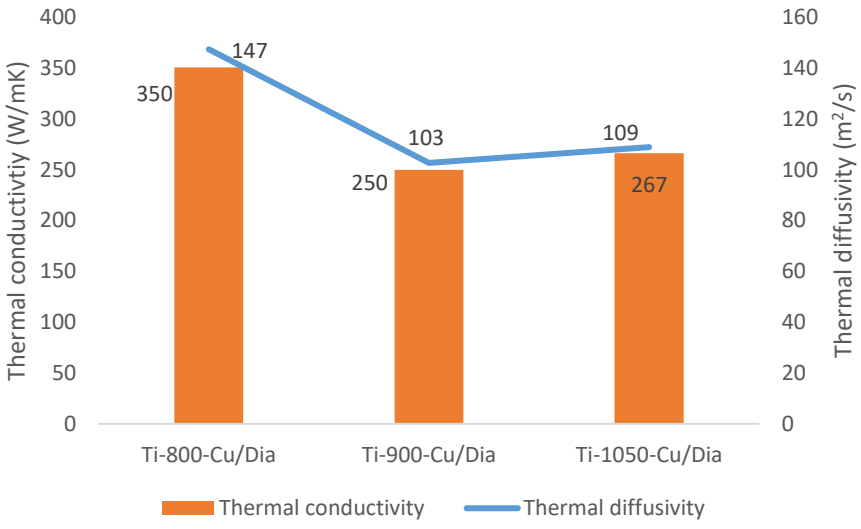

Figure 4-12 Thermal diffusivity and thermal conductivity of the Ti-800-Cu/Dia, Ti-900-Cu/Dia, and Ti-1050-Cu/Dia composites

4.2.5 Theoretical thermal conductivity

The differential effective medium (DEM) model is used to calculate the theoretical thermal conductivity value to compare the measured and theoretical thermal conductivity. The influence of interfacial thermal conductance and the particle size of the diamond is considered in this model. The equation shows below [3]:

$$(1-V_d)\left(\frac{k_c}{k_m}\right)^{\frac{1}{3}}=\frac{(k_d^{eff}-k_c)}{(k_d^{eff}-k_m)} \text{ with } k_d^{eff}=\frac{k_d}{1+\frac{k_d}{RG_c}} \quad 4\text{-}2$$

where k_c, k_d and k_m are the thermal conductivity of composite, diamond, and copper matrix respectively. k_d^{eff} is the effective thermal conductivity of diamond reinforcement. R is the average radius of the diamond, V_d is the volume fraction of diamond and G_c is the interfacial thermal conductance. In this study, the volume fraction of the diamond is 55% in all of the composites. The thermal conductivity of diamond and hot forged copper is 1500W/ (mK) and 224 W/ (mK) [65], respectively. The average diamond diameter is about 230/270 mesh. In this study, the interfacial layer is TiC in the composite of pre-annealed diamond and copper, thus, the interfacial thermal conductance (G_c) can be expressed by,

$$\frac{1}{G_c}=\frac{1}{G_{Cu/TiC}}+\frac{d}{k_{TiC}}+\frac{1}{G_{TiC/diamond}} \quad 4\text{-}3$$

where k_{TiC} is the thermal conductivity of TiC, d is the thickness of the interfacial layer, and $G_{Cu/TiC}, G_{TiC/diamond}$ are the thermal conductance of the interface between copper and TiC, and between TiC and diamond. The thermal conductance can be calculated by the acoustic mismatch model (AMM),

$$G=\frac{1}{4}c_{AB}\upsilon_{AB}q_{AB}\alpha_{AB} \quad 4\text{-}4$$

where c is the heat capacity, ν is the phonon velocity, q is the fraction of photons incident with a critical angle at the interface, and α is the transmission coefficient of phonons incident with the critical angle. The subscript "AB" means the incident and exist side of the phonon.

$$q_{AB}=\frac{1}{2}\left(\frac{v_A}{v_B}\right)^2 \quad 4\text{-}5$$

$$\alpha_{AB} = \frac{4Z_A Z_B}{(Z_A+Z_B)^2} \; wtih \; Z = \rho v \qquad 4\text{-}6$$

where $Z_A \; and \; Z_B$ are the acoustic impedances which are calculated by the density ρ and sound velocity v of material A and B respectively.

According to the calculations from Equation 4-4, we obtain the interfacial thermal conductance of $G_{Cu/TiC}$ =2.01×10^5 W/m^{2}K, $G_{TiC/diamond}$ =5.8×10^5 W/m^{2}K. To calculate the thickness of the interface, assuming the original Ti-coating is 50nm and the reaction between titanium and diamond is uniform on diamond particles and based on the amount of the titanium is constant before and after the chemical reaction, we obtain the thickness of the TiC interface is about 50nm as well, and then we apply these data to equation 4-3, to obtain that G_c=1.5×105 W/m^{2}K. Substituting the related value to the equation 4-2, the theoretical thermal conductivity of Cu/55vol%Diamond composite is about 541W/ (mK). The material properties used in the calculation are listed in Table 4-4. This suggests that the measure thermal conductivity of Ti-800-Cu/Dia is significantly smaller than its theoretical value.

Table 4-4 Materials properties for theoretic thermal conductivity calculation of Cu/Ti-diamond composites [3, 66]

Materials	**Thermal conductivity (W/mK)**	**Density(kg/m^3)**	**Specific heat (KJ/ m^{3}K)**	**Phonon velocity (m/s)**	**Acoustic impedance (10^7 kg/m^{2}s)**
Diamond	1500	3520	1784	13430	4.73
TiC	36.4	4903	2770	6777	3.34
Cu	224	8900	3426	2801	2.49
Ti	22	4540	2354	3730	1.69

4.2.6 Discussion

4.2.6.1 Effect of pre-annealing temperature on the formation of Ti-diamond particles

When the annealing temperature is 800℃, the titanium coating starts to react with diamond particles to generate TiC particles on the diamond surface. However, the formation of TiC particles is easier to happen on the diamond-{111} facet than on the diamond-{100} facet. This may be due to the sp^3 structure is easy to transform into the sp^2 graphite cluster structure on the diamond-{111} facet that is relatively disordered and highly active at its edge, leading to the reaction of Ti and graphite carbon cluster happens to form TiC particles. The transformation of sp^3 into sp^2 is likely active at 800℃, and this is also confirmed in the Al/diamond composites [67].

Regarding the formation of TiC particles on the diamond-{100} facets, it is reported that small {111} facets are formed on the diamond-{100} surface first under pre-annealing temperature at 800℃ due to the surface energy of diamond-{111} facet is lower than that of diamond-{100} facets (5.4 J/m^2 vs 9.4 J/m^2) [68], and then the sp^3 structure transforms into sp^2 graphite cluster structure and TiC particles are formed follow the similar reaction occurred on the diamond-{111} facet. The 800℃-annealed temperature for 30 min is not enough for a large amount of TiC nucleation on diamond-{100} facets.

With increasing the pre-annealing temperature to 900℃, the transformation of sp^3 to sp^2 structure becomes more active on the diamond-{111} facet, and this further promotes the reaction between Ti coating and graphite, leading to more TiC particles are formed on the diamond-{111} facets. And the activation of forming small {111} facets on the diamond -{100} surface is influenced by pre-annealing temperature, the higher the pre-annealing temperature is, the higher the activity of forming new {111} facets on the diamond-{100} surface. At annealing of 900℃, the small {111} facets are formed first on the diamond-{100} surface, and the TiC is further formed on the newly formed {111} facets. In this situation, the nucleation of TiC has the same nucleation rate on the diamond-{100} and -{111} facets. This is caused by (1) less C-C bonds are bonded of the carbon atoms on diamond-{100} facet compared to on the diamond-{111}facet (two vs three C-C bonds [69]), this makes carbon atoms are easier to break its original structure to react with titanium atoms on the diamond-{100} facet and the structure reviews in Figure 4-14; (2) smaller size of the TiC nucleation required on small {111} facets of diamond-{100} facets (the nucleation sites are the small dents) than the big steps on diamond-{111} facets. These lead to forming more TiC nucleation and growth sites on the diamond-{100} facet and the TiC particles are as dense as on the diamond-{111} facet with increasing the pre-annealing temperature from 800℃ to 900℃. The detailed nucleation mechanism of the carbides on both diamond-{100} and -{111} facets is shown in Figure 4-13 a and b, based on the explained in [70]. The nucleation of the carbides on both diamond-{100} and -{111} facets is heterogeneous. It can be seen that perpendicular steps are active and in low density which provides the sites for carbides nucleation on the diamond-{111} facets, while high-density dents are formed on the diamond-{100} facet for carbides nucleation (refers to the formation of the small {111} facets) and the carbides nucleation sites are relatively small due to they have an angle of 55° with the diamond surface.

When the pre-annealing temperature increase to 1050℃, the nucleation of TiC particles is nearly finished on both diamond-{100} and -{111} facets, and the TiC particles start to grow up. The

growth rate of the formed TiC particles on the diamond-{100} and -{111} facets is different, results in relatively bigger carbides particles on the diamond-{111} facet than on the diamond-{100} facet. The reason can be explained by Figure 4-13 c and d [49]. The growth of the carbides on diamond-{111} facet depends on both surface diffusion and bulk diffusion, this leads to a relatively fast growth rate of the carbides on diamond-{111} facets. On the diamond-{100} facet, due to the limitation of the dents, only bulk diffusion of the diamond can contribute to the growth of the carbides particles and bulk diffusion is at low speed which limits the growth rate of the carbides on the diamond-{100} facet. This results in the bigger TiC particles are observed on diamond-{111} facet than on diamond-{100} facet.

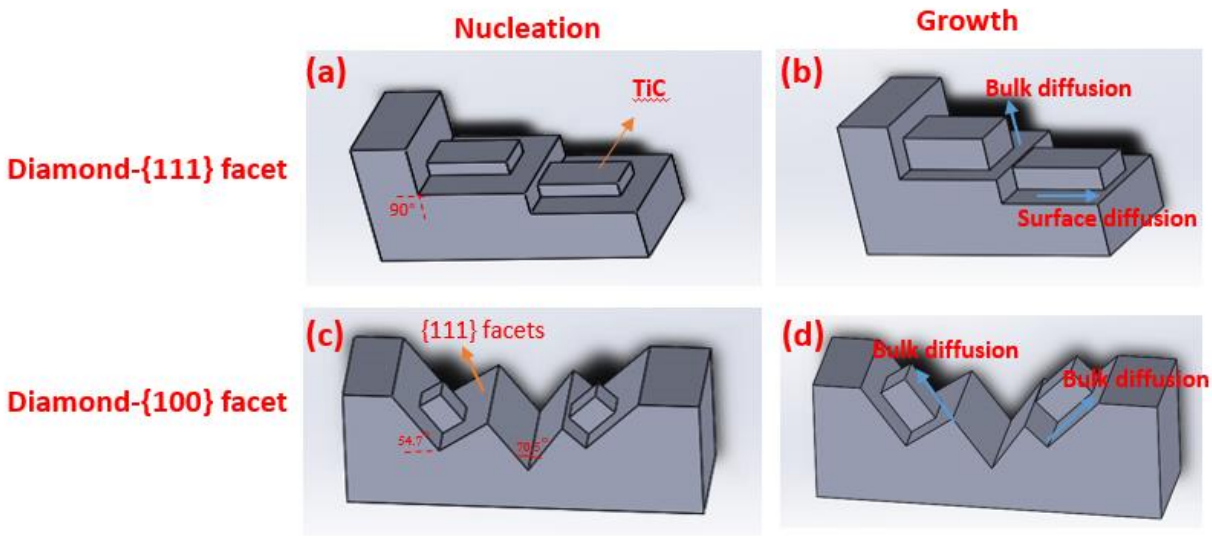

Figure 4-13 The nucleation and growth mechanisms of TiC carbides on diamond-{111} and -{100} facets [70]

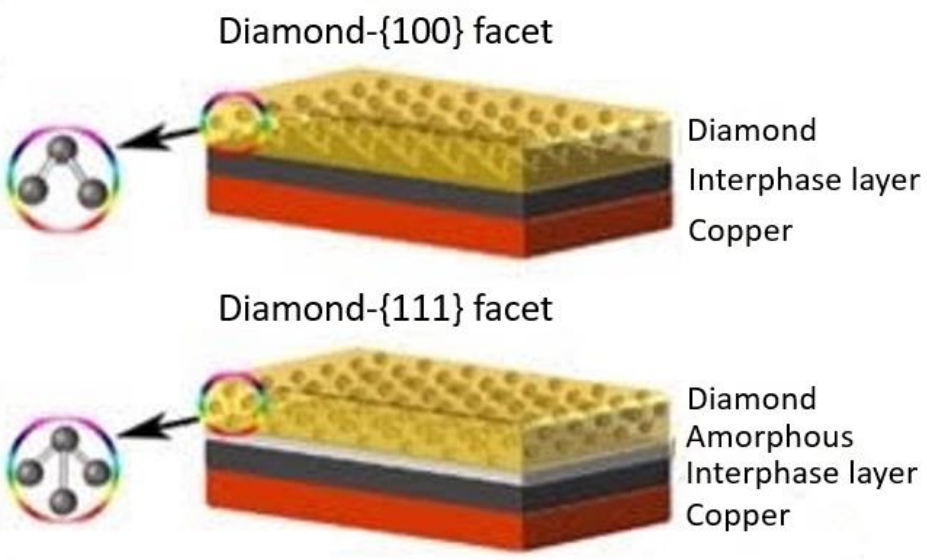

Figure 4-14 Structure of the diamond-{100} and -{111} facets [59]

4.2.6.2 Effect of pre-annealing temperature on the microstructure of Cu/Ti-diamond composite

Pre-annealing has a significant effect on the diamond particles. It was reported that vacuum heat treatment can alter the phase compositions and roughness of diamond [67]. In this study, the diamond particles were pre-annealed at 800℃, 900℃, and 1050℃ first and then are used to prepare the copper/diamond composite. After annealing, the coating composition of original Ti-coated diamond particles is changed. For 800-annealed diamond particles, the coating consists of a large amount of Ti and a very small amount of fine TiC particles (protrusion) that are mainly distributed on the diamond-{111} facet. A large amount of fine TiC particles and the un-reacted Ti are distributed on both diamond-{100} and -{111} facets after annealing at 900℃. In addition, TiC particles form a denser layer on both diamond-{100} and-{111} facets, which completely envelop the diamond particles after annealing at 1050℃.

During hot forging at 800℃, the unreacted Ti in the annealing process is continually reacted with the diamond to form TiC particles on both diamond-{100} and -{111} facets, as shown in Figure 4-15. TiC particles are attached to the diamond surface directly after pre-annealing, and the unreacted titanium distributes beside or above the TiC particles. Carbon atoms will diffuse to react with the unreacted titanium because of the smaller radius of C than Ti atoms. Due to the combined effects from the pressure introduced by large plastic deformation and temperature in the hot forging, a strong interfacial layer structure is formed between the copper and the diamond in the copper/diamond composites, attributed to the formed nano-spherical TiC particles have rough surface morphology and are strongly mechanical interlocked with the copper matrix through certain

orientation [65]. However, the preformed TiC particles are continually growing coarse during the forging process, and this reduces the interface surface roughness and forms a smooth and flat interface structure (as shown in Figure 4-10). Because of the brittle nature of ceramic, the coarsening of the preformed TiC particles in the annealing process would be possible to become crack initiation cites during the process of hot forging and subsequent cooling (as indicated by the arrow in Figure 4-15).

More preformed TiC particles during annealing, much serious spallation occur in hot forging. These cause the coverage rate of the diamond by interfacial layer for Ti-800-Cu/Dia, Ti-900-Cu/Dia, and Ti-1050-Cu/Dia composites are decreased with increasing of the pre-annealing temperature. As reported, the diamond particles are nearly completely covered by the formed interface for the Cu/Ti-coated diamond composites that are directly forged at 800℃ without pre-annealing diamond particles[65]. This further confirms that the preformed TiC particles in the pre-annealing process are easily peeled off from the diamond particle surface during hot forging. The formation of a strong interface with less spallation possibility in the Cu/Ti-coated diamond is mainly attributed to the in-suit formation of TiC particles with less growth possibility and higher mechanical interlock with copper matrix than a preformed TiC layer.

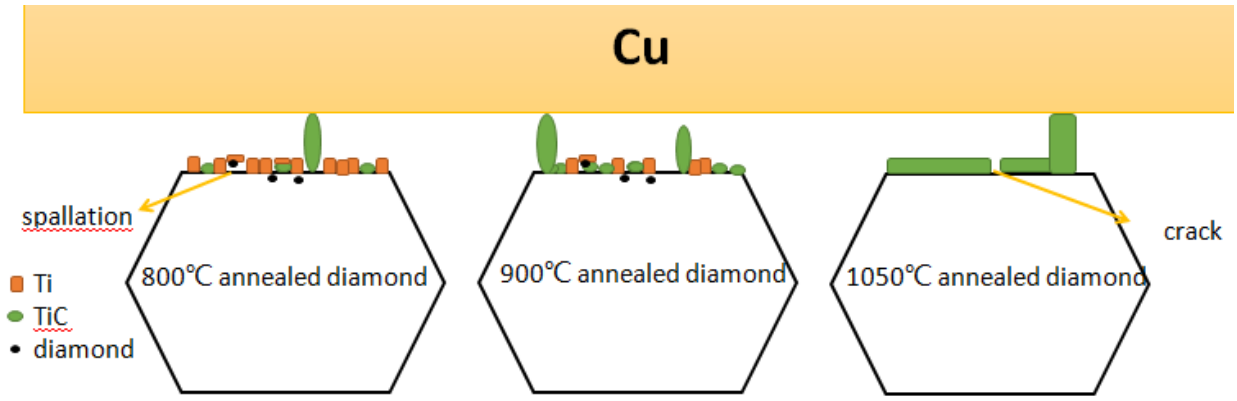

Figure 4-15 Further reaction mechanism between the diamond and titanium during hot forging

4.2.6.3 Effect of pre-annealing temperature on TC of the composites

Pre-annealing significantly changes the formed interface structure of fabricated composites, and this further affects the composite's thermal conductivity. Relative high thermal conductivity is achieved for the Ti-800-Cu/Dia composite, and this is mainly because (1) only a small amount of TiC particles are formed in the pre-annealing process, leading to a large amount of in-suit TiC particles form and grow during hot forging, which helps limit the interface spallation from the diamond

particles; (2) rough surface enlarge the contact area between the copper and the TiC interphase layer, leading to the formation of strong interface bonding; and (3) the formed TiC interface with strong interface bonding with both copper matrix and diamond particles facilitate the phonon transfer from the copper to the diamond [65]. For Ti-900-Cu/Dia and Ti-1050-Cu/Dia composites, the presence of voids and pores near the interface is the main reason that leads to big thermal resistance at the interface, results in low thermal conductivity is achieved for those two composites.

4.2.7 Summary

This chapter studies the interface structure and thermal conductivity of the fabricated copper/diamond composites from the pre-annealed Ti-coated diamond particles. The primary results are:

(1) At the pre-annealing of 800℃, the nucleation of TiC particles can be active, the TiC is easier to form on the diamond-{111} facet than the diamond-{100} facet, showing more TiC particles (protrusion) on the diamond-{111} facet rather than on the diamond-{100} facet. This is mainly attributed to the sp^3 structure is easy to transform to the sp^2 graphite cluster structure and then react with titanium to form TiC. With increasing annealing temperature to 900℃ and 1050℃, TiC particles can be formed on the diamond-{100} and -{111} facets, the anisotropic TiC formation characteristics are not obvious, and the entire diamond particles are enveloped by relative coarse and dense TiC layers for the 1050-annealed Ti-coated diamond particles.

(2) The coating's phase constitutions consist of large Ti and a small amount of TiC for the 800℃-annealed Ti-coated diamond particles, a large amount of TiC particles, and a small amount of unreacted Ti for the 900℃-annealed Ti-coated diamond particles, and TiC particles for the 1050℃-annealed Ti-coated diamond particles.

(3) Ti-800-Cu/Dia, Ti-900-Cu/Dia, and Ti-1050-Cu/Dia composites are successfully fabricated by hot forging, the powder mixture of pre-annealed Ti-coated diamond particles and copper powders, at 800℃, and the diamond particles are uniformly distributed in those three composites.

(4) The TiC interface can be observed in the Ti-800-Cu/Dia composite, and the interface bonding is strongly attributed to the formation of fine TiC particles and the interface layer have a rough surface. However, both Ti-900-Cu/Dia and Ti-1050-Cu/Dia have a smooth and flat interface layer with relative coarse TiC particles. In addition, the coverage of diamond by the interface is about 79.5% for 800-Ti-Cu/Dia, 65.3% for 800-Ti-Cu/Dia, and 57.7% for 1050-Ti-Cu/Dia, respectively.

(5) Ti-800-Cu/Dia has the highest thermal conductivity among the three fabricated copper/diamond composites, with a value of 350W/ (mK). This is mainly attributed to a strong interface that is formed in the Ti-800-Cu/Dia, which promotes the phonon transfer between the diamond particles and the copper matrix.

5 Interface characteristics and thermal conductivity of Cu/55vol%Diamond (W-coated) composites

In Chapter 4, Ti-coated diamond particles are pre-annealed before hot forging to tune the interface characteristics of Cu/55vol%Ti-diamond composites. The results show that it is easier for the TiC particles form in the pre-annealing process and then the parts of the formed TiC particles are peeled from the diamond surface during hot forging, compared to the in-suit formed TiC nucleation in hot forging. The thermal conductivity of the Cu/55vol%Ti-diamond composites decreases with increasing the pre-annealing temperature. Due to the difference of metal elements' carbide forming ability and the acoustic properties of different carbides, pre-annealing different metal-coated diamond particles may cause different effects on the interface's characteristics and thermal conductivity of the fabricated composites.

Tungsten is another strong carbide forming element, tungsten carbides (WC and W_2C) can be obtained by the chemical reaction between tungsten atoms and the diamond. In this chapter, W-coated diamond particles are used to fabricate Cu/W-diamond composites, the interface characteristic of Cu/W-diamond composites is tailored by pre-annealing W-coated diamond particles before the fabrication process. We aim to investigate how the phase constitutions and the interface microstructure of the fabricated Cu/W-coated diamond composites vary before and after hot forging, and understand how the interface characteristics affect the thermal conductivity of the fabricated composite materials.

5.1 Pre-annealing of W-coated diamond

The microstructure of the as-received W-coated diamond particles is showed in Figure 5-1. It is clear to see that the W-coated diamond particles are in regular Cubo-octahedral shape and the tungsten layer on the diamond particles is uniform. Comparing with the backscatter image of non-coated diamond particles (Figure 4-1 a), W-coated diamond particles are much brighter due to the deposition of the tungsten layer on the diamond surface. In the high magnification, it can see that the coating is flat and small particles are observed on both diamond-{100} and -{111} facets (Figure 5-1 a1 and a2). The particles are tungsten due to the magnetic sputtering is operated in the room or low temperature, and no chemical reactions between tungsten and carbon.

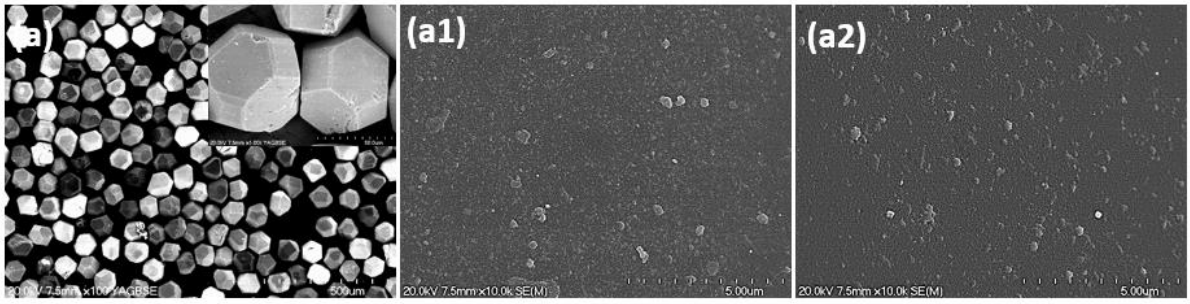

Figure 5-1 SEM microstructure of as-received W-coated diamond particles

In order to modify the W-coated diamond particles' microstructure, the diamond particles are pre-annealed at different temperatures, following the process carried for Ti-coated diamond particles. And also using the characterization technology of SEM, and XRD to observe the surface microstructure and phase compositions of the composites, respectively.

5.1.1 Diamond phase transformation after annealing

Figure 5-2 shows XRD patterns of the W-coated diamond particles before and after pre-annealing. The peaks of W and diamond are detected for the as-received W-coated diamond particles (Figure 5-2a), this can confirm that the particles on the W-diamond surface are tungsten (Figure 5-1 a1 and a2). XRD spectrum shows that the phase compositions of annealed W-coated diamond particles are still W and diamond when the pre-annealing temperature is below 1050℃, and become diamond, W, and W_2C when annealing at 1050℃ (Figure 5-2b). It suggests that the phase constitutions of W-coated diamond particles are not significantly changed when the annealing temperature is below 1050℃, and the kinetic conditions of the chemical reaction between diamond and tungsten to form W_2C can be satisfied when the pre-annealing temperature is over 1050℃. The formation of W_2C follows equation 5-1.

$$2W + C_{diamond} = W_2C \qquad 5\text{-}1$$

In addition, the intensity of W is stronger than that of W_2C in the XRD pattern when the pre-annealing temperature is 1050℃, suggesting that only a small amount of tungsten coating is reacted with the diamond to form W_2C. Furthermore, no graphite peaks are identified in the XRD patterns, indicating that the graphitization of diamond is not caused by these pre-annealing temperature profiles for 30min, this is consistent with the results of annealed Ti-coated diamond particles (Figure 4-2b). Thus, it can conclude that the reaction between tungsten and diamond is incomplete

(a large amount of W is not reacted) when the pre-annealing temperature is between 950℃ and 1050℃.

To further confirm the phase constitutions of W-coated diamond particles after pre-annealing at1050℃, EDS point analysis is carried out and the results are shown in Figure 5-3. The chemical compositions are composed of 89.75wt%W and 10.25wt%C at point 1, and 77.76 wt% W and 22.4wt%C at point 2, and 85.13wt% W and 14.87wt%C at point 3. The results of point 1 suggest that the white particles are likely uncoated tungsten atoms from the sputtering process. And the weight percentage of tungsten at position 2 and 3 slightly decrease compared to that at point 1, and they are possible to be W_2C. This indicates that the partial original tungsten coating layer is reacted with diamond, and this agrees with the XRD results (Figure 5-2b).

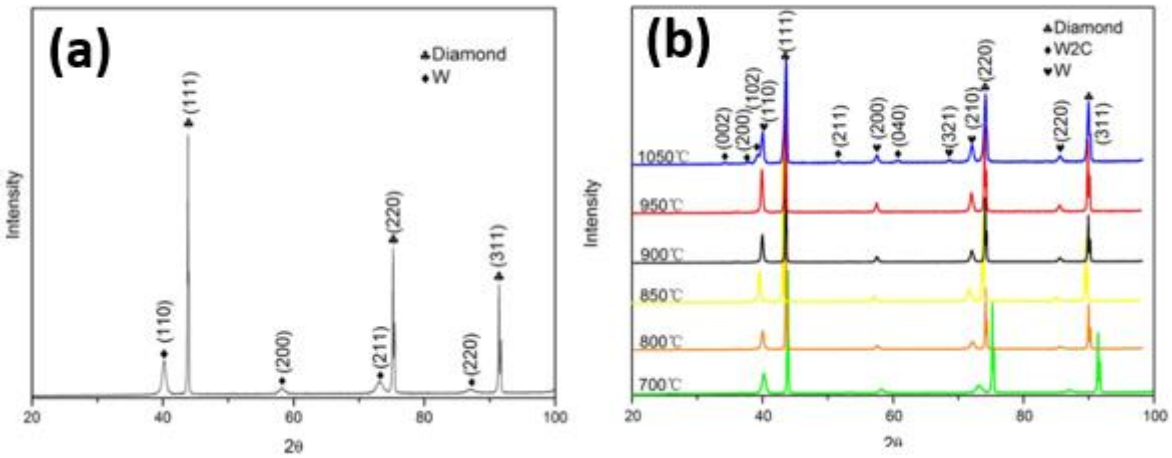

Figure 5-2 XRD patterns of the W-coated diamond after (a) magnetic sputtering; (b) pre-annealing at different temperatures

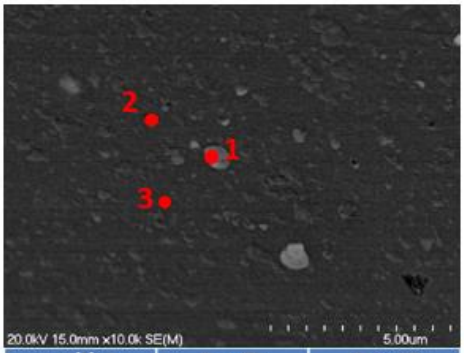

position	C- wt%	W- wt%
1	10.25	89.75
2	22.24	77.76
3	14.87	85.13

Figure 5-3 EDS point analysis of 1050℃-annealed W-coated diamond particles

5.1.2 Diamond surface characterization after annealing

Figure 5-4 presents the SEM microstructures of the W-coated diamond particles annealed at 900℃ and 1050℃ (referred to as W900, and W1050). W-coated diamond particles are fully enveloped with the coating layer after sputtering (Figure 5-1), while black areas are exposed on W900 and W1050 diamond particles, as shown in low magnification images (Figure 5-4a, b). According to the calculations, the coverage rate of W900 and W1050 diamond particles by the coating is 91.3% and 91.8%, respectively (Table 5-1).

Figure 5-4 a1 and a2 display the detailed morphology on diamond-{100} and -{111} facets of W900. The coating layer is flat and some particles are visible (as indicated by the circle) on both diamond-{100} and -{111} facets. The distinct morphology on the diamond-{100} and -{111} facets is the distribution of these particles. The particles on the diamond-{100} facet (Figure 5-4 a1) are more evenly dispersed than that on the diamond-{111} facet (Figure 5-4 a2). These particles on W900 are similar to that on as-received W-coated diamond (Figure 5-1). XRD patterns in Figure 5-2b suggest that no new phase forms after the W-coated diamond particles are annealed at 900℃ for 30min. Thus, it can conclude that the particles on W900 are tungsten. The grain boundary of these tungsten particles is much clearer and the grain size is bigger on both diamond-{100} and -{111} facets of W900 compared to the as-received W-coated diamond surface. This suggests pre-annealing at 900℃ will not cause the reaction between the diamond and tungsten coating but lead to the growth of the original tungsten particles on the diamond surface. Moreover, tungsten particles are agglomerated on the diamond-{111} facet and uniformly distribute on the diamond-{100} facet (as indicated by the red circle in Figure 5-4).

In the high magnification images of W1050, the coating layer is rougher on both diamond-{100} (Figure 5-4b1) and -{111} facets (Figure 5-4b2) than that on W900. And two types of particles are observed on the diamond-{100} and -{111} facets, which are white and grey particles (as indicated by the red circle and blue circle, respectively). XRD results reveal that a small amount of W_2C is formed by the reaction between the diamond and tungsten when the diamond particles are annealed at 1050℃ (Figure 5-2b). Thus, we can speculate that the white particles are W and the grey one is W_2C. From Figure 5-4 b1 and b2, a big amount of the un-reacted W particles are observed on the diamond-{100} facet than on the diamond-{111} facet. Moreover, relatively large W_2C particles can be observed on the diamond-{111} facet compared to the diamond-{100} facet from the detailed morphology of W1050 diamond particles, as shown in Figure 5-5a and b, respectively.

These indicate that W_2C nucleation and growth are more likely to occur on diamond {111} facets than on diamond {100} facets during annealing. This is because small {111} facets will form on diamond-{100} facet first, and then, the carbides will nucleate on those small {111} facets, similar to on the diamond-{111} facet. This confirms the results of the annealed Ti-coated diamond particles and the reason has been discussed in 4.2.6.1.

Table 5-1 Coverage rate by tungsten coating after pre-annealing

Samples	**The coverage rate of diamond particles by coating (%)**
W900	91.3
W1050	91.8

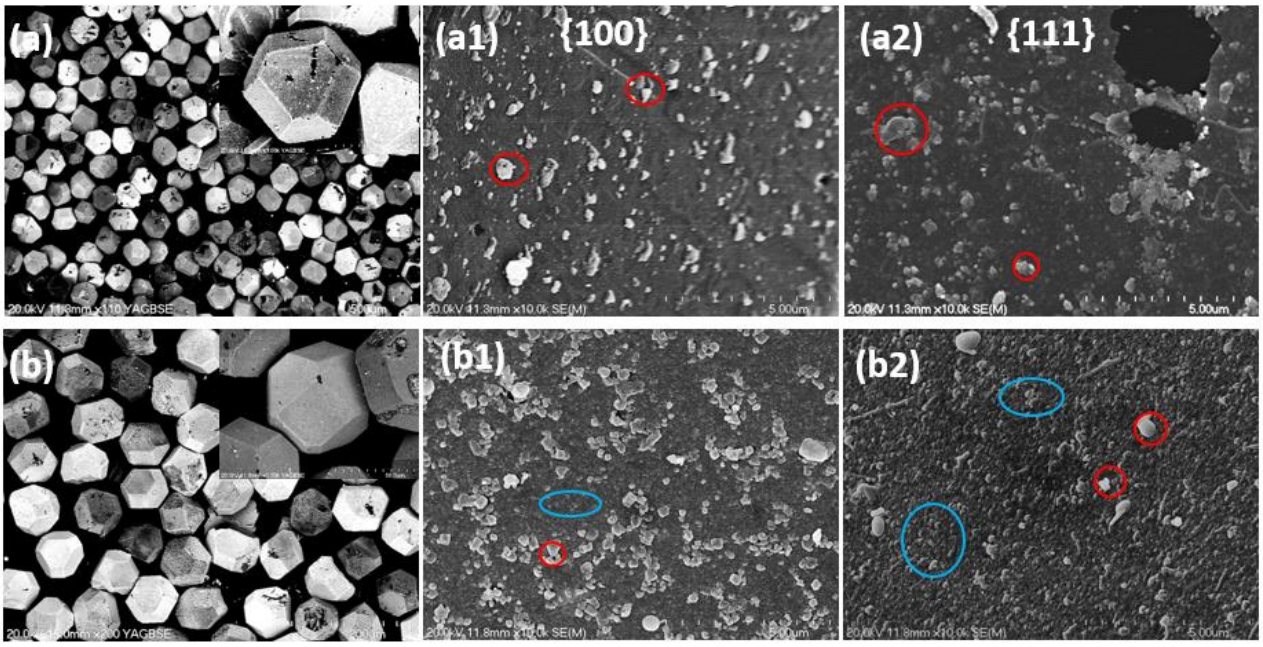

Figure 5-4 SEM microstructure of: (a) W900; (b) W1050. (a1) (b1) are corresponding diamond-{100} facets and (a2) (b2) are corresponding diamond-{111} facets

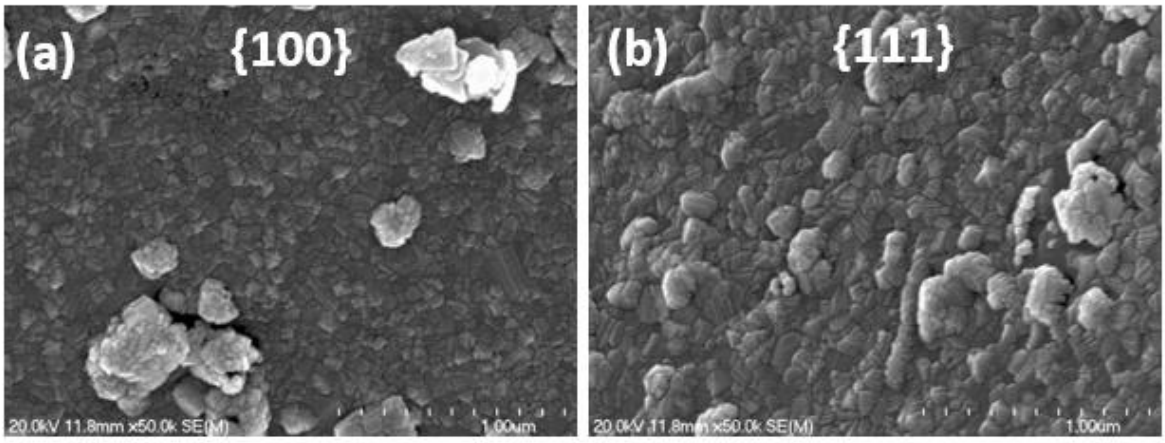

Figure 5-5 The detailed SEM microstructures of W1050 diamond particles: (a) diamond-{100} facet; and (b) diamond-{111} facet

5.2 Copper /55vol%Diamond (W-coated) composites

From Section Pre-annealing of W-coated diamond5.1, it can confirm that the phase compositions of W-coated diamond particles annealed at 900℃ are the same as the as-received W-diamond (including W and diamond), but their microstructure are different. The phase compositions of the 1050℃-annealed diamond particles are composed of diamond, W, and a small amount of W_2C. Thus, the as-received W-coated diamond, W900, and W1050 are used, respectively, to mix with copper to fabricate Cu/W-diamond composites by hot forging at 800℃. The three composites are named W-0-Cu/Dia, W-900-Cu/Dia, and W-1050-Cu/Dia, respectively. The details of the process parameters are listed in Table 5-2.

Table 5-2 Details of copper/55vol%diamond (W-coated) diamond composites

Samples	**Matrix**	**Diamond**		**Composites**
		Pre-annealing T(℃)	Holding Time (min)	Hot Forging T(℃)
W-0-Cu/Dia	Copper	-	-	800
W-900-Cu/Dia		900	30	800
W-1050-Cu/Dia		1050	30	800

5.2.1 Relative density

Figure 5-6 reveals the measured relative density of W-0-Cu/Dia, W-900-Cu/Dia, and W-1050-Cu/Dia composites. The relative density of the three composites is higher than 95% and it is 95.4% for the W-0-Cu/Dia, 97% for W-900-Cu/Dia, and 95.04% for W-1050-Cu/Dia. This suggests the

changes in the diamond coating characteristics can improve the density of the fabricated composites, and the reason to cause W-1050-Cu/Dia having a relatively low density will be discussed in the following sections.

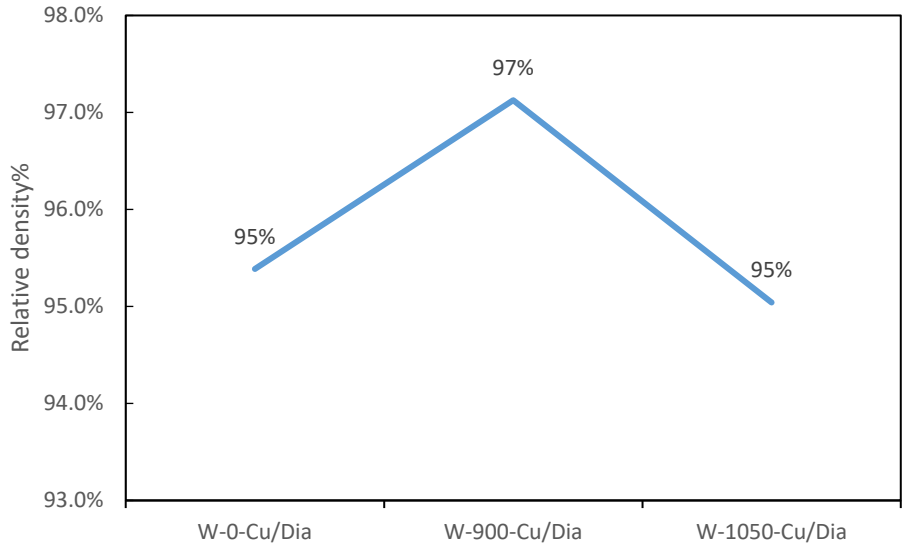

Figure 5-6 The measured relative density of W-0-Cu/Dia, W-900-Cu/Dia, and W-1050-Cu/Dia composites

5.2.2 Phase constitutions

The X-ray diffraction patterns of the fabricated Cu/W-coated diamond composites (W-0-Cu/Dia, W-900-Cu/Dia, and W-1050-Cu/Dia) are displayed in Figure 5-7. The diffraction peaks of copper, diamond, W_2C, and WC are detected in the XRD patterns of W-0-Cu/Dia composite, and the number and the intensity of the W_2C are more than that of WC. The same peaks of copper, diamond, W, and WC are identified in the W-900-Cu/Dia and W-1050-Cu/Dia composites and no W_2C peaks are identified in both composites. However, the intensity of the W and WC peaks is different, the intensity of the W peak is higher than that of WC in W-900-Cu/Dia composite, while WC is the domain phase in W-1050-Cu/Dia composite.

The phase compositions in W-0-Cu/Dia and W-900-Cu/Dia are the same (W, diamond, and copper) before hot forging, but different after hot forging. This suggests that pre-annealing can cause the chemical reactions between the tungsten coating and the diamond to form different tungsten carbides during hot forging. For W-0-Cu/Dia, the tungsten coating reacts with the diamond to preferentially form W_2C, and the W_2C will further react with the diamond to form WC, as seen in equation 5-1 and 5-2. For W-900-Cu/Dia, the diamond reacts with tungsten to generate the WC

phase during the hot forging process, as shown in equation 5-2. This indicates that pre-annealing is beneficial for improving the activation of the chemical reaction between the tungsten coating and diamond during hot forging at 800℃.

$$W + C_{diamond} = WC \quad (5\text{-}2)$$

$$W_2C + C_{diamond} = WC \quad (5\text{-}3)$$

For W-1050-Cu/Dia composite, the preformed W_2C during annealing can be further reacted with the diamond to form WC, as seen in equation 5-3. Therefore, the WC phase in W-1050-Cu/Dia composite is formed in two ways: (1) the partial WC is obtained by the reaction of W_2C formed in the pre-annealing stage with the diamond during hot forging, due to the WC is more stable compared to the metastable W_2C; (2) the rest of the WC is formed by the reaction between the diamond and the tungsten coating directly during hot forging, as listed in equation 5-2. The comparison of phase compositions of the three composites before and after hot forging is listed in Table 5-3.

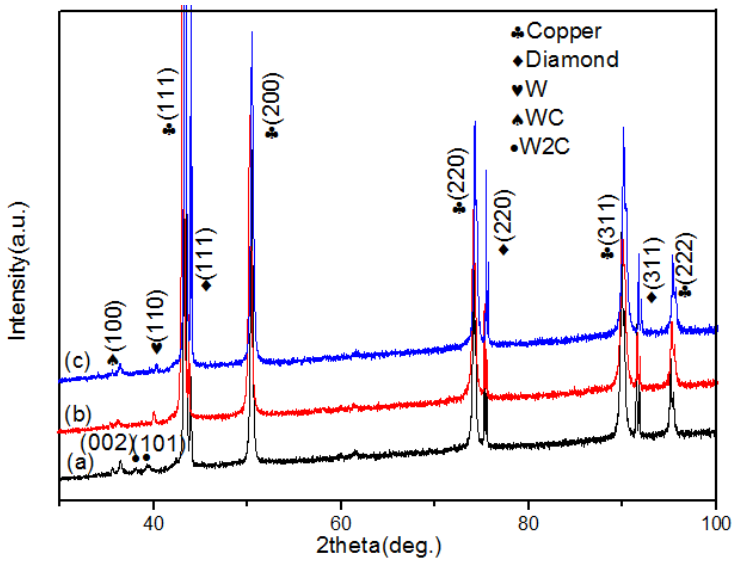

Figure 5-7 X-ray diffraction of (a) W-0-Cu/Dia; (b) W-900-Cu/Dia, and (c) W-1050-Cu/Dia composites

Table 5-3 Phase constitutions of Cu/55vol%diamond (W-coated) composites before and after hot forging at 800℃

Specimens	Before hot forging	After hot forging
W-0-Cu/Dia	Copper, Diamond, W	Copper, Diamond, A large amount of W_2C, A small amount of WC
W-900-Cu/Dia	Copper, Diamond, W	Copper, Diamond, A relatively large amount of W, A small amount of WC
W-1050-Cu/Dia	Copper, diamond, W, little W_2C	Copper, Diamond A relatively large amount of W, A large amount of WC

5.2.3 Microstructure

5.2.3.1 Microstructure of 800℃-forged composite materials

Figure 5-8 illustrates the SEM microstructure of Cu/55vol%W-diamond (W-0-Cu/Dia, W-900-Cu/Dia, and W-1050-Cu/Dia) composites. It is clear to see that the diamond particles are uniformly dispersed in the copper matrix for all those three composites and no diamond particles are detached from the copper matrix in W-0-Cu/Dia and W-1050-Cu/Dia composite (Figure 5-8a, and g), this attributes to the formation of the interphase layer improve the chemical affinity between the copper and the diamond. However, in W-900-Cu/Dia, several diamond particles are detached from the cooper matrix (as indicated by the red arrows, in Figure 5-8d) as preparing the SEM specimen, indicating the poor interfacial bonding between the copper and the diamond.

In W-0-Cu/Dia composites, from the observation of the high magnification images, the interface is visible on the diamond particles (as indicated by the blue arrow), which is not continuous and in sporadic distribution, as shown in Figure 5-8 c, and small voids and gaps can be observed between the copper and the diamond (as indicated by the circle). The interface layer is composed of a large amount of W_2C and a small amount of WC, as proved by the XRD results (Figure 5-7).

In W-900-Cu/Dia and W-1050-Cu/Dia, the interface is found in both composites (as indicated by the blue arrows), and no visible cracks and voids are found at the vicinity of the interface in both fabricated Cu/W-diamond composites (Figure 5-8 f and i). For W-900-Cu/Dia, it can see a thin interface layer, which is relatively continuous compared to the W-0-Cu/Dia. In the W-1050-Cu/Dia composite, the interface is much thicker than that in W-900-Cu/Dia. XRD results reveal that the interface's phase composition includes W and a small amount of WC in W-900-Cu/Dia, and a large

amount of WC and a small amount of W in W-1050-Cu/Dia composite, as shown in Figure 5-7. In addition, it is reported that the interfacial bonding in the copper/diamond composites with W interface is weaker than that with WC interface [48, 60]. Therefore, we can speculate the formed interface is composed of W and WC in the W-900-Cu/Dia and W-1050-Cu/Dia composites, and the W-1050-Cu/Dia composite has the strongest interface bonding between the diamond and the copper among the three fabricated composites.

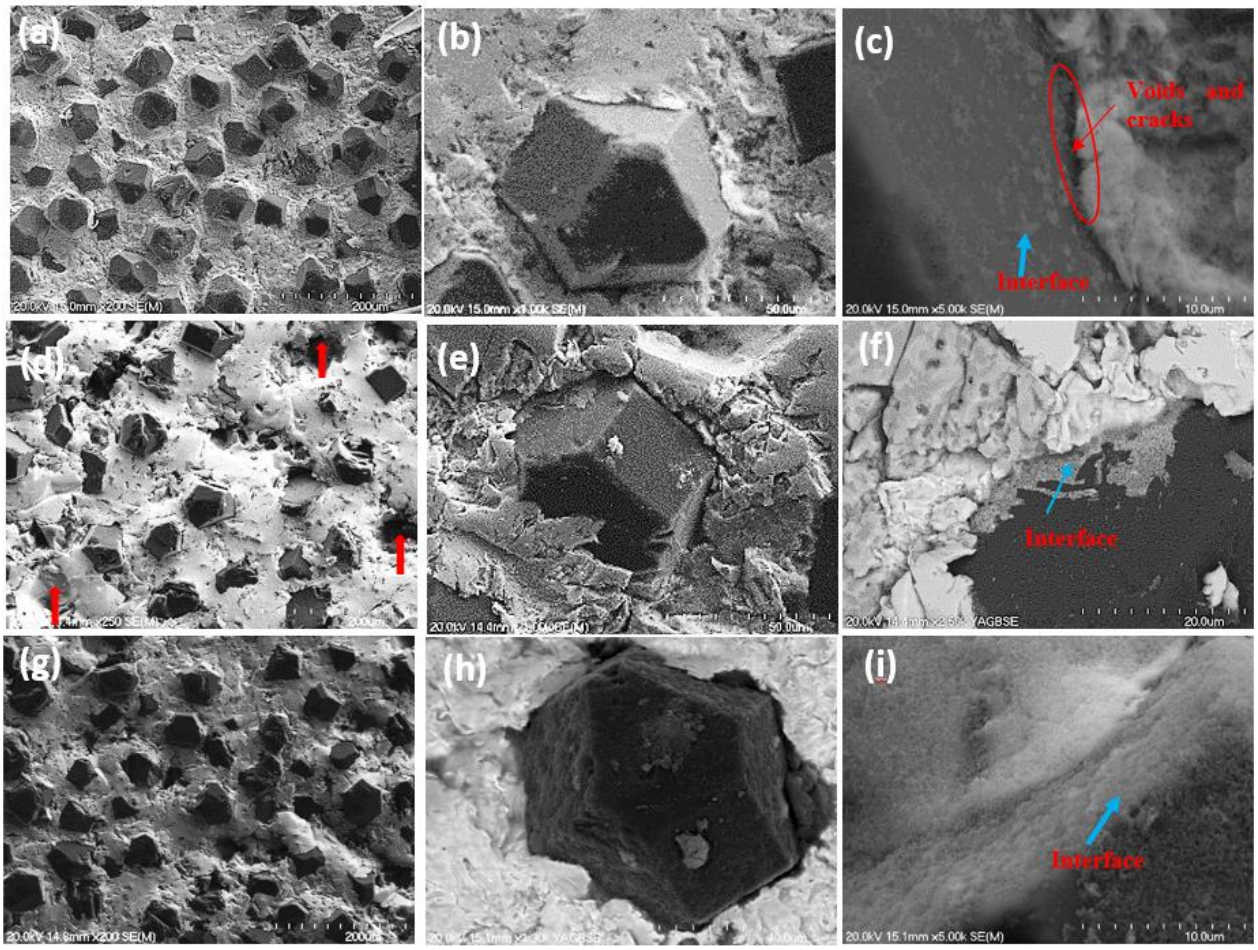

Figure 5-8 Microstructure of (a-c) W-0-Cu/Dia, (d-f) W-900-Cu/Dia, and (g-i) W-1050-Cu/Dia composites

5.2.3.2 Morphology of extracted diamond particles from the fabricated copper/W-coated diamond composites

To further research on the characteristics of the interface in the W-0-Cu/Dia, W-900/Cu/Dia, and W-1050-Cu/Dia composites, the diamond particles are extracted from the three composites will also be characterized by SEM, respectively, as shown in Figure 5-9. It is clear to see the most of the diamond particles extracted from W-0-Cu/Dia and W-1050-Cu/Dia composites are covered by the

interface (mainly W_2C for W-0-Cu/Dia, and WC for W-1050-Cu/Dia), as shown in bright color (Figure 5-9a, c), and the coverage rate of diamond particles extracted from the two composites by the interface is 75% and 83%, respectively. However, the coverage rate of diamond particles by the interface is only about 10% for the W-900-Cu/Dia, and most diamond particles are without interface attached (diamond particles show dark color), as shown in Figure 5-9b. The details of the statistic coverage rate of diamond particles by the formed interface for the three composites are listed in Table 5-4.

Before hot forging, the as-received W-coated diamond particles are completely enveloped with original W-coating, this indicates that most of the spallation of the interface from W-0-Cu/Dia diamond particles occurs during hot forging. The coverage rate of W900 and W1050 diamond particles by original W-coating or formed W_2C interfacial layer (only for W1050) is about 91%, and the observed spallation from the diamond particles is caused by the diffusion of the tungsten atoms during annealing. The phase compositions of W-900-Cu/Dia and W-1050-Cu/Dia composites are composed of diamond, copper, tungsten, and WC. Therefore, the exposed diamond area for W-900-Cu/Dia and W-1050-Cu/Dia composites is due to (1) the spallation of the formed interface during hot forging; (2) the acid corrosion of tungsten during the acid extraction process. The high coverage rate of extracted diamond particles by the interface for the W-1050-Cu/Dia composite indicates that a large amount of WC is formed at the interface, compared to W-0-Cu/Dia and W-900-Cu/Dia composites, and WC particles have stronger interfacial bonding with diamond than W_2C.

The high magnification images in Figure 5-9 reveals the detailed morphology on the diamond-{100} facet (Figure 5-9 a1, b1, and c1) and diamond-{111} facets (Figure 5-9 a2, b2, and c2) extracted from W-0-Cu/Dia, W-900-Cu/Dia, and W-1050-Cu/Dia composites, respectively. In the case of the diamond particles extracted from W-0-Cu/Dia (Figure 5-9), it is clear to see the diamond coating on both diamond-{100} and -{111} facets is not flat as that of the original W-coated diamond particles. This attributes to the nucleation of the W_2C and WC occurs due to the chemical reaction between the diamond and tungsten during hot forging. The interface on the diamond-{100} facet is a double-layer structure (Figure 5-9 a1), while only one interface layer can be observed on the diamond-{111} facet (Figure 5-9 a2).

For the diamond particles extracted from W-900-Cu/Dia, the interphase layer on the extracted diamond is relatively rough on both diamond-{100} and -{111} facets compared to the 900-annealed W-diamond particles, as shown in Figure 5-9b1 and b2. It can be seen that only one coating layer forms on both diamond-{100} and-{111} facets for W-900-Cu/Dia composites, and it

is not continuous. The rough surface and the one-layer coating are caused by the nucleation of the WC particles through the reaction between tungsten and the diamond during hot forging. We know that the pre-annealing of W-coated diamond particles at 900°C has no significant change on phase composition but it does change the tungsten element distribution, and this leads to the preference of the WC formation (confirmed by XRD results in Figure 5-7). In addition, the morphology of WC particles has no significant difference on diamond -{100} and -{111} facets, and this suggests that the anisotropic chemical reaction between tungsten and diamond can be eliminated by pre-annealing the W-coated diamond particles at 900℃.

The details of the interface morphology on both diamond-{100} and -{111} facets extracted from W-1050-Cu/Dia illustrate in Figure 5-9 c1 and c2, respectively. WC particles can be observed on both diamond-{100} and -{111} facets, and these WC particles cause a rough diamond surface. It finds that the WC layer in W-1050-Cu/Dia composites is more continuous and denser and its grain boundary is much clearer, comparing to the W-900-Cu/Dia. We know that partial W-coating is transferred to W_2C particles after annealing at 1050℃ for 30min (Figure 5-2b), and the un-reacted tungsten is still attached to the diamond surface. During hot forging, the un-reacted tungsten will further react with the diamond to form WC and the W_2C will also react with tungsten to form WC, resulting in a continuous, rough and relatively thick interfacial layer is formed in the W-1050-Cu/Dia. This is beneficial for forming an adhesion bonding between the interface and the copper in the composites.

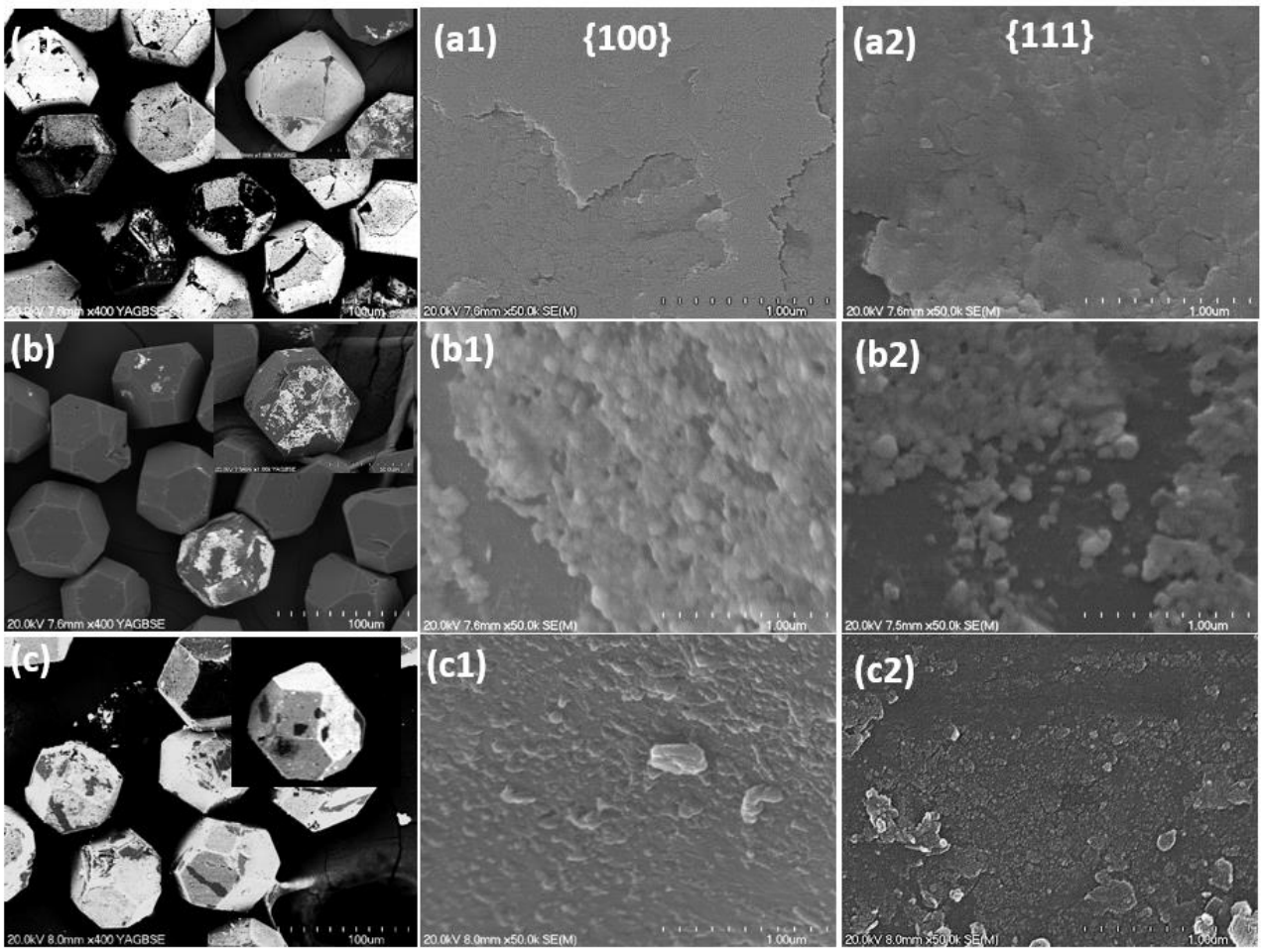

Figure 5-9 Extracted diamond particles from: (a)W-0-Cu/Dia; (b) W-900-Cu/Dia; (c)W-1050-Cu/Dia composites, (a1), (b1), (c1) are corresponding the diamond-{100} facets and (a2), (b2), (c2) are the corresponding the diamond-{111} facets

Table 5-4 Coverage rate of the diamond by coating before and after hot forging

Coverage diamond area (%)	**W-0-Cu/Dia**	**W-900-Cu/Dia**	**W-1050-Cu/Dia**
Before hot forging	100	91.3	91.8
After hot forging (800℃)	75	10	83.6

5.2.4 Thermal conductivity

The thermal diffusivity (α) and thermal conductivity (k) of the three fabricated Cu/W-coated diamond (W-0-Cu/Dia, W-900-Cu/Dia, and W-1050-Cu/Dia) composites are plotted in Figure 5-10. The thermal conductivity for W-1050-Cu/Dia composites is 223W/ (mK), which is higher than that

of W-0-Cu/Dia (184 W/ (mK)) and W-900-Cu/Dia (208 W/ (mK)) composites. It suggests that pre-annealing of W-coated diamond particles has positive effects on the thermal conductivity of the fabricated Cu/W-diamond composites. W-1050-Cu/Dia composite has a higher thermal conductivity but lower relative density in the three composites, this indicates that the interface structure has more contribution to the thermal conductivity of Cu/W-diamond composites compared to the composite's relative density. This agrees with the results obtained for the Cu/Ti-diamond composites (Section 4.2.4).

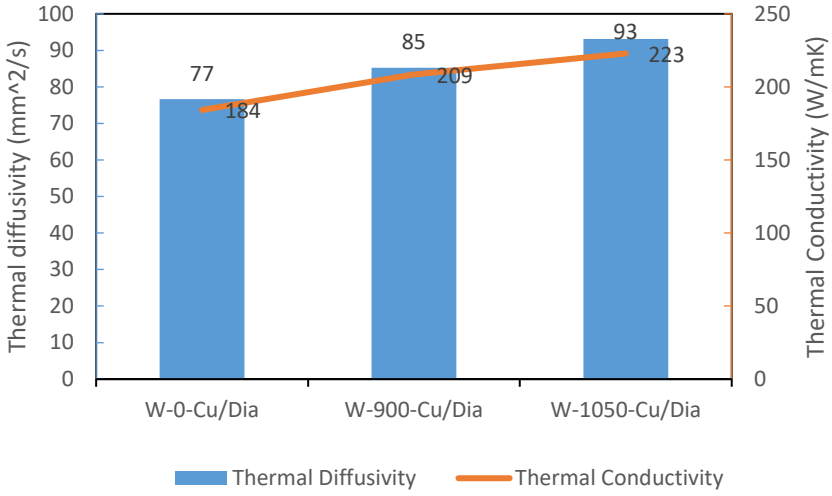

Figure 5-10 Thermal diffusivity and thermal conductivity of W-0-Cu/Dia, W-900-Cu/Dia, and W-1050-Cu/Dia composites

5.2.5 Theoretical thermal conductivity

For Cu/55vol%W- diamond composites, differential effective medium (DEM) is also used to calculate the theoretical thermal conductivity value to compare the measured theoretical thermal conductivity with the theoretical thermal conductivity. The calculated equation and process are shown in 4.2.5.

The theoretical thermal conductivity of Cu/W-diamond composite is calculated based on equation 4-2. In this study, the particle size of the W-coated diamond is 230/270 mesh on average, and the volume fraction of the diamond is 55% for the three composites (W-0-Cu/Dia, W-900-Cu/Dia, and W-1050-Cu/Dia). In addition, the thermal conductivity of diamond is 1500W/ (mK) and 224W/ (mK) for copper, the thermal conductivity of copper is lower than the standard pure copper (400W/ (mK)) due to the deformed structure of the hot-forged copper [65]. Tungsten and tungsten carbides

are coexisting at the interface in Cu/W-diamond composites prepared from the annealed W-diamond particles. Therefore, the extreme condition for Cu/W-diamond composites is that tungsten is fully covered on the diamond surface after hot forging, or tungsten is fully transferred into WC.

If there is no phase transformation during hot forging, only tungsten exists at the interface. The thermal resistance in Cu/W-diamond composites is from the interfaces of Cu/W, W interlayer, and W/diamond, like a thermal resistance series mode, as shown in Figure 5-11. The interfacial thermal conductance (G_C) can be expressed:

$$\frac{1}{G_C} = \frac{1}{G_{Cu/W}} + \frac{d}{k_W} + \frac{1}{G_{G_{W/diamond}}} \qquad 5\text{-}4$$

where k_W is the thermal conductivity of W, d is the thickness of the W interfacial layer, and $G_{Cu/W}, G_{W/diamond}$ are the thermal conductance of the interface between copper and W, and W and diamond.

When the tungsten is fully transferred into tungsten carbides after hot forging, the thermal resistance for the Cu/W-diamond composites is from the Cu/W interface, W interlayer, and W/diamond the interfacial thermal conductance (G_C) can be expressed:

$$\frac{1}{G_c} = \frac{1}{G_{Cu/WC}} + \frac{d}{k_{WC}} + \frac{1}{G_{WC/diamond}} \qquad 5\text{-}5$$

where k_{WC} is the thermal conductivity of WC, d is the thickness of the WC interfacial layer, and $G_{Cu/W}, G_{W/diamond}$ are the thermal conductance of the interface between copper and WC, and WC and diamond.

The thermal conductance of Cu/W and W/diamond is determined by equation 4-4, we obtain the thermal conductance of the composites with the tungsten interface is 8 ×10^4 W/ m^2K, while 2.5×10^5 W/ m^2K for WC interface composites. The thickness of both W and WC interface is estimated to be 50nm, assuming the W-coating (50nm) is uniformly reacted with diamond and the interface is continuous for both tungsten and tungsten carbides, and based on the balance of the tungsten amount before and after the reaction, the thickness of the interface is about 50nm. Substituting the related value to equation 4-2, the theoretical thermal conductivity of Cu/W-diamond composite with W interphase layer and WC interface layer is 800 W/ (mK) and 808W/ (mK), respectively. The material properties used in the calculation are listed in Table 5-5. The measured results are lower than the theoretical value, this is because of the spallation of the formed interface from the diamond surface after hot forging.

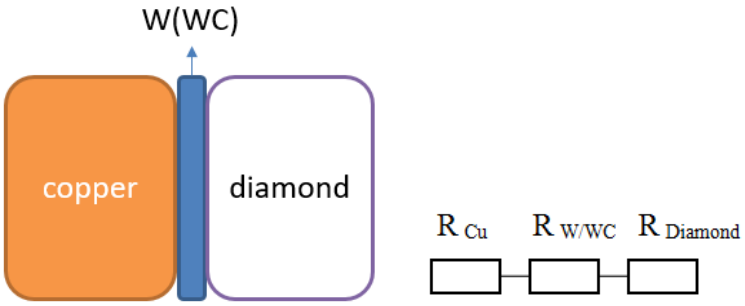

Figure 5-11 Interface structure in Cu/W-diamond composites

Table 5-5 Material properties for theoretic thermal conductivity calculation of Cu/W-diamond composites [66], [71]

Materials	**Thermal conductivity (W/mK)**	**Density (kg/m3)**	**Specific heat (KJ/ m^3K)**	**Phonon velocity (m/s)**	**Acoustic impedance (10^7 kg/m^2s)**
Diamond	1500	3520	1784	13430	4.73
Cu	224	8900	3426	2801	2.49
W	178	19320	2570	4029	7.79
WC	120	14900	3025	4697	7

5.2.6 Discussion

5.2.6.1 Effect of pre-annealing temperature on the formation of W-diamond particles

When the annealing temperature is below 1050℃, the tungsten coating has no significant change in phase compositions. It is reported that the reaction temperature of the carbon and the tungsten is 1000℃ [60], therefore, it is reasonable that the phase composition of the W-coated diamond does not change when the annealing temperature is below 1050℃. Other researchers reported that the phase compositions of the W-coated diamond are composed of W_2C and WC when the annealing temperature is 900℃ for 2h [72], this is likely due to the long holding time prompts the reaction between the diamond and the tungsten at 900℃. Thus, increasing holding time or temperature can speed up the reaction between tungsten and diamond.

Furthermore, the XRD results suggest that there is no new phase formed on W900, but the coating spallation area is observed on both W900 and W1050 diamond particles. This is because the high pre-annealing temperature can promote atomic diffusion and this leads to unstable coating structure and poor interfacial bond strength between the tungsten and the diamond, resulting in tungsten

coating is peeled off from the diamond surface. The formation of the tungsten carbide needs more tungsten elements, so tungsten atoms will diffuse to the preferential location to form carbide particles, such as the defect sites. When the annealing temperature is 1050℃, it can see that W_2C particles and unreacted W particles disperse on both diamond-{100} and -{111} facets from the SEM microstructure (Figure 5-5). However, diamond atoms on diamond-{100} facet have a slower reaction with tungsten coating than diamond-{111} facet during pre-annealing at 1050℃. This is because it is easy for the diamond-{111} facet to have the transformation from sp^3 to sp^2. This has explained in Chapter 4.2.6.1.

5.2.6.2 Effect of pre-annealing temperature on the microstructure of Cu/W-diamond composites

The phase composition of the W coating on the diamond particles is only changed when the annealing temperature is above 1050℃, and it primarily includes a large amount of W and a small amount of W_2C particles, and the W_2C particles are mainly distributed on the diamond-{111} facet. W900 and the as-received W-diamond particles have the same coating composition (only tungsten), but different coating microstructure. The tungsten particles are aggregation on W900 the diamond particles especially on the diamond-{111} facet, compared to the as-received W-diamond particles that have a uniform distribution of W.

During hot forging at 800℃, the tungsten reacts with the diamond first to form W_2C, and then W_2C reacts with the diamond to form WC at the interface in W-0-Cu/Dia, the second reaction is incomplete due to the short fabrication time. Surprisingly, the W_2C and WC are identified in the W-0-Cu/Dia composite after hot forging at 800℃ even if the fabricating temperature is lower than the reaction temperature of the diamond and the tungsten (1000℃[60]). This suggests the reaction between the diamond and the tungsten coating can be promoted by the combined effects of the pressure introduced by large plastic deformation and temperature (800℃).

The reaction between the tungsten and the diamond also displays in the W-900-Cu/Dia and W-1050-Cu/Dia, however, the WC is directly obtained by the reaction between the diamond and tungsten. This is due to the pre-annealing changes in the distribution or the phase compositions of the W coating. Except that, the preformed W_2C in W-1050-Cu/Dia will also react with the diamond to form WC during hot forging, leading to the formation of a rough and continuous interphase layer (Figure 5-9c) and thus enlarging the contact area with the copper matrix to help improve the interfacial bonding strength between the copper and the diamond. However, a large amount of WC

formed in W-1050-Cu/Dia that induces a lot of defects at the interface, and this causes the densification of W-1050-Cu/Dia composites is slightly lower than the W-900-Cu/Dia.

Figure 5-12 sketches the internal stress variation during Cu/W-diamond composites fabrication process. For W-0-Cu/Dia, the spallation of the interface from the diamond is mainly caused by the variation of the internal stress during the hot forging. During the hot forging, the large plastic deformation will induce compressive stress at the interface and large tensile stress will be induced at the interface when the sample is cooled from the high temperature due to the different CTE between the copper and the diamond (17ppm for Cu, and 2ppm for diamond). The tensile stress can release the formed compressive stress at the interface and also result in the delamination of the interface [65]. The reason for the low interface coverage of diamond particles by the interface of W-900-Cu/Dia composite is because only a small amount of WC is formed at the interface during the hot forging process and W interface is etched during the corrosion process. The further reaction between the diamond and the diamond coating (W or W_2C) in W-1050-Cu/Dia during hot forging displays in Figure 5-13. Diamond prefers to react with W_2C to form WC due to the W_2C particles directly contacts with the diamond after pre-annealing. After that, carbon atoms diffuse to react with W to form new WC particles through the formed WC layer. Besides, W_2C formed in the annealing can be broke due to it is brittle phase (same as the spallation of TiC, see in 4.2.6.2). These lead to the spallation of the WC interface in W-1050-Cu/Dia.

From the resultant composite's microstructure, visible voids and gaps are observed between the copper and the diamond in W-0-Cu/Dia composite, but not identified in W-1050-Cu/Dia, suggesting that the W_2C interface forms the weaker interfacial bonding with the copper matrix than WC. The detached diamond particles from the copper in W-900-Cu/Dia also means the formed interfacial bonding between the copper and the diamond is poor, this is ascribed to a large amount of tungsten remains on the diamond surface. It reported that the interfacial bonding in the copper/diamond composites with W interface is weaker than that with WC interface [48, 60].

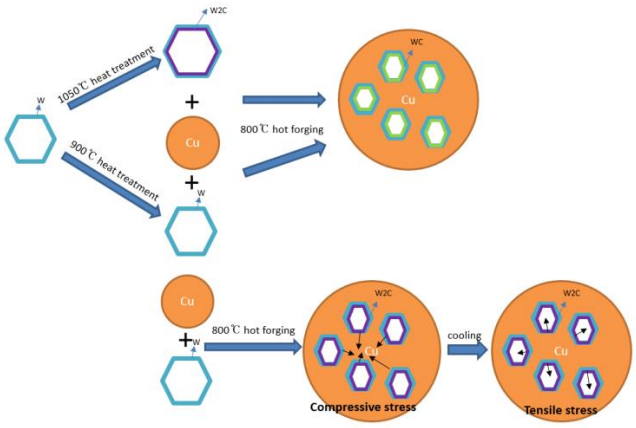

Figure 5-12 The fabrication process of Cu/W-diamond composites

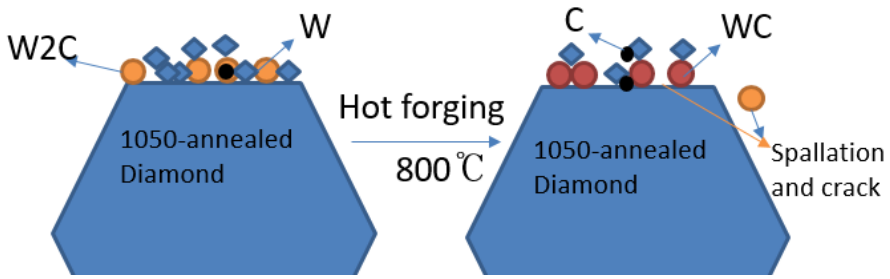

Figure 5-13 Further reaction in W-1050-Cu/Dia composite during hot forging

5.2.6.3 Effect of pre-annealing temperature on Cu/W-diamond composites' TC

Pre-annealing on W-diamond particles is a benefit for improving the thermal conductivity of the hot-forged Cu/W-diamond composites. The thermal conductivity is higher for W-1050-Cu/Dia composite than for W-900-Cu/Dia and W-0-Cu/Dia composites is because: (1) the formation of W_2C during pre-annealing prompts the reaction between the diamond and tungsten coating leads to more in-suit tungsten mono-carbides can form in the short hot forging process compared to W-900-Cu/Dia composites, and the formed WC layer acts as a bridge for phonons transport between copper and diamond; and (2) the phase compositions at the interface are consists of a large amount of WC and a small amount of W. Although tungsten is fully transferred into tungsten carbides (WC and W_2C) for W-0-Cu/Dia composites after hot forging, the thermal conductivity of tungsten semi-carbides (29-36W/ (mK)) [71] is lower than that of the metal tungsten (178W/ (mK)) and tungsten mono-carbides (29-121 W/ (mK)) [66], the existence of the large amount of W_2C increase the thermal resistance at the interface and leads to the low thermal conductivity of Cu/W-diamond composites.

5.2.6.4 Effect of the coating type on Cu/diamond composites

Pre-annealing on Ti-diamond and W-diamond particles have different influences on the coated-diamond particles and the thermal conductivity of resultant Cu/coated-diamond composites. Comparing the phase compositions and microstructure of annealed W-coated diamond with annealed Ti-coated diamond, it finds that the annealing temperature for the formation of the TiC and tungsten carbides is different. Titanium has a higher specific heat capacity (522 J/kg K) than tungsten (133 J/kg K), which means titanium has a strong ability to absorb or dissipate heat, therefore, the formation of TiC is much easier than WxC at the same pre-annealing temperature.

Also, TiC can be gained from one reaction step between the diamond and the titanium. However, the reaction between tungsten and diamond is complicated. During hot forging, TiC particles start to grow due to most of the TiC particles has nucleated in the annealing, and it is easy for the pressure to act on the interface directly, resulting in the spallation of TiC particles from the diamond, which is too brittle to undertake high external pressure. However, due to a small amount of W_2C formed during annealing, the spallation of the interface caused by this reason is in a small proportion and the nucleation of the WC still occurs by the reaction between the diamond and the tungsten, and the diamond and the W_2C. This leads to more in-suit metal carbides particles forms during hot forging, thus decreasing the spallation possibility of the formed interface from the diamond particles and then improving the chemical affinity between the copper and the diamond. Thus, the pre-annealed Ti-coated diamond and W-coated diamond particles lead to a different influence on the thermal conductivity of Cu/diamond composites.

In the copper/diamond composites, the Debye temperature of the transition layer should be approximately the square root of the product of the Debye temperature of the copper (310K) and diamond (1860K), which is about 760K [73]. The Debye temperature for TiC and WC is 614K [74] and 653K [75], respectively. Therefore, both TiC and WC are suitable for being the interphase layer in the copper/diamond composites to increase the phonon transfer across the interface. In this study, Cu/Ti-diamond composites show higher thermal conductivity than Cu/W-diamond composites. This is mainly because (1) the coverage rate of the diamond particles by TiC interface is more than that by WC; and (2) from the interface morphology, the TiC interface covered on the diamond is rougher than the WC interface which is helpful to improve the interfacial bonding strength and the thermal conductivity of the composites; (3) Ti coating can enhance the interfacial bonding between the copper and the diamond due to Ti atoms can diffuse to the copper matrix to form a solid solution [76] (not detected in this study, probably due to a small amount of Cu-Ti is formed).

5.2.7 Summary

This chapter studies the interface structure and thermal conductivity of the fabricated copper/ diamond composites from the pre-annealed W-coated –diamond particles. The results show below:

(1) The coating's phase constitution is not changed when the W-coated diamond particles are annealed below 1050℃ (only tungsten), and it has changed for the 1050-annealed diamond which includes a small amount of W_2C and a large amount of W.

(2) The reaction between the diamond and tungsten only can occur at pre-annealing of 1050℃ for 30mins, and it is more active on diamond-{111} facet than on diamond-{100} facet. The pre-annealing temperature of lower than 1050℃ has no evident effects on the diamond coating phase compositions, but it changes the distribution of the W atoms, which is beneficial for the reaction between the tungsten and the diamond to directly form WC in the fabrication.

(3) W-0-Cu/Dia, W-900-Cu/Dia, and W-1050-Cu/Dia composites are successfully prepared by hot forging at 800℃, the diamond particles are evenly distributed in the copper matrix.

(4) The phase compositions in the W-0-Cu/Dia (primarily include a large amount of W_2C and a small amount of WC) are different from the composites prepared by the annealed W-diamond particles (consist of W and WC). W_2C has relatively high thermal resistance than WC and W, which will decrease the interfacial conductance. The WC interface can be observed in W-900-Cu/Dia and W-1050-Cu/Dia, with a coverage value of 10% and 83.6%, respectively. The formation of the WC ensures good interfacial bonding performance between diamond and copper.

(5) The thermal conductivity of W-1050-Cu/Dia is 223W/ (mK), which is the highest one among the three fabricated copper/W-diamond composites. This attributes to the strong interfacial bonding between the interface and the diamond and the copper matrix, which improve the phonon transport in the composites. Controlling the degree of the reaction between tungsten and diamond can affect the formation of the W_2C particles formed in annealing and the nucleation of the WC during hot forging. Therefore, the thermal conductivity of the Cu/W-diamond composites may be adjustable by varying the pre-annealing temperature.

6 Effect of fabrication process on the interface characteristics and thermal conductivity of Cu/Ti-diamond composites.

In previous chapters, we investigated the influence of pre-annealing of the Ti-coated/ W-coated diamond particles on the interface characteristics and thermal conductivity of Cu/Ti-diamond and Cu/W-diamond composites, respectively. It demonstrates that the carbide forming ability of Ti and W is different during annealing, and pre-annealing of diamond particles can promote both reactions between the diamond and the titanium or tungsten coating, which has different effects on the interface microstructure and thermal conductivity of the Cu/Ti-diamond and Cu/W-diamond composites.

In this chapter, we will further investigate Cu/Ti-diamond prepared by vacuum sintering (refer to as Cu/Ti-Dia-VS), and the combination of vacuum sintering and hot forging (refer to as Cu/Ti-Dia-VSHF). The results of the two composites are used to compare with our previous work (Cu/Ti-diamond composite, which is directly fabricated by hot forging at 800℃, refers to as Cu/Ti-Dia-HF [65]), and then to analyze how the interface forms and evolves during the processing and affects the resultant thermal conductivity of the fabricated composites.

6.1 Cu/Ti-diamond composites

6.1.1 Relative density

The measured relative density of Cu/Ti-Dia-VS and Cu/Ti-Dia-VSHF composites is listed in Table 6-1. The data reveals that the relative density of the fabricated Cu/Ti-diamond composite is only 73% after vacuum sintering, the relative density of sintered composites (Cu/Ti-Dia-VSHF) is increased to 93% after hot forging. This suggests that the hot forging is suitable to prepare copper/diamond composites with a low porosity level.

Table 6-1 The measured the relative density of the Cu/Ti-Dia-VS and Cu/Ti-Dia-VSHF composites

Composite	Relative Density %
Cu/Ti-Dia-VS	73
Cu/Ti-Dia-VSHF	93

6.1.2 Phase constitutions

Figure 6-1a, and b show the phase constitutions of the fabricated copper/diamond composites (Cu/Ti-Dia-VS and Cu/Ti-Dia-VSHF, respectively). The peaks of the copper, diamond, and TiC are detected in the XRD spectra of the two composites, and no titanium peak is identified. These suggest that the Ti coating can react with the diamond to form the TiC phase during vacuum sintering process, and this reaction is almost complete. Except that, it is worth noticing that the intensity of the TiC peak in Cu/Ti-Dia-VS is higher than in Cu/Ti-Dia-VSHF, which means that the relative higher quantity of TiC in Cu/Ti-Dia-VS composite. XRD pattern of Cu/Ti-Dia-HF [65] is shown in Figure 6-1c, the same peaks of copper, diamond and TiC are identified. After hot forging, the interface constitution in Cu/Ti-Dia-VSHF and Cu/Ti-Dia-HF are both TiC, but the initial phase at the interface is Ti and TiC, respectively. This indicates that the formed TiC during vacuum sintering will not evolve and new phase will not be formed in Cu/Ti-Dia-VSHF during the hot forging process.

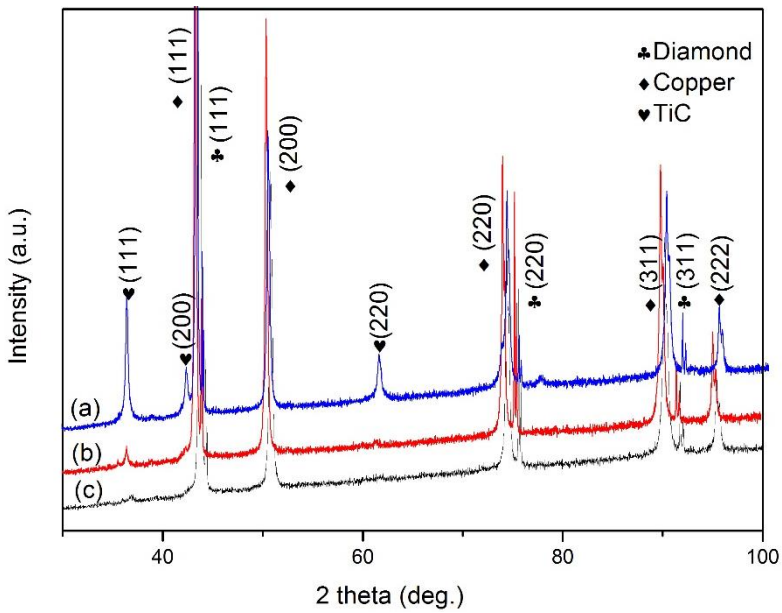

Figure 6-1 XRD patterns of Cu/Ti-Dia composites prepared by (a) vacuum sintering (Cu/Ti-Dia-VS); (b) the combination of the vacuum sintering and hot forging (Cu/Ti-Dia-VSHF); (c) hot forging (Cu/Ti-Dia-HF [65])

6.1.3 Microstructure

6.1.3.1 Microstructure of 800℃-forged composites

Figure 6-2 displays the SEM microstructure of the Cu/Ti-Dia-VS, Cu/Ti-Dia-VSHF and Cu/Ti-Dia-HF composites. It can be clearly seen that the distribution of diamond particles in the copper matrix is uniform for Cu/Ti-Dia-VS and Cu/Ti-Dia-VSHF composites (Figure 6-2a, d). For Cu/Ti-Dia-VS, several diamond particles are peeled off from the copper matrix, this is caused by mechanical polishing as preparing SEM samples (as indicated by the red arrow in Figure 6-2a). This suggests the interface has a poor interfacial connection with the copper leads to the diamond particles peel off from the copper matrix. In the high magnification images, the interfaces are found on both diamond-{100} and -{111} facets, which are very continuous and dense (Figure 6-2 b and c). Moreover, there are no visible voids and gaps can be seen between the copper and the diamond. After vacuum sintering, only the TiC peak is detected in the XRD pattern of the composite, we can speculate that the formed interface is TiC (Figure 6-1).

For Cu/Ti-Dia-VSHF, there are more pits leave on the copper matrix by the detachment of diamond particles from the copper matrix (Figure 6-2d), this means that the worse interfacial bonds are formed between the copper and the diamond in Cu/Ti-Dia-VSHF composite compared to the Cu/Ti-D-VS. Besides, from Figure 6-2 e and f, the TiC interface is also observed on both diamond-{100} and -{111} facets in Cu/Ti-Dia-VSHF composites, but the interface on the diamond surface is discontinuous and only a few TiC particles are dispersed on the diamond surface, and gaps and cracks are visible between the diamond and the copper (as shown by the circle in Figure 6-2f). This suggests that the amount of TiC particles is reduced after the hot forging of the pre-sintered composite material (also confirmed by XRD, in Figure 6-1), which weakens the interfacial bonding between the diamond and the copper.

As reported, the TiC interface is attached to the diamond closely and a strong TiC interface is formed between the diamond and the copper in Cu/Ti-Dia-HF composite, as shown in Figure 6-2g-h [65]. This indicates that stronger interfacial bonding is formed between the copper and the diamond in Cu/Ti-Dia-HF than both Cu/Ti-Dia-VS and Cu/Ti-Dia-VSHF.

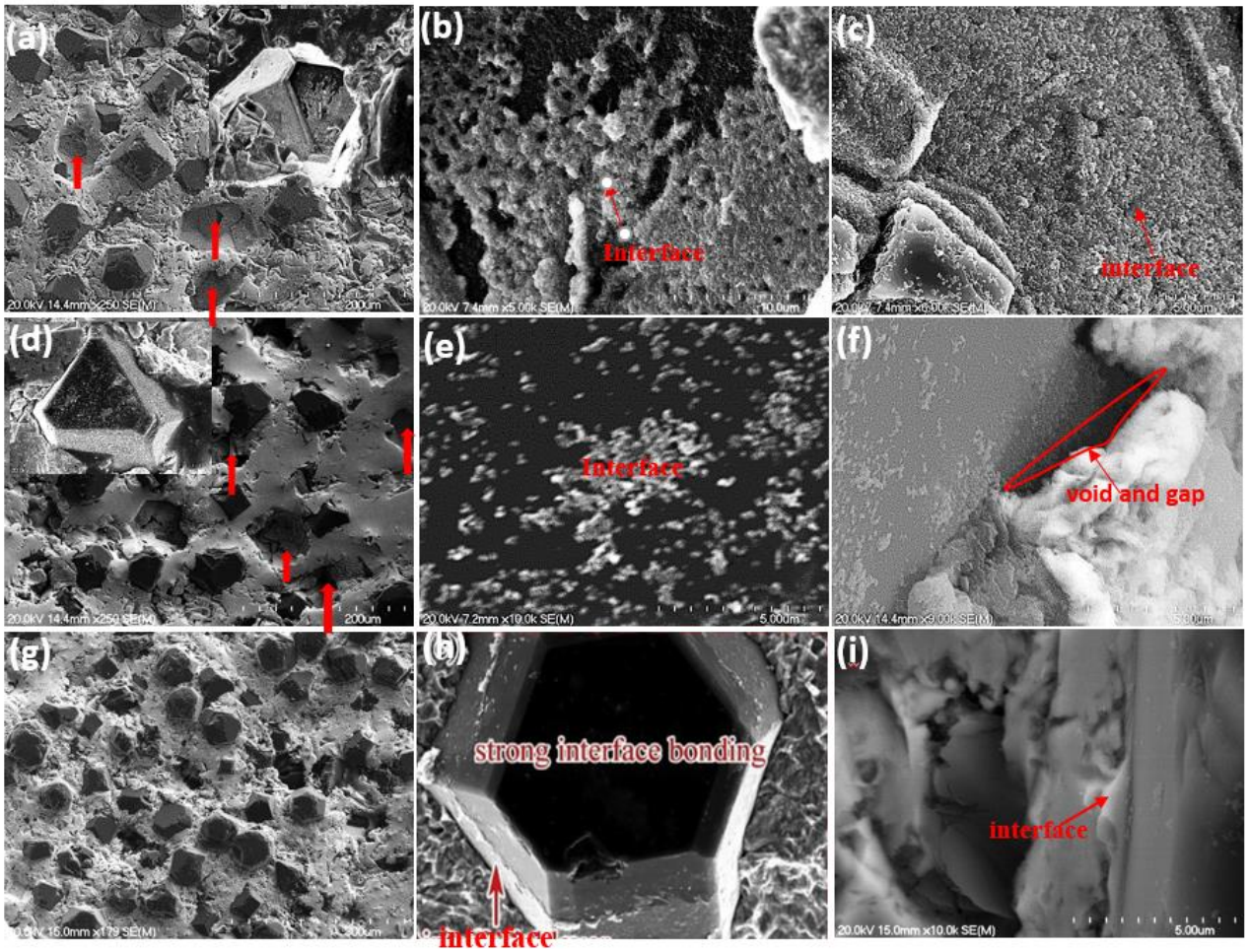

Figure 6-2 SEM microstructure of (a-c) Cu/Ti-Dia-VS; (d-f) Cu/Ti-Dia-VSHF; (g-i)Cu/Ti-Dia-HF [65] composites

6.1.3.2 Morphology of extracted diamond particles form the fabricated copper/Ti- coated diamond composites

The morphology of diamond particles extracted from Cu/Ti-Dia-VS and Cu/Ti-Dia-VSHF composites is shown in Figure 6-2 a and b, respectively. It can be seen that the bright area is the TiC interface and the black area is the bare diamond surface (Figure 6-2a and b). The diamond surface is not completely covered by the TiC interface, and the exposure of the bare diamond surface is caused by the interface peeling off from the diamond surface. According to calculations, the coverage rate of the diamond surface area by the interface is 53% for Cu/Ti-Dia- VS composite, only 35% for Cu/Ti-Dia-VSHF composite, the results are listed in Table 6-2. This suggests that the coverage rate of the diamond by the interface is low for the Cu/Ti-Dia-VS and Cu/Ti-Dia-VSHF composites and hot forging will lead to the spallation of the formed interface during vacuum sintering for Cu/Ti-Dia-VSHF composite.

For the detailed morphology of the TiC interface on the diamond surface of Cu/Ti-Dia-VS composite, it is clear to see the diamond surface is slightly rough and a large number of protrusions can be observed on both diamond-{100} (Figure 6-2a1) and -{111} facets (Figure 6-2a2). This is likely caused by the nucleation of the TiC particles through the reaction between the Ti coating and the diamond during vacuum sintering. It is also clear to see the TiC particles on the diamond-{111} facet is bigger than that on the diamond-{100} facet.

From the high magnification of diamond particles extracted from Cu/Ti-Dia-VSHF composite, we can see that the formed TiC interface tends to be coarse and flat (Figure 6-2b1 and b2). It is confirmed by XRD results that almost all Ti-coating has reacted with the diamond to form TiC after vacuum sintering, and this means the preformed TiC particles start growing coarse during hot forging, leading to a dense and flat interface forms in the Cu/Ti-Dia-VSHF. However, the preformed TiC particles are likely to break and spall from the diamond surface due to the plastic deformation (confirmed by the decreased coverage rate). The morphology on diamond-{100} and -{111} facets are almost the same, and the TiC particles are in flakes, with the grain size is greater than that of Cu/Ti-Dia-VS. This suggests vacuum sintering can eliminate the morphology discrepancy between diamond-{100} and -{111} facets.

The coverage rate of the diamond particles by the interface is relatively high for Cu/Ti-Dia-HF, with a value of 96%, compared to Cu/Ti-Dia-VS and Cu/Ti-Dia-VSHF composites. Besides, the formed interface layer on diamond particles extracted from Cu/Ti-Dia-HF is with a relatively rough and fine surface, and this leads to form an effective mechanical bonding with the copper matrix [65].

Table 6-2 Coverage rate of the diamond by TiC interface

Specimens	Coverage diamond area (%)
Cu/Ti-Dia-VS	53%
Cu/Ti-Dia-VSHF	35%

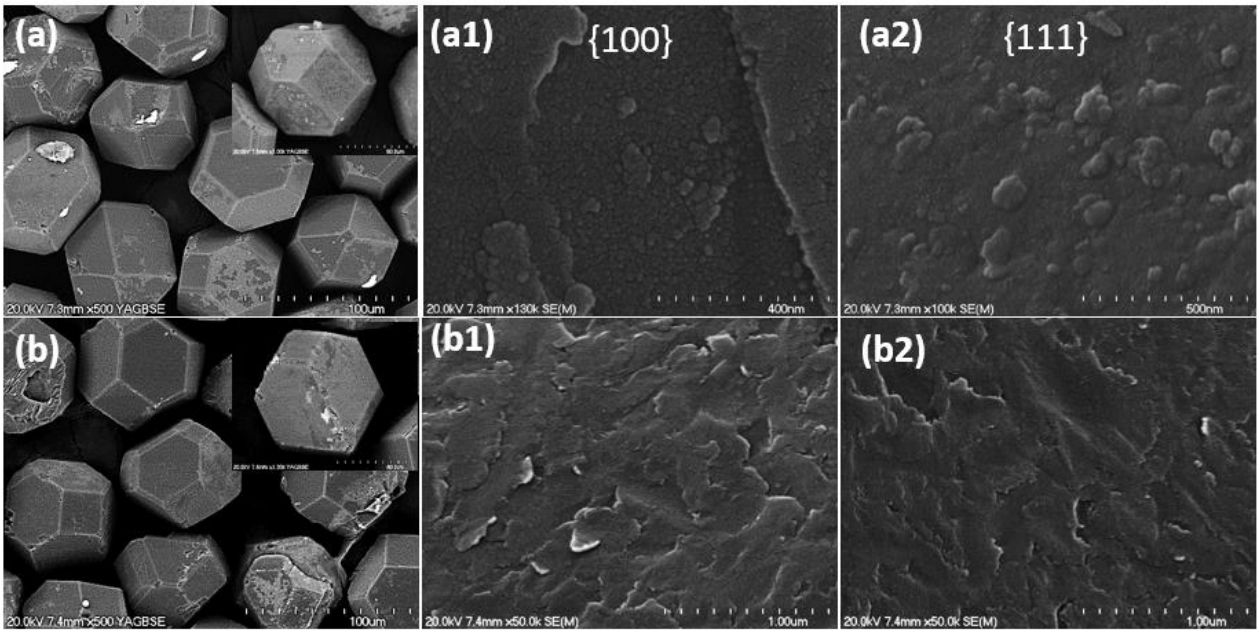

Figure 6-3 Microstructure of diamond particles extracted from (a) Cu/Ti-Dia-VS; (b) Cu/Ti-Dia-VSHF composites

6.1.4 Thermal conductivity

The thermal diffusivity (α) and thermal conductivity (k) of the Cu/Ti-Dia-VS and Cu/Ti-Dia-VSHF composites are shown in Figure 6-4. The thermal conductivity of Cu/Ti-Dia-VS is only 46W/ (mK), and the thermal conductivity of Cu/Ti-Dia-VSHF is increased to 241W/ (mK). Cu/Ti-Dia-VS has the lowest TC, this attributes to (1) the existence of the pores and gaps between the copper and the diamond in the composite leads to the low relative density of the composite; (2) poor interfacial bonding between the copper and the TiC interface result in diamond particles are easy to peel off from the copper matrix, which increases phonon scattering. After hot forging, the thermal conductivity is greatly increased due to the increased density of forged composite materials.

The thermal conductivity of Cu/Ti-Dia-HF is 550W/ (mK) [65], which is greatly higher than that of Cu/Ti-Dia-VSHF and Cu/Ti-Dia-VS composites. The high thermal conductivity value of Cu/Ti-Dia-HF is mainly attributed to the high the coverage rate of the diamond by the TiC interface, the formed TiC interfacial layer promotes the interface bonding strength between the copper and the diamond, and this enables phonon transfer at the interface.

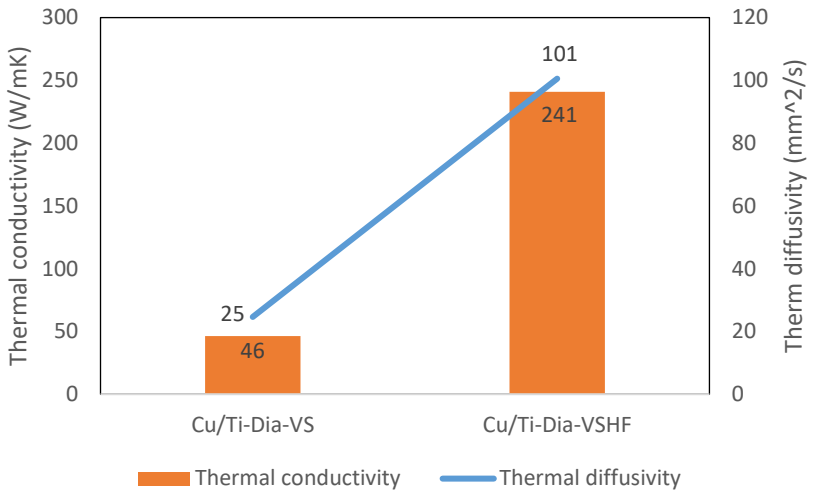

Figure 6-4 Thermal diffusivity and thermal conductivity of composites Cu/Ti-Dia-VS and Cu/Ti-Dia-VSHF composites

6.2 Discussion

6.2.1 Effect of vacuum sintering on Cu/Ti-diamond composites

The relative density of Cu/Ti-Dia-VS is lower than the copper/diamond composites prepared with the same process in literature [77], this is because the sintering temperature (800℃) in our study is lower than theirs (900℃). In the vacuum sintering process, the densification of the material is achieved by mass transfer including the surface and the bulk transport mechanisms. The mass transfer of these two mechanisms requires sufficient energy to support the mass transfer from the surface and the interior of the composite material. In this work, the sintering temperature of 800°C is relatively low, which makes it difficult to consolidate the copper/diamond composite material. This will adversely affect the shrinkage of the pores and reduce the diffusion of the matrix particles between each other, resulting in poorly dense composite materials.

During vacuum sintering, the original Ti coating almost completely reacts with the diamond to form the TiC interface layer, however, a large amount of the formed TiC layer is easy to spall from the diamond surface as the sample is cooling from 800℃ to room temperature, due to large CTE difference between TiC and the diamond (7.7ppm vs 2 ppm) and poor interfacial bonding between the copper and the interface leads to the copper matrix cannot restrict the spallation of the interface from the diamond surface.

6.2.2 Effect of hot forging on Cu/Ti-diamond composites

Cu/Ti-Dia-VSHF composite is prepared by vacuum sintering and hot forging. Ti coating has fully reacted with the diamond to form TiC during vacuum sintering at 800℃ for 2h, thus, the preformed TiC particles start growing coarse on both diamond-{100} and -{111} facets, and a large quantity of the TiC particles are spalled from the diamond surface during hot forging. The growth of the TiC particles reduces the roughness of the interface which leads to the reduction of the contact area with the copper, and the spallation of the TiC particles leads to the presence of the voids and gaps between the copper and the diamond. After hot forging, the relative density of the Cu/Ti-Dia-VSHF composite is increased from 73% (Cu/Ti-Dia-VS) to 93%, due to the pores are closed by the large plastic deformation. This is the primary reason to help improve the thermal conductivity of Cu/Ti-Dia-VSHF compared to the Cu/Ti-Dia-VS.

6.3 Summary

This chapter introduces Cu/Ti-diamond composite materials prepared by different methods, vacuum sintering, and a combination of vacuum sintering and hot forging. The conclusions are:

(1) Cu/Ti-Dia-VS and Cu/Ti-Dia-VSHF composites are successfully prepared by vacuum sintering, and the combination of vacuum sintering and hot forging, respectively. The diamond particles are uniformly distributed in the two composites, some diamond particles are peeled off from the copper matrix.

(2) The TiC interface can be observed in both Cu/Ti-Dia-VS and Cu/Ti-Dia-VSHF composites, but the interface bonding is weak due to the relative flat interface and low interface coverage rate of diamond particles. The coverage rate of the diamond by the interface is only 53% for Cu/Ti-Dia-VS, and 35% for Cu/Ti-Dia-VSHF. It suggests that the formed TiC particles during vacuum sintering are spalled from the diamond surface.

(3) For Cu/Ti-Dia-VS, the Ti coating is completely reacted with the diamond to form the TiC phase during vacuum sintering. The thermal conductivity of Cu/Ti-Dia-VS is only 46.31W/mK due to the low relative density of the composites (76%). The relative density and the thermal conductivity of Cu/Ti-Dia-VSHF composites are 93% and 241W/mK, respectively. The increased thermal conductivity is mainly attributed to the hot forging increase the relative density of the composite.

(4) By contrast with Cu/Ti-Dia-HF, it concludes that the TiC interface formed during hot forging is beneficial for improving the interfacial bonding strength between the copper

and the diamond and getting high thermal conductivity of the composite compared to the preformed.

7 Conclusion

(1) Pre-annealing on coated-diamond particles is an effective way to modify the interface of the Cu/Ti (W)-coated diamond composites. The reaction between the diamond and the coating element is controlled by the diffusion mechanism, and the reaction products varied by changing the pre-annealing temperature. The carbides formation ability of titanium and tungsten is different. TiC can be formed as the pre-annealing temperature is higher than 800℃, whilst tungsten carbides only formed as the annealing temperature is over 1050℃ in this study. High pre-annealing temperature can active more positions for carbides nucleation and growth;

(2) The nucleation of the carbide particles prefers to occur on the diamond-{111} facet rather than diamond-{100} facet during the process of pre-annealing because the graphitization of the diamond is easy to happen on the diamond-{111} facet;

(3) The thermal conductivity of Cu/Ti-diamond composite is decreased with increasing the pre-annealing temperature of Ti-coated diamond particles, while the thermal conductivity of Cu/W-diamond composite has a positive linear relationship with the pre-annealing temperature. The highest thermal conductivity Cu/Ti-diamond composite is 350W/ (mK) as the annealing temperature of Ti-diamond particles is 800℃ (Ti-800-Cu/Dia), attributed to high interface coverage rate and formation of the rough interface on the diamond particle surface. Because more WC interface are formed in the resultant composites, W-1050-Cu/Dia composite has the highest thermal conductivity among the fabricated Cu/W-diamond composites, with a value of 223 W/ (mK);

(4) The carbides forming ability of metal elements (such as Ti and W) and the acoustic properties of different carbides are different, thus, annealing of Ti- and W-coated-diamond particles prior to the fabrication of composites has different effects on the interface characteristics and thermal conductivity of the resultant composites. It is helpful to control the Cu/diamond composites' interface characteristics by tuning the pre-annealing temperature of the coated-diamond particles.

Reference

1. Razeeb, K.M., et al., *Present and future thermal interface materials for electronic devices.* International Materials Reviews, 2017. **63**(1): p. 1-21.
2. Wang, L., et al., *Combining Cr pre-coating and Cr alloying to improve the thermal conductivity of diamond particles reinforced Cu matrix composites.* Journal of Alloys and Compounds, 2018. **749**: p. 1098-1105.
3. Chang, G., et al., *Effect of Ti interlayer on interfacial thermal conductance between Cu and diamond.* Acta Materialia, 2018. **160**: p. 235-246.
4. Sinha, V. and J.E. Spowart, *Influence of interfacial carbide layer characteristics on thermal properties of copper–diamond composites.* Journal of Materials Science, 2012. **48**(3): p. 1330-1341.
5. He, J., et al., *Thermal conductivity of Cu–Zr/diamond composites produced by high temperature–high pressure method.* Composites Part B: Engineering, 2015. **68**: p. 22-26.
6. Kang, Q., et al., *Effect of molybdenum carbide intermediate layers on thermal properties of copper–diamond composites.* Journal of Alloys and Compounds, 2013. **576**: p. 380-385.
7. Weber, L. and R. Tavangar, *On the influence of active element content on the thermal conductivity and thermal expansion of Cu–X (X=Cr, B) diamond composites.* Scripta Materialia, 2007. **57**(11): p. 988-991.
8. Azina, C., et al., *Effect of titanium and zirconium carbide interphases on the thermal conductivity and interfacial heat transfers in copper/diamond composite materials.* AIP Advances, 2019. **9**(5).
9. Moore, G.E., *No exponential is forever: but Forever can be delayed! [semiconductor industry]*. Vol. 1. 2003. 20-23 vol.1.
10. Moore, G.E., *Cramming more components onto integrated circuits, Reprinted from Electronics, volume 38, number 8, April 19, 1965, pp.114 ff.* IEEE Solid-State Circuits Society Newsletter, 2006. **11**(3): p. 33-35.
11. Liu, T.L.C.P.R.W.X.W.B., *Research Progress in Ceramic Substrate Material for Electronic Packaging.* p. 1365-1374.
12. Zhang, H.B., *Electronic packaging materials and technology development status.* Applied Physics Letters, 2003. **8**(3).
13. Van Schilfgaarde M, A.I., Johansson B., *Origin of the Invar effect in iron-nickle alloys.* Nature, 1999. **400**(6739).
14. Huang, F.Y., et al., *The machinability of KOVAR material.* Journal of Materials Processing Technology, 1999. **87**(1): p. 112-118.
15. Clyne, T.W. and P.J. Withers, *An Introduction to Metal Matrix Composites*. Cambridge Solid State Science Series. 1993, Cambridge: Cambridge University Press.
16. Gui, M., S. Kang, and K. Euh, *Al-SiC Powder Preparation for Electronic Packaging Aluminum Composites by Plasma Spray Processing.* Journal of Thermal Spray Technology, 2004. **13**: p. 214-222.
17. Wu, L., et al., *Wear Resistance of Graphite / Aluminium Composites that Prepared by Stirring Casting.* Advanced Materials Research, 2013. **683**: p. 333-338.
18. Fadavi Boostani, A., et al., *Strengthening mechanisms of graphene sheets in aluminium matrix nanocomposites.* Materials & Design, 2015. **88**: p. 983-989.
19. Qu, X.-h., et al., *Review of metal matrix composites with high thermal conductivity for thermal management applications.* Progress in Natural Science: Materials International, 2011. **21**(3): p. 189-197.
20. Cho, S., et al., *Multiwalled carbon nanotubes as a contributing reinforcement phase for the improvement of thermal conductivity in copper matrix composites.* Scripta Materialia, 2010. **63**(4): p. 375-378.
21. Schubert, T., et al., *Interfacial design of Cu/SiC composites prepared by powder metallurgy for heat sink applications.* Composites Part A: Applied Science and Manufacturing, 2007. **38**(12): p. 2398-2403.
22. Johnson, J.L. and R.M. German. *Powder metallurgy processing of Mo-Cu for thermal management applications*. 1999.
23. Guo-Qin, C., et al., *Fabrication and characterization of high dense Mo/Cu composites for electronic packaging applications*. 2007. S580-S583.
24. Zifan, C., *The mechanism of interfacial structure formation and thermal properties of Al/diamond composites.* 2017.
25. Harkins, W.D., *Energy Relations of the Surface of Solids I. Surface Energy of the Diamond.* The Journal of Chemical Physics, 1942. **10**(5): p. 268-272.
26. Brillas, E., C.A. Martínez-Huitle, and I. Wiley, *Synthetic diamond films : preparation, electrochemistry, characterization, and applications*. 2011, Hoboken, N.J.: Hoboken, N.J. : Wiley.
27. Mizuuchi, K., K. Inoue, and Y. Agari, *Trend of the development of metal-based heat dissipative materials.* Microelectronics Reliability, 2017. **79**: p. 5-19.
28. Sidambe, A., *Biocompatibility of Advanced Manufactured Titanium Implants—A Review.* Materials, 2014. **7**: p. 8168-8188.
29. Abyzov, A.M., S.V. Kidalov, and F.M. Shakhov, *Filler-matrix thermal boundary resistance of diamond-copper composite with high thermal conductivity.* Physics of the Solid State, 2012. **54**(1): p. 210-215.

30. Tan, Z., et al., *Diamond/aluminum composites processed by vacuum hot pressing: Microstructure characteristics and thermal properties.* Diamond and Related Materials, 2013. **31**: p. 1–5.
31. Monachon, C., L. Weber, and C. Dames, *Thermal Boundary Conductance: A Materials Science Perspective.* Annual Review of Materials Research, 2016. **46**(1): p. 433-463.
32. Yang, F., et al., *Effect of Minor Titanium Addition on Copper/Diamond Composites Prepared by Hot Forging.* JOM, 2018. **70**(10): p. 2243-2248.
33. Moustafa, S., *Hot Forging and Hot Pressing of AlSi Powder Compared to Conventional Powder Metallurgy Route.* Materials Sciences and Applications, 2011. **02**: p. 1127-1133.
34. Tang, Y., L. Wang, and C. Zhao, *Enhancement of the thermal properties of silver-diamond composites with chromium carbide coating.* Applied Physics A, 2014. **115**.
35. Edtmaier, C., et al., *Temperature dependence of the thermal boundary conductance in Ag–3Si/diamond composites.* Diamond and Related Materials, 2015. **57**: p. 37-42.
36. Long, J., et al., *Fabrication of diamond particles reinforced Al-matrix composites by hot-press sintering.* International Journal of Refractory Metals and Hard Materials, 2013. **41**: p. 85-89.
37. Tan, Z., et al., *Diamond/aluminum composites processed by vacuum hot pressing: Microstructure characteristics and thermal properties.* Diamond and Related Materials, 2013. **31**: p. 1-5.
38. Schubert, T., et al., *Interfacial design of Cu-based composites prepared by powder metallurgy for heat sink applications.* Materials Science and Engineering: A, 2008. **475**(1): p. 39-44.
39. Losego, M.D., et al., *Effects of chemical bonding on heat transport across interfaces.* Nat Mater, 2012. **11**(6): p. 502-6.
40. Sinha, V., et al., *Effects of disorder state and interfacial layer on thermal transport in copper/diamond system.* Journal of Applied Physics, 2015. **117**(7).
41. Xu, Y., D.D.L. Chung, and C. Mroz, *Thermally conducting aluminum nitride polymer-matrix composites.* Composites Part A: Applied Science and Manufacturing, 2001. **32**(12): p. 1749-1757.
42. Mehra, N., et al., *Thermal transport in polymeric materials and across composite interfaces.* Applied Materials Today, 2018. **12**: p. 92-130.
43. Aleksandr, et al., *Thermal Transport in Nanostructured Materials*. 2012, Bosa Roca, United States: Taylor Francis Inc.
44. Schubert, T., et al., *Interfacial characterization of Cu/diamond composites prepared by powder metallurgy for heat sink applications.* Scripta Materialia, 2008. **58**(4): p. 263-266.
45. Chung, C.-Y., et al., *High thermal conductive diamond/Cu–Ti composites fabricated by pressureless sintering technique.* Applied Thermal Engineering, 2014. **69**(1): p. 208-213.
46. Chu, K., et al., *On the thermal conductivity of Cu–Zr/diamond composites.* Materials & Design, 2013. **45**: p. 36-42.
47. Bai, G., et al., *High thermal conductivity of Cu-B/diamond composites prepared by gas pressure infiltration.* Journal of Alloys and Compounds, 2018. **735**: p. 1648-1653.
48. Kang, Q., et al., *Microstructure and thermal properties of copper–diamond composites with tungsten carbide coating on diamond particles.* Materials Characterization, 2015. **105**: p. 18-23.
49. Wang, L., *Interficial structure and thermal conductivity of Cu/diamond composites*. 2019: University of Science and Technology Beijing
50. Xiaoguang Guo., T.L., Changheng Zhai., Zewei Yuna., Zhuji Ji., Dongming Guo., *Study on the Mechanism of Diamond Graphite with the Action of Transition Metals* 2016. **52**((20)): p. 23-29.
51. Feng, B., Z. Li, and X. Zhang, *Prediction of size effect on thermal conductivity of nanoscale metallic films.* Thin Solid Films, 2009. **517**(8): p. 2803-2807.
52. Hua, Y., Y. Dong, and B. Cao, *Monte carlo simulation of phonon ballistic diffusion and heat conduction in silicon nanometer films.* Acta Phys. Sin., 2013. **62**.
53. Wang, L., et al., *Enhanced thermal conductivity in Cu/diamond composites by tailoring the thickness of interfacial TiC layer.* Composites Part A: Applied Science and Manufacturing, 2018. **113**: p. 76-82.
54. Huang, X., et al., *Effects of particle size and film thickness of chrome-plated diamond on thermal properties of diamond-copper composites.* 2018. **28**: p. 53-56.
55. Abyzov, A.M., S.V. Kidalov, and F.M. Shakhov, *High thermal conductivity composites consisting of diamond filler with tungsten coating and copper (silver) matrix.* Journal of Materials Science, 2010. **46**(5): p. 1424-1438.
56. Ren, S., et al., *Effect of coating on the microstructure and thermal conductivities of diamond–Cu composites prepared by powder metallurgy.* Composites Science and Technology, 2011. **71**(13): p. 1550-1555.
57. Li, J., et al., *Optimized thermal properties in diamond particles reinforced copper-titanium matrix composites produced by gas pressure infiltration.* Composites Part A: Applied Science and Manufacturing, 2016. **91**: p. 189-194.
58. Pan, Y., et al., *Optimized thermal conductivity of diamond/Cu composite prepared with tungsten-copper-coated diamond particles by vacuum sintering technique.* Vacuum, 2018. **153**: p. 74-81.
59. Zhang, H., et al., *Unveiling the interfacial configuration in diamond/Cu composites by using statistical analysis of metallized diamond surface.* Scripta Materialia, 2018. **152**: p. 84-88.
60. Abyzov, A.M., et al., *Diamond–tungsten based coating–copper composites with high thermal conductivity produced by Pulse Plasma Sintering.* Materials & Design, 2015. **76**: p. 97-109.

61. Sang, J., et al., *Regulating interface adhesion and enhancing thermal conductivity of diamond/copper composites by ion beam bombardment and following surface metallization pretreatment.* Journal of Alloys and Compounds, 2018. **740**: p. 1060-1066.
62. Wheeler, D.W. and R.J.K. Wood, *High velocity erosion of CVD diamond coatings by diamond particles.* Diamond and Related Materials, 2018. **84**: p. 32-40.
63. Grzonka, J., et al., *Interfacial microstructure of copper/diamond composites fabricated via a powder metallurgical route.* Materials Characterization, 2015. **99**: p. 188-194.
64. Wu, Y., et al., *Critical effect and enhanced thermal conductivity of Cu-diamond composites reinforced with various diamond prepared by composite electroplating.* Ceramics International, 2019. **45**(10): p. 13225-13234.
65. Lei, L., L. Bolzoni, and F. Yang, *High thermal conductivity and strong interface bonding of a hot-forged Cu/Ti-coated-diamond composite.* Carbon, 2020. **168**: p. 553-563.
66. Tan, Z., et al., *A predictive model for interfacial thermal conductance in surface metallized diamond aluminum matrix composites.* Materials & Design, 2014. **55**: p. 257-262.
67. Che, Z., et al., *Effect of diamond surface chemistry and structure on the interfacial microstructure and properties of Al/ diamond composites.* RSC Adv., 2016. **6**.
68. Harkins, W., *Energy Relations of the Surface of Solids I. Surface Energy of the Diamond.* Journal of Chemical Physics, 1942. **10**: p. 268-272.
69. Chen, H., C. Jia, and S. Li, *Interfacial characterization and thermal conductivity of diamond/Cu composites prepared by two HPHT techniques.* Journal of Materials Science, 2012. **47**(7): p. 3367-3375.
70. Wang, L., et al., *Interfacial structure evolution and thermal conductivity of Cu-Zr/diamond composites prepared by gas pressure infiltration.* Journal of Alloys and Compounds, 2019. **781**: p. 800-809.
71. Abyzov, A.M., S.V. Kidalov, and F.M. Shakhov, *High thermal conductivity composites consisting of diamond filler with tungsten coating and copper (silver) matrix.* Journal of Materials Science, 2011. **46**(5): p. 1424-1438.
72. Zhang, C., et al., *Effects of dual-layer coatings on microstructure and thermal conductivity of diamond/Cu composites prepared by vacuum hot pressing.* Surface and Coatings Technology, 2015. **277**: p. 299-307.
73. Liang, Z. and H.-L. Tsai, *Reduction of solid–solid thermal boundary resistance by inserting an interlayer.* International Journal of Heat and Mass Transfer, 2012. **55**(11): p. 2999-3007.
74. Azina, C., et al., *Effect of titanium and zirconium carbide interphases on the thermal conductivity and interfacial heat transfers in copper/diamond composite materials.* AIP Advances, 2019. **9**(5): p. 055315.
75. Cheng, X.Y., et al., *First-principles thermal equation of state of tungsten carbide.* Computational Materials Science, 2012. **59**: p. 41-47.
76. Huang, S., et al., *Comparative study on the properties and microscopic mechanism of Ti coating and W coating diamond-copper composites.* Materials Research Express, 2020. **7**(7): p. 076517.
77. Raza, K. and F.A. Khalid, *Optimization of sintering parameters for diamond–copper composites in conventional sintering and their thermal conductivity.* Journal of Alloys and Compounds, 2014. **615**: p. 111-118.